Structural Investigation of the Ryôké Metamorphic Rocks of the Area between Iwakuni and Yanai, Southwestern Japan*

By

Terukazu NUREKI

with 72 Text-figures, and 6 Plates

ABSTRACT: Structural features of various scales were described, and, on the basis of geometrical and petrofabric analyses of these structures, the metamorphic history of the Ryôké metamorphic rocks has been discussed. The "Ryôké metamorphism" has been interpreted by predecessors as a progressive metamorphism of single generation, through which the Ryôké metamorphic rocks ranging from schistose hornfelses to banded gneisses and migmatites were produced. The metamorphic history of the area between Iwakuni and Yanai has, however, been considered by the present author as an overlapping series of events in which two phases have been discriminated: schistose hornfelses were formed during the first, earlier phase, and banded gneisses and migmatites during the second, later phase. The earlier phase is characterized by regional thermal metamorphism accompanied by penetrative movement, while the later phase by metasomatism or intense granitization under high temperature and relatively static condition.

CONTENTS

I. INTRODUCTION

The most interesting subject which has hitherto been a focus of discussion among Japanese geologists is when and how the Upper Palaeozoic sediments, deposits on the floor of so-called Chichibu geosyncline, in Japan underwent extensive crustal movements, and what meaning these metamorphosed sediments have in the history of development of the Japanese Islands.

It is in general believed among Japanese geologists that in Southwestern Japan there are three metamorphic zones derived from the Upper Palaeozoic formations, i.e., the Sangun metamorphic zone, the Ryôké metamorphic zone, and the Sambagawa

* Thes is presented for the degree of D. Sc. of the Hiroshima University.

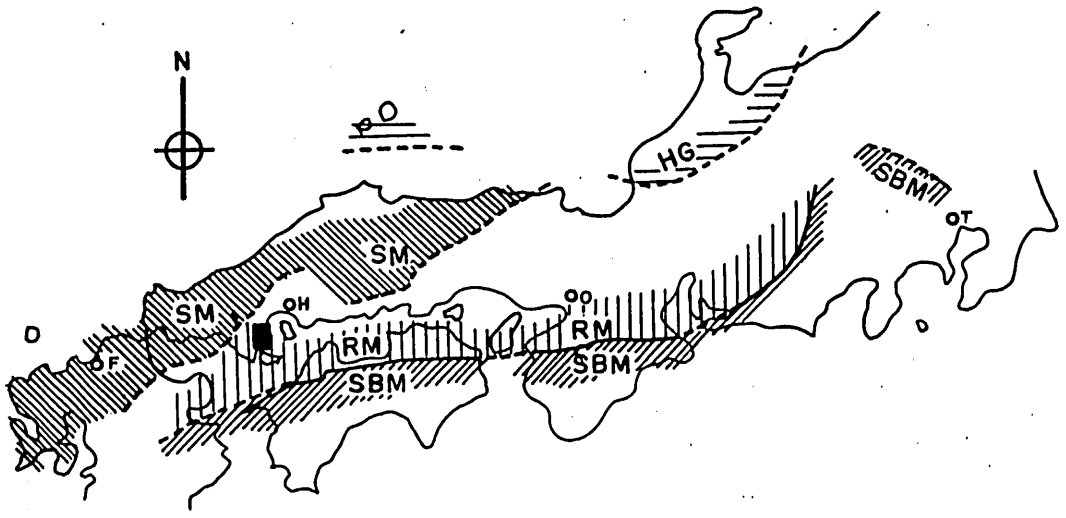

FIG. 1 Sketch map of three metamorphic zones in Southwestern Japan (after G. KOJIMA (1953)). HG: Hida gneiss complex SM: Sangun metamorphic zone RM: Ryôké metamorphic zone SBM: Sambagawa metamorphic zone F: Fukuoka H: Hiroshima O: Ôsaka T: Tokyo ■: Area investigated.

metamorphic zone. The Ryôké metamorphic zone in question is situated between the Sangun metamorphic zone to the north and the Sambagawa metamorphic zone to the south (Fig. 1).

Since the summer of 1955, the writer has been engaged in the geological and structural-petrological studies on the Ryôké metamorphic and granitic rocks* of the area between Iwakuni and Yanai, Yamaguchi Prefecture (Fig. 2).

In this article, the writer intends to study mainly the structural petrology of the Ryôké metamorphic and granitic rocks of the area between Iwakuni and Yanai. The area represents a type area comprising most types of the Ryôké metamorphites, accordingly, it may be expected to be able to extend the results of study of the area to dissolve structural problems of other areas of the Ryôké metamorphic zone, and furthermore, it may be expected that the method applied and the results obtained in this study will contribute to the study of other metamorphic zones.

Historical review: Since 1910, the Geological Survey of Japan has presented many valuable geological maps, which dealt with the geology of and near the area now concerned, such as Matsuyama-sheet (1:200,000; S. KÔZU & S. NODA, 1910), Hiroshima-sheet (1:200,000; S. KÔZU & S. NAKAMURA, 1911), Murozumi-sheet (Sheet 266; 1:75,000; T. AKAGI, 1922), Tokuyama-sheet (Sheet 262; 1:75,000; T. OGURA,

* The name "Ryôké metamorphic rocks" has been given to those rocks such as schistose hornfelses or mica-schists and banded gneisses, which are metamorphic derivatives of the Upper Palaeozoic sediments. Migmatites, granites and their derivatives in the Ryôké zone, which occur in intimate relation to the metamorphic rocks, are generally called the "Ryôké granitic rocks". The Ryôké metamorphic zone is composed of these metamorphic and granitic rocks.

1926), and Yanaizu-sheet (Sheet 241; 1:75,000; H. SATÔ, 1933). By the valuable contributions of these pioneers' works became the geology of the area in problem increasingly elucidated, in particular, Sheet 241 by SATÔ seems even now to be worthy of confidence in the light of modern structural geology.

From 1936 to 1940, S. IWAO published several papers (1936a, 1936b, 1936c, 1938, 1940) dealing with problems of geology and petrology of the area. Discussions submitted by him were based exclusively on the petrographical researches but not on the structural-petrological studies of the Ryôké metamorphic and granitic rocks.

Meanwhile, in 1941, T. KOBAYASHI summarized the Palaeozoic and Mesozoic geology of Southwestern Japan. On the basis of the idea of comparative tectonics of H. STILLE, KOBAYASHI introduced a hypothesis that in Japan two great orogenic cycles can be distinguished: the older one is the Akiyoshi orogenic cycle (Late Palaeozoic—Early Mesozoic) and the younger one the Sakawa orogenic cycle (Middle — Late Mesozoic). After him the phases of the Ryôké and the Sambagawa metamorphism belong to the Sakawa orogenic cycle, and that of the Sangun metamorphism to the Akiyoshi orogenic cycle.

Since 1946, G. KOJIMA and his collaborators have been engaged in the geological and petrological researches of the Ryôké metamorphic zone in Southwestern Japan. Some results of their researches have been published in several papers, such as, A. SHIMOYAMA, 1948; K. WATANABÉ, 1951; G. KOJIMA et al., 1951; G. KOJIMA and Y. OKAMURA, 1952; G. KOJIMA, 1953; Y. OKAMURA, 1957. SHIMOYAMA studied schistose hornfelses and gneisses in the northern half of the area now concerned, while, WATANABÉ and OKAMURA studied gneisses migmatites, and granites in the southern half of the area. OKAMURA concluded that gneisses, migmatites and granites in the Ryôké metamorphic zone of the area have been formed during a single phase of metamorphism.

With increase in the knowledge of structural and petrological characteristics of many metamorphic zones in Japan, the view of KOBAYASHI has become questionable. In 1952, M. GORAI discussed the origin of the Japanese Islands, and denied the opinion of KOBAYASHI. He interpreted the age of formation of the metamorphic zones in Southwestern Japan as that the Ryôké metamorphic rocks and associated granites were, along with crystalline schists of the Sangun and the Sambagawa metamorphic zone, formed during the orogenesis of the Late Palaeozoic or the Early Mesozoic. Most of Japanese geologists, e.g. KOJIMA (1953) and recently K. ICHIKAWA (1958), have supported GORAI's view being the most probable interpretation.

The writer has above described the outline of history of researches of the area now in question, but, of course, it can not be overlooked many valuable contributions to the knowledge of geology and petrology of the Ryôké metamorphic and granitic rocks in the other areas: in particular, the research of H. KOIDÉ (1949) in the Dando district and that of the members of the Research Group of the Ryôké Metamorphic Zone in Central Japan (1955).

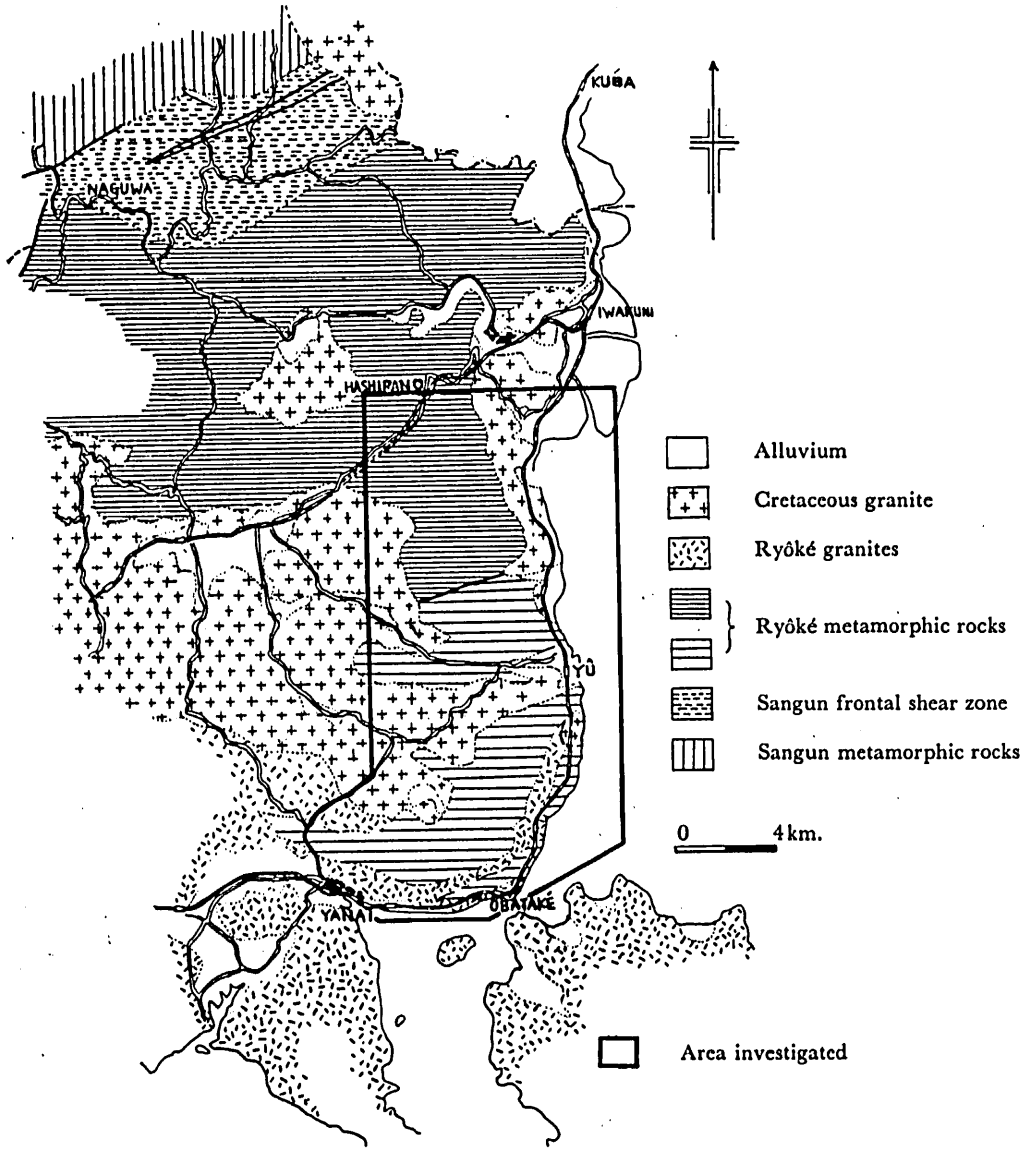

FIG. 2. Geologic situation of the area between Iwakuni and Yanai. (after "Geological Map of Yamaguchi Prefecture" (1954)).

Acknowledgement: The writer wishes to record his great indebtedness to Prof. G. KOJIMA of Hiroshima University for advice, discussions and encouragement during four years spent on this work. Professor KOJIMA read this manuscript and offered valuable criticism. Thanks are also due to Mr. Y. OKAMURA, Yamaguchi University, for his cooperation in the fabric analysis and many helpful discussions; to staffs of the

Institute of Geology and Mineralogy, Hiroshima University, for many fruitful discussions; and to Messrs. Y. OKIMURA, T. SUZUKI, and M. NAKAGAWA for valuable assistance with the drawings. Finally, the writer is indebted to the Grants in Aid for Scientific Research from the Ministry of Education in Japan in 1955, 1956, 1957, and 1958, which enabled him to carry on his field and laboratory work.

II. GEOLOGICAL SETTING AND PETROGRAPHIC PROPERTIES

GEOLOGICAL SETTING

KOJIMA (1953, p. 30) defined the extension of the Ryôké zone as follows: "The southern boundary of the zone is marked by the Median Dislocation Line, while the northern boundary is obscured by the intrusion of the Cretaceous granites, which are extensively exposed on the northern half of Seto-naikai (the Inland Sea) and on the southern half of Chûgoku. The Ryôké metamorphic zone proper may be tentatively defined as demarcated by the Median Dislocation Line and the southern intrusion boundary of the Cretaceous granites". The distribution of the Ryôké metamorphic rocks, especially schistose hornfelses, is rather patchy, and the area between Iwakuni and Yanai is the most extensive area of the Ryôké metamorphites in Southwestern Japan which enables the systematic study of the metamorphic rocks.

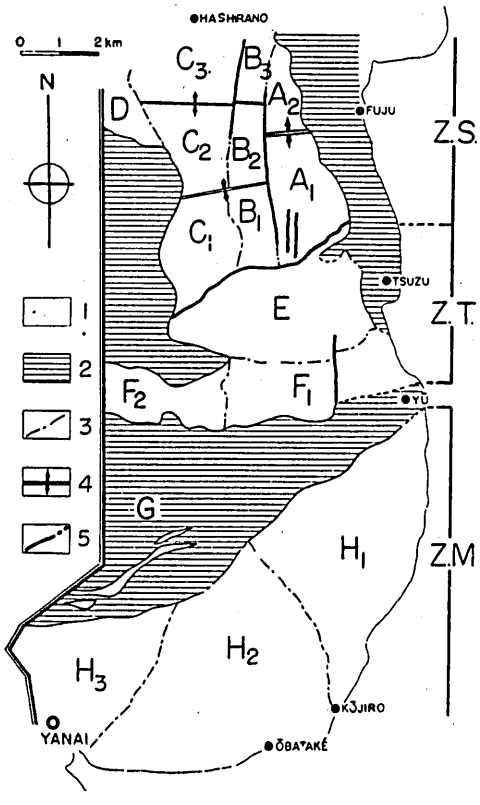

FIG. 3. Index map showing the three zones and 16 subareas. Z.S.: Zone of schistose hornfelses Z.T.: Zone of transitional rocks Z.M.: Zone of migmatites. 1: Ryôké metamorphic rocks 2: Cretaceous granite and Ryôké granites 3: boundaries between subareas 4: Axes of anticlines 5: Faults.

KOJIMA and OKAMURA have named the Palaeozoic formations, from which the Ryôké metamorphites were derived, the "Kuga Group" (KOJIMA & OKAMURA, 1952; KOJIMA, 1953). The upper and the lower limit of the group have not been ascertained, but, after KOJIMA, the total thickness of the group may attain 3000 m or more.

As to the age of sedimentation of the Kuga group in the area concerned, there are no direct palaeontological data available. In some places farther north of the area, however, the Kuga group contains some fossils. Several years ago, OKAMURA found fossils of the Permian fusulinids (Neoschwagerina or Yabeina) from a limestone lense near the

northern boundary of the Kuga group to the Sangun metamorphic zone.*

OUTLINE OF GEOLOGY

In the area between Iwakuni and Yanai there can be found four groups of rocks in mutually intimate relations, i.e., schistose hornfelses, banded gneisses, migmatites, and granites. In addition to these Ryôké metamorphic and granitic rocks, Cretaceous intrusive granite and its derivatives are also found in the northern half of the area.

Ryôké metamorphic rocks

The Ryôké metamorphic terrain in the area can be divided into three zones from the north to the south; i.e., (1) the zone of schistose hornfelses,** (2) the zone of transitional rocks,** and (3) the zone of migmatites*** (Fig. 3). The petrographic and structural properties of each zone change gradually across the mutual boundary.

Zone of schistose hornfelses: The northern part of the area belongs to the zone of schistose hornfelses (Fig. 3 and Plate XII). The main rock types of the zone are banded chert and pelite. The subordinate rocks are semi-pelite, limestone, calcareous-pelitic rock, sandstone, basic (diabasic) rock, and aplite. Semi-pelite consists of alternating thin bands of chert and pelite, and in the field it changes gradually into either banded chert or pelite. Sandstone lenses are found very scarcely. Calcareous-pelitic rock and limestone occur generally as lenses. The horizon of occurrence of calcareous-pelitic rock and limestone is not fixed, but they occur either in banded chert or in pelite. Basic rock occurs also as small lens-like bodies, and now they have schistose characters. The basic rock can be considered as derived from dyke rock of diabasic character, which was probably intruded prior to or during the Ryôké phase.**** Aplite dykes related to the Ryôké granites are sporadically found.

---

* G. KOJIMA (1953, p.31) explains: "As the limestone lens in question has been found in shear-slate in the frontal shear-zone ,the original horizon of bed is not ascertainable. But judging from the associated rocks, it can safely be said that the limestone belongs to the Kuga formation."

** H.KOIDÉ (1949) studied the Ryôké metamorphic rocks and the related granites of the Dando district, Aichi Prefecture. He has classified the Ryôké terrain of the district into three zones; i.e., the zone of schistose hornfelses (zone of potash-alumina-addition and silica subtraction), the zone of transitional rocks (zone of potash-alumina metasomatism, accompanied by metamorphic differentiation), and the zone of banded gneisses (zone of soda-addition and alumina-subtraction, accompanied by metamorphic differentiation). The zone of schistose hornfelses and the zone of transitional rocks after the present writer are petrographically identical with those of KOIDÉ.

*** In the southern part of the area in problem, gneisses and migmatites occur in intimate relation, and the more intense admixture of materials is expected than in the zone of banded gneisses of KOIDÉ. It may therefore be convenient in describing these plutonic rocks to use READ's definition of "Zone of migmatites" as applied in central Sutherland (H.H.READ, 1931, p. 91) or in Crohy Hills area in Donegal (A.R.GINDY, 1952). Intrusive granites in the Ryôké terrain were excluded from this zoning.

**** Though now the basic rock has a shistose character and its structure is in complete harmory with the surrounding schistose hornfelses, the lense like bodies of basic rock occur not always conformably to the surrounding formation. The basic rock has chilled margin near the contact with the surrounding schistose hornfelses.

The stratigraphy of original sediments from which schistose hornfelses were derived has not yet been decided in detail. It can safely be said, however, that pelite is prevalent at the lower horizon, and that, through alternating group (semi-pelite), banded chert becomes predominant at the upper horizon. The total thickness of schistose hornfelses may attain at least 700m or more.

There is a large anticline, which runs E.-W. through the central part of the zone in question and is called "major anticline" by the writer. The wave-length of the anticline attains about six km, and its axis plunges moderately towards the east. On both limbs of the major anticline are there two or more subordinate anticlines, the wave-length of which attains commonly one km or more.

Zone of transitional rocks: The central part of the area belongs to the zone of transitional rocks. The northern boundary of the zone is demarcated by a thrust-fault, which runs east and west. This thrust-fault, however, does not represent a boundary fault genetically related to the difference in metamorphic character between the northern and the central zone. Schistose hornfelses of the northern zone change gradually their petrographic characters towards gneisses of the zone of transitional rocks, the southern-most part of the northern zone consisting of gneisses of transitional type. The southern and western borders of the zone are demarcated by intrusion boundaries of the Ryôké granites.

The zone of transitional rocks is essentially composed of siliceous banded gneiss, micaceous banded gneiss, and micaceous gneiss, and subordinate members are basic gneiss and the Ryôké granite. In the northern half of the zone is exposed micaceous banded gneiss, which is the most predominant rock type in the zone. In the southern half of the zone siliceous banded gneiss is predominant, being often accompanied by micaceous gneiss. Basic gneiss occurs as a large lens-like body, which is conformable to structures of the surrounding gneisses. Some small stocks of fine-grained granites, probably derived from the Ryôké granites, are found here and there in the zone.

Because of the lack of good exposures within the zone in problem, the structure on larger scale can not be decided.

Zone of migmatites: The zone of migmatites occupies the southern part of the Iwakuni Yanai area. This zone continues farther towards the west. The northern and southern borders of the zone are bounded by the Gamano gneissose granodiorite.

The zone of migmatites consists mainly of siliceous banded gneiss, micaceous gneiss, and migmatites or "autochthonous granite"*.

The subordinate rock types are micaceous banded gneiss, crystalline limestone,

* The word "autochthonous" is here used in the sense of H. H. READ (1949). OKAMURA (1957), who has studied the Ryôké granites since 1951, has adopted the words "autochthonous", "parautochthonous", and "intrusive" granites, presented by H. H. READ, to granites in the Ryôké zone. He has classified the Ryôké granites into two groups of different generation, i.e., the older and younger complexes. According to his view, the older complex corresponds to the "autochthonous" and "parautochthonous" granites, and the younger one to the "intrusive" granites. The writer agrees with his view of the Ryôké granites, and intends to use the names of rock bodies which have been used by him.

aplitic rock and fine-grained granite, the latter two of which are related to the Ryôké granites.

Siliceous banded gneiss occupies the greater part of the zone, within which thin but continuous beds of micaceous gneiss and micaceous banded gneiss are concordantly inserted. Crystalline limestone occurs as a small lens.

There are some bodies of migmatites, most of which lie in concordance with the structure of the surrounding siliceous banded gneiss (Plate XII). Considering petrologic characteristics of migmatites, the writer has grouped them into two types: the migmatite in the southern part of the zone has been named the "Ôbataké gneissose granodiorite", and the other the "Ôbataké gneissose granite"* (Plate XII). Summarizing field data, the Ôbataké gneissose granite lies strictly concordant with the structure of the surrounding gneisses; that is, it appears to be completely "autochthonous". While, the Ôbataké gneissose granodiorite is not always concordant with the surrounding structure: the eastern half of the body shows "parautochthonous" features at the contact with the surroundings.

The foliation (compositional banding) in banded gneisses is generally inclined either north or south at high angles. It is very significant that, as seen on the geologic map, the general trend of banded gneisses draw a gentle convex curve towards the southeast.

Ryôké granites

As mentioned above, the Ryôké granites in the area can be divided into two groups (OKAMURA, 1957), i. e., the older and the younger. Migmatites and the Gamano gneissose granodiorite belong to the former, and the Kibé and Namera granites to the latter. The Kibé granite and the Gamano gneissose granodiorite lie in wedge-shaped form between the zone of migmatites and the zone of transitional rocks.

The Gamano gneissose granodiorite lies concordantly in part or sub-concordantly in another part with the structure of banded gneisses of the zone of migmatites. Four or more bodies of siliceous banded gneiss are found within the Gamano gneissose granodiorite. No recognizable thermal effects can be found from the surroundings of the Gamano gneissose granodiorite. While, the Kibé and Namera granites, which may probably synchronous with each other, exerted intense thermal effects upon the surroundings; in particular, the former has a fine-grained facies along the contact with siliceous banded gneiss of the zone of transitional rocks.

Igneous rocks of the Late Cretaceous period

The eastern and the western side of the zone of schistose hornfelses are bounded by the Cretaceous granite, which is the extension of the so-called Hiroshima granite expansively exposed in Chûgoku Province, Southwestern Japan. The zone of schistose hornfelses lies on the Cretaceous granite as a huge roof-pendant, and schistose horn-

* All the migmatite bodies in the zone have, however, been called by OKAMURA the "Ôbataké gneissose granodiorite".

felses near the intrusion contact have suffered strong thermal metamorphism. In the zone of schistose hornfelses, small to large dykes of quartz-porphyry and aplite related to the Cretaceous granite are found here and there. They are also found in the northern part of the zone of transitional rocks, but have never been found in the zone of migmatites.

Petrographic Properties of the Ryôké Metamorphic Rocks and Granites

Rocks in the zone of schitose hornfelses

Banded chart: Banded chert is composed of alternating bands of chert and pelite, the latter being very thin.

Chert bands are built up of quartz and muscovitic mineral. Quartz, average size of which is 0.03 mm in diameter, makes up more than 90% of each band, and always shows mosaic texture. Muscovitic mineral is colourless or faint green and shows no pleochroism, and is too small to determine its optic character under the ordinary microscopic method. The subordinate minerals in chert bands are biotite, feldspars, carbonaceous material and garnet. Biotite is pale brown. Feldspars and garnet are very rare.

Pelite bands consist of muscovitic mineral, biotite, carbonaceous material, quartz, and occationally garnet. Biotite and carbonaceous material are abundant in pelite bands. Biotite is also pale brown. In some places near Sugaki and Shimobata, pelite bands contain many small grains of garnet, which is idiomorphic and includes many minute grains of opaque minerals.

Segregated veins of quartz or of quartz and chlorite are often found in network in banded chert.

Pelite: Pelite is often accompanied by thin quartzose layers (chert). Biotite and muscovitic mineral, which is more abundant than the former, are the essential ingredients in pelite. Carbonaceous material, quartz, and plagioclase are the subordinate. In some quartzose layers, rounded grains of plagioclase are occasionally found. Micas show preferred orientation along the plane of original compositional banding.

Semi-pelite: Semi-pelite consists of quartzose bands and pelite bands, each being commonly alternated nearly in the same proportion. The mineral assemblage of quartzose bands varies from that of chert to that of sandstone.

Sandstone: Sandstone is composed essentially of quartz, muscovitic mineral, accompanied with biotite, carbonaceous material and plagioclase. Quartz is mostly equigranular, but in part it shows sub-angular forms. Angular grains of plagioclase are sporadically found.

Limestone and calcareous-pelitic rock: Limestone as well as calcareous-pelitic rock are now completely recrystallized by the thermal metamorphism exerted by the Cretaceous granite. Accordingly, the schistose nature of them is completely obscured.

Basic (diabasic) rock: Basic rock consists of actinolite, brown hornblende, and plagioclase, accompanied by opaque minerals, epidote, muscovite and quartz. Brown

hornblende appears to be a relic mineral, but relics or alteration products of pyroxene have not been found. Saussuritisation of the rock seems to have been effective.

The writer has above described schistose hornfelses in the main part of the zone in problem. Near the southern border of the zone, schistose hornfelses change gradually their petrographic features into those of gneisses towards the zone of transitional rocks, as follows:—

1) The mineral assemblages of banded chert and pelite show no essential change, but the grain-size of quartz and micas remarkably increases: the average size of quartz attains 0.05 mm or more in diameter.

2) Brown or reddish-brown biotite gradually increases in amount, and minute grains of muscovitic mineral disappear. Now, unmistakable muscovite becomes an essential ingredient and co-exists with biotite.

3) Segregated veins of quartz increase remarkably in amount.

Rocks in the zone of transitional rocks

Micaceous gneiss, micaceous banded gneiss and siliceous banded gneiss: As in the case of schistose hornfelses, various rock types found in the zone of transitional rocks have been grouped according to the relative proportion of white (quartzose) band to black (micaceous) band: the rock composed of thick black bands and thin white bands is called micaceous gneiss; on the contrary, the rock of thick white bands and thin black bands is named siliceous banded gneiss; and the intermediate rock type micaceous banded gneiss. Accordingly, no essential differences in mineralogical assemblage can not be detected between these rock types.

Quartzose bands are commonly composed of quartz, potash-feldspar, biotite and muscovite, with less common plagioclase and garnet. Quartz is 0.05 mm in average diameter and shows mosaic texture. Many porphyroblasts of quartz are found in every section. Potash-feldspar is commonly found but inferior in amount. Minute grains of biotite are commonly found in the porphyroblast of quartz*. Muscovite is less abundant than biotite.

Micaceous bands are composed of biotite, muscovite, cordierite, quartz, plagioclase and potash-feldspar, with subordinate zircon, garnet, and carbonaceous material. Porphyroblastic quartz is not rare. Muscovite is rather rare or absent, while biotite is universally found.

Petrographic features of rocks in the zone are thus characterized by the appearance of potash-feldspar, which can not be found in schistose hornfelses. In siliceous banded gneiss of the southern part of the zone, the grain-size of quartz becomes larger, attaining 0.1 mm or more in diameter, and potash-feldspar increases in amount.

Basic gneiss: The rock consists of brown or greenish-brown hornblende, plagioclase and quartz, with carbonaceous material. Hornblende makes up about 80% of the rock, and quartz is fairly abundant than plagioclase. The rock shows typical mosaic

* Detailed descriptions of the porphyroblast of quartz are referred to the paper of S. IWAO (1938).

texture. Alternation of hornblendic bands and felsic bands is common. Although the original rock of the basic gneiss is not certain, it seems probable that the basic gneiss have been derived from an impure calcareous rock or calcareous-pelitic rock.

Rocks in the zone of migmatites

Micaceous gneiss, micaceous banded gneiss and siliceous banded gneiss: The banded nature of these rocks is also due to the alternation of quartzose bands and micaceous bands. Quartzose bands are composed of biotite, muscovite, quartz, potash-feldspar and plagioclase, with subordinate zircon, garnet, iron ores and carbonaceous material. Quartz always shows slight elongation parallel to the foliation, and undulatory extinction of quartz is commonly found. The diameter of quartz grains is very variable from 0.1 to 1 mm. Porphyroblasts of quartz are common, and attain often to 2～3 mm in diameter. Parallel arrangement of flakes of biotite and muscovite accentuates the banded nature of the rock.

Micaceous bands consist of biotite, muscovite, cordierite, quartz, potash-feldspar and plagioclase, accompanied with sillimanite, iron ores, carbonaceous material and garnet. In some sections, sillimanite occurs as an essential component and coexists with biotite and cordierite. Cordierite can commonly be found in most samples, not rarely forming porphyroblasts. Large porphyroblasts of quartz, attaining up to 2 mm, are also common.

The most significant petrographic feature of banded gneisses in this zone is that feldspars, in particular plagioclase, increase remarkably in amount, compared with those in banded gneisses in the zone of transitional rocks. Considering their petrographic characters, it can safely be said that banded gneisses in this zone have suffered more intense alkali-alumina-metasomatism accompanied by metamorphic differentiation than those in the zone of transitional rocks.

Migmatites (*Ôbataké gneissose granite and Ôbataké gneissose granodiorite*): The Ôbataké gneissose granite consists of quartz, potash-feldspar, plagioclase, biotite and muscovite, accompanied with less prominent zircon, apatite, sphene and iron ores. The migmatite often contains small amount of cordierite and less commonly sillimanite. The rock shows an inequigranular fabric, the feature having been noticed as an characteristic feature of granitic rocks of metasomatic origin. Potash-feldspar generally shows perthitic structure and is more abundant than plagioclase. Zonal structure of plagioclase is lacking. Biotite and muscovite are arranged parallel to the foliation and accentuate the gneissose nature of the migmatite.

The Ôbataké gneissose granodiorite strongly resembles the Gamano gneissose granodiorite in many petrographic features. As essential components are found hornblende and pyroxene, which have not been found in the Ôbataké gneissose granite. The minerals however can not always found from every section. The most essential mafic mineral is biotite. Potash-feldspar is far inferior to plagioclase in quantity. Glomeroporphyroblasts of plagioclase are often found, and the zonal structure of plagioclase

is rare.

On the basis of various data obtained from the field as well as from microscopic observations, it can safely be inferred that the Ôbataké gneissose granite may have been derived from siliceous banded gneiss, while the Ôbataké gneissose granodiorite from micaceous banded gneiss which was in part probably rich in calcareous materials, and that the former probably corresponds to the autochthonous granite, as Y. OKAMURA has reported in detail. It is questionable, however, to regard the whole rock body of the latter as corresponding to the autochthonous granite. The Ôbataké gneissose granodiorite is conceivably autochthonous in some parts, but parautochthonous in other parts.

Ryôké granites

Gamano gneissose granodiorite: The Gamano gneissose granodiorite resembles strongly the Ôbataké gneissose granodiorite in the field as well as in petrographic features under the microscope. The essential minerals found in the granodiorite are hornblende, pyroxene, biotite, potash-feldspar, quartz and plagioclase. Hornblende and pyroxene occur only in the western area of Yû.* Zonal structure of plagioclase is common.

Judging from detailed observations in the field, it may safely be concluded that the Gamano gneissose granodiorite may correspond to the parautochthonous granite as interpreted by Y. OKAMURA.

Younger (intrusive) Ryôké granites: The Kibé granite is coarse-grained and somewhat porphyritic in appearance, but it shows less commonly weak gneissose structure. The essential components of the granite are biotite, quartz, potash-feldspar and plagioclase. The porphyritic appearance of the granite is due to the sporadic presence of large grains of perthitic potash-feldspar.

The Namera granite is also coarse-grained and homogeneous. Biotite, quartz, potash-feldspar and plagioclase are the essential ingredients of the granite, and garnet and zircon are generally found as accessories. A characteristic mineral of the granite is garnet which has not been found from the Kibé granite.

III. MESOSCOPIC AND MACROSCOPIC STRUCTURE

GENERAL STATEMENT

There is a tendency among modern structural petrologists to explain the metamorphic history of certain field on the basis of geometrical analysis of minor structures (mesoscopic structures of L. E. WEISS) and major structures (macroscopic structures of L. E. WEISS). Especially, structural petrologists in Scottish Highlands and in Rheinische Schiefergebirge have made much contributions to the structural petrology (D. B.

* It is an interesting fact that the pyroxene-hornblende bearing Gamano gneissose granodiorite is found in the area of Ôsato to Yû, and the pyroxene-hornblende bearing Ôbataké gneissose granodiorite occurs exclusively in the area of Kôjiro to Yû. It can be inferred that these granodiorites are genetically closely related to each other.

McINTYRE, L. E. WEISS, J. SATTON, J. WATSON *et al.* in Scottish Highlands; R. HOEPPENER, S. KIENOW, W. JANKOWSKY *et al.* in Rheinische Schiefergebirge).

The structural geometry of the Ryôké metamorphic rocks of the area in question will be described systematically in the following order: (1) to describe different kinds of mesoscopic structures,* (2) to examine the degree of structural homogeneity in each zone, (3) to systematize the macroscopic structures of the region as a whole, and (4) to clarify the structural relation between the Ryôké metamorphic rocks and the Ryôké granites.

The writer has divided the Iwakuni-Yanai area into 16 subareas, as shown in Fig. 3.

MESOSCOPIC STRUCTURE

Mesoscopic structures of schistose hornfelses

Foliation and cleavage: One of the important planar structures of schistose hornfelses is the foliation (here termed S_1), which is the most prominent set of structural surfaces. In most rocks, especially in banded chert, S_1 corresponds to the surface of bedding or lamination of original rocks.

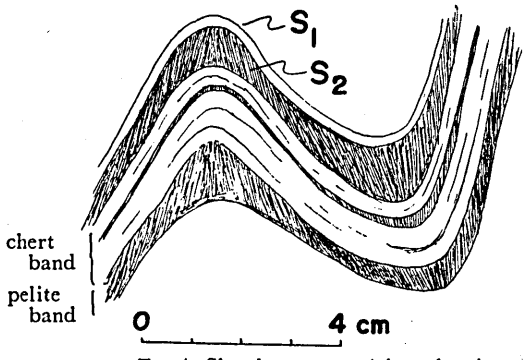

FIG. 4. Sketch on an ac-joint; showing the relation of S_1 and S_2 in semi-pelite, near Rokuroshi, Iwakuni city.

In semi-pelite, in particular near the crest of minor folds, the second planar structure (here termed S_2) can often be found. This planar structure is restricted in pelite bands and may correspond to the "fracture-cleavage" of DE SITTER (1956). Locally, S_2 is also found in pelite. In strongly folded semi-pelite, however, S_2 is not always developed. Often away from the crest, S_2 becomes more and more weaker, and finally at the limb it becomes invisible. The number of the surface of S_2 exceeds 10 within 1 cm. The surface of S_2 converges towards the crest of minor folds (Fig. 4), and does not cut chert bands in semi-pelite as well as in pelite.

In some places, especially in the northern-most part of the zone of schistose hornfelses, a set of another planar structure is developed. This surface clearly cuts S_1 and S_2, and the inclination of the surface is commonly steep or nearly vertical, exceeding generally 70°. The structure is here termed S_3, which may correspond to the "slaty cleav-

* The writer uses the terms "mesoscopic" and "macroscopic" after the definition presented by L. E. WEISS (1957). He defined them as follows (p.577):
(1) "Mesoscopic: This covers fields ranging in size from a single hand specimen to a single continuous exposure (generally, but not always, of small size) in which data can be measured with sufficient accuracy and continuity to alow determination of its over-all structural geometry."
(2) "Macroscopic: This covers fields of any size containing discontinuously observable structures. It stands apart from the other scales, in that structures within macroscopic fields are determined indirectly."

age" of DE SITTER (1956) (Fig. 5.)

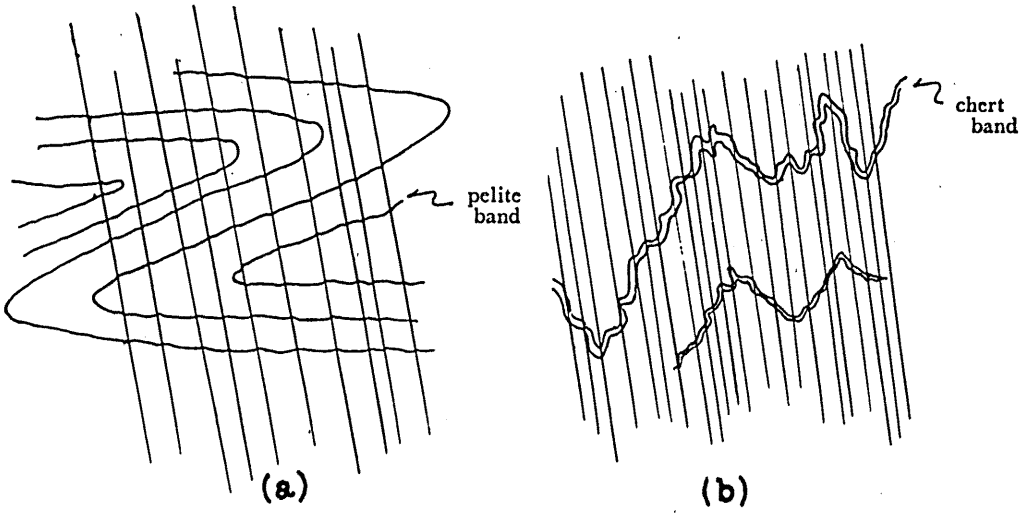

FIG. 5. Schematic sketch of S_3 in banded chert (a) and in pelite (b). (see text).

S_3 has been found only from three subareas, regardless of rock types, i.e., subarea C_3 (and B_3), the northern part of subarea B_2, and the southwestern part of subarea A_1. In particular, a large exposure along the road-cutting south of Hashirano is most suited for the statistic study of S_3. In the other exposures, S_3 is locally found, but the statistical study of S_3 were practically impossible, because of either lacking in good exposure or local development of S_3.

The strike and dip of S_3 are rather constant throughout the zone in problem. The general trend of S_3 is E.-W., and it dips to the south at very steep angles. Sometimes, S_3 is practically parallel to the axial plane of minor folds, but most commonly they intersect at variable angles (Fig. 5 and Plate XI-B). In banded chert S_1 is visibly displaced along the surface of S_3, the distance of displacement being very short. The spacing of the set of S_3 is generally $0.5 \sim 1$ mm. S_3 in pelite is more closely spaced than that in banded chert. Sometimes, the surface of S_3 is partly filled with segregated quartz veins.

Careful examinations in the field strongly suggest that the formation of S_3 is clearly later than that of folds most commonly found in schistose hornfelses* (later described).

Joints: There are at least two kinds of joint in the zone of schistose hornfelses. The most commonly occuring joint is that perpendicular or subperpendicular to the lineation. This may correspond to the *ac*-joint of E. CLOOS (1937). This type of joint has all the characteristics of tension fractures. Comparing the *ac*-joint in pelite (Plate IX-A)

* S_3 has not been found from rocks in the other two zones, i.e., the zone of transitional rocks and the zone of migmatites. This fact will become significant in the later chapter, when the history of the Ryôké metamorphic rocks in the Iwakuni-Yanai area is considered.

with that in banded chert (Plate IX-B), the surface of the former is more even and continuous than the latter. In an exposure, however, individual surface of *ac*-joints is rarely perpendicular to the lineation, and most commonly they are subnormal to the lineation or form slight angles with the *ac*-position, the fact having been observed by many workers in deformed rocks of many different styles.

Beside the *ac*-joint are observable oblique (*hk0*)-joints (E. CLOOS, 1937) in some localities. They are subnormal to the foliation surface and lie symmetrically to the lineation. They are, however, not always found in pairs. The oblique joints are typically developed near the crest of the major anticline. Shear joints of other types have been observed locally, but the statistic examination of them could have not been carried out.

Most *ac*-joints have been conventionally interpreted as tension fractures, and several alternatives concerning the genesis of them have been presented by many authors. Considering the mode of occurrence of the *ac*-joint, the writer believes that the *ac*-joint may be the ruptural expression of strain parallel to the axes of major folds during folding (FAIRBAIRN, 1949, p. 156–157).

Lineation: The most conspicuous mesoscopic structure is the distinct lineation that is present in almost all the rock types in the area concerned. The lineation can be divided into two groups acconding to the following features:—

Regardless of rock types, one can find a distinct linear structure expressed by axes of microfold of S_1, most of which are accompanied by folds on every scale. Judging from characters of these folds, it is evident that the rock structure generally shows a monoclinic symmetry with one plane of symmetry normal to the fold axis. The lineation is thus parallel to the fabric axis *b* and is by definition $B(=b)$-lineation (B. SANDER, 1948, p. 65–68).

Parallel arrangement of mineral grains defines another type of lineation. Lineation in basic rocks may be due to parallel arrangement of hornblende grains. Quartz grains in schistose hornfelses are most commonly equigranular and show no elongated character in any thin section. While, parallel arrangement of mafic minerals, such as muscovitic mineral and biotite, is observable on S_1, especially in pelite and semi-pelite. This type of lineation is to be attributable to the intersection of planar structures. There are at least three types of lineation due to the intersection of *s*-surfaces, i.e., intersection of S_1 with S_2 (here designated as $\widehat{S_1 S_2}$), intersection of S_1 with S_3 (as $\widehat{S_1 S_3}$), and intersection of S_2 with S_3 (as $\widehat{S_2 S_3}$). The lineation $\widehat{S_1 S_2}$ is most prominently found in pelite and in semi-pelite. In subareas C_3 and B_3, the lineation $\widehat{S_1 S_3}$ has been generally found regardless of rock types, wherever S_3 is developed, but, in the other localities, megascopically visible $\widehat{S_1 S_3}$ is rather rare. $\widehat{S_2 S_3}$ has been found from some localities, where S_3 is developed. Semi-pelite and pelite are the essential rock types in which $\widehat{S_2 S_3}$ can be observed. All these lineations, $\widehat{S_1 S_2}$, $\widehat{S_1 S_3}$ and $\widehat{S_2 S_3}$, are practically parallel to each other and also to the axis of microfold of S_1. It is therefore often very difficult

to distinguish megascopically the one type from the other. It can safely be said that this type of lineation found in schistose hornfelses is also $B(=b)$-lineation.

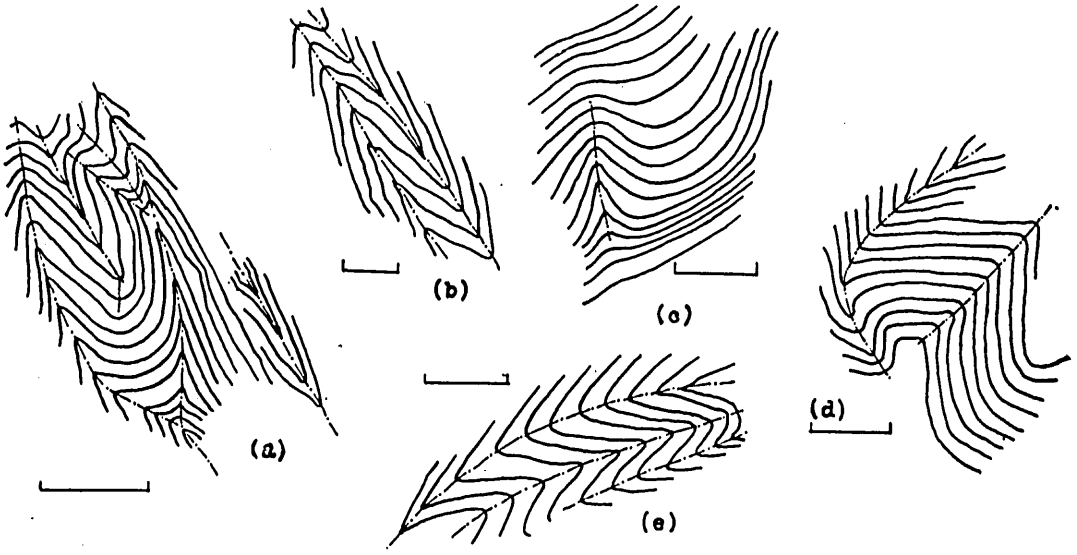

FIG. 6. Profiles of folds in banded chert. Scale: 50 cm.

Folds: S_1 is generally folded about gently or moderately plunging axes. These folds occur on every scale, throughout the zone of schistose hornfelses. Folds are most frequently found in the central part of the zone, which corresponds to the axial zone of the major anticline.

There are no significant differences in style of fold among various rock types, except basic rock, limestone, and calcareous pelitic rock, which show no definable fold on any scale. Folds on minor scale in banded chert and semi-pelite are characterized with the following features:—

1) All folds are "concentric" rather than "similar" in style (DE SITTER, 1956, p. 181–183). The symmetry of them varies from the monoclinic to the nearly orthorhombic. Folds showing nearly orthorhombic symmetry closely resemble those described from Moine by M.R.W. JOHNSON (1956), who has called them the "conjugate fold system". The fold shown in Fig. 6-d approximates to this style. Most of folds show monoclinic symmetry, and sometimes their limbs make very acute angles (20° or less) at the hinge.

Chert and pelite bands in banded chert or semi-pelite show fairly contrasted features in the style of fold. The thickness of chert bands is commonly unvarying regardless of position in the fold structure, unless the hinge makes a very acute angle. While, pelite bands become generally more or less thicker at the hinge of fold (Plate VIII). Such contrast in the style of fold between chert and pelite bands suggests that pelite bands behaved as highly plastic material between less plastic chert bands during the folding.

2) The attitude of axial surfaces of folds is highly variable as shown in Fig. 6. They are not always plane but often visibly curved, and sometimes, two or three axial surfaces of adjoining folds are joined (Fig. 6-a). On the other hand, Fig. 6-e shows another example that axial surfaces of adjoining folds are nearly parallel to each other. There are various intermediate types between these extreme attitudes of axial surfaces. Planar and curved axial surfaces occur side by side (Fig. 6-d). It is of interest that all axes of these folds are, at least in a small field, parallel to each other, regardless of attitude or orientation of the axial surfaces.

3) In some places where S_3 is well-developed, a cleavage fold or "similar fold" in the sense of DE SITTER can be found. Fig. 5, along with Plate XI-B, illustrates a typical cleavage fold found in the northern part of subarea C_3. Folds of this style are also observed here and there in other subareas.

β-axis: In recent years, "β-axis"* has been used often by some workers, such as F. KARL (1952), and L. E. WEISS (1954, 1957), as an important linear element to elucidate tectonic history of an area of complex structure.

After the method of B. SANDER, the writer has made many β-diagrams for S_1 from the area concerned. There are no essential differences between the patterns of β-diagrams prepared from pelite and those from banded chert and semi-pelite (later will be described). The maximum of β-diagrams prepared from one or two adjoining exposures coincides completely or nearly completely with the maximum of lineation diagrams of the same exposures.

Mesoscopic structures of banded gneisses and granites

Foliation: The banded structure due to the alternation of white band and black band, the foliation, is the sole planar structure. The foliation is in general clearly boservable in banded gneisses but is not so clear in migmatites.

Concerning the origin of the foliation in banded gneisses of the zone of transitional rocks, the following facts must be mentioned:—

1) In the field, S_1 of banded chert in the zone of schistose hornfelses is turned gradually into compositional banding (foliation) in siliceous banded gneiss at the southernmost part of the zone, just north of the thrust-fault above mentioned.

2) The boundary surface (bedding surface) between siliceous banded gneiss and micaceous banded gneiss is evidently parallel to the surface of compositional banding in either rock. Such parallelism between bedding and banding is still clearly retained, even where gneisses have been intensely folded.

Judging from the facts above mentioned, it is concluded that the foliation in banded gneisses of the transitional zone corresponds to S_1 in schistose hornfelses, and that it has not been derived from planar structures other than S_1.

In banded gneisses and migmatites in the zone of migmatites, the only visible planar

* See, B. SANDER, 1948, p. 132-146; L. E. WEISS, 1954, p. 12-15.

structure is also the compositional banding, the foliation. The foliation becomes sometimes obscured in the Ôbataké gneissose granite and granodiorite, and often in the Gamano gneissose granodiorite. It disappears almost completely in the Kibé and Namera granites.

The compositional banding found in banded gneisses and granites is probably remnant of S_1 in the original rocks, from which banded gneisses and granites have been derived.

Joints: Joints have been measured and plotted on an equalarea net, but data are too insufficient to discuss the structural geometry of joints. There seems to be present also *ac*-joints and oblique joints, the latter appearing more predominant than the former.

Lineation: Lineation is also an important mesoscopic structure in gneisses, but is not always distinct in migmatites. In the Gamano gneissose granodiorite and the Kibé and Namera granites, measurable lineation is lacking. The lineation in banded gneisses are characterized followingly:—

1) The lineation found in the zone of transitional rocks may belong to a single style: it is expressed by the axis of microfold of the foliation surface, most of which are accompanied by folds on larger scales. The orientation of the lineation in an exposure are nearly constant. Accordingly, the lineation in problem is of the same style as that in schistose hornfelses, i.e., $B(=b)$-lineation.

2) The lineation in banded gneisses of the zone of migmatites is also the axis of microfold, i.e., $B(=b)$-lineation. It is most significant, however, that the orientation of lineation in this zone commonly more or less varies even in an exposure. In some localities, there is another fold on moderate scale, the axes of which generally intersect the axis of microfold, the lineation, at angles 30°~60°, sometimes 90°. Folds of the latter style are predominant particularly in the central and southern part of this zone, and, as discussed later, the orientation of the lineation varies remarkably.

Evidences described above suggest that the lineation in banded gneisses also corresponds to $B(=b)$-lineation, which is just correlatable with the lineation in schistose hornfelses.

Folds: Folds on every scale in banded gneisses in the zone of transitional rocks always show simple styles, but those in the zone of migmatites have fairly complicated styles. Detailed examination of the mesoscopic geometry of folds in the zone of migmatites shows that these folds can be classified into two types which seem to suggest two distinct generations of structure.

The first type of folds (here termed *B*-folds) is most prominent throughout gneisses. Axes of the *B*-folds are usually parallel to the lineation. The style of *B*-folds is "concentric" in the sense of DE SITTER and monoclinic in symmetry. There can be found no cleavage-surfaces cutting the *B*-folds, axial surfaces of which are not always plane but often curved (Plate X-A). All mesoscopic features of the *B*-folds are just similar to those of folds on small scale in schistose hornfelses.

The second type of folds (here termed *F*-folds*) is characteristic in gneisses of the zone of migmatites, in particular in subarea H_2. The *F*-folds show in general relatively gentle waves on moderate scale, and axes of the *F*-folds are steeply inclined and their orientation is variable from one exposure to another. Sometimes the *F*-folds have a symmetry plane normal to the axis of fold, but commonly they have no definite symmetry plane. In places, where *F*-folds are prominent, axes of *B*-folds, along with the lineation, have various orientations, either easterly or westerly, with plunges of various angles (Plate X-B), and the general monoclinic symmetry of *B*-folds is turned often into triclinic symmetry.

These data show that the *B*-folds were bent about axes of the *F*-folds, and consequently, the *B*-folds have lost their monoclinic symmetry.

β-axis: β-diagrams for the foliation in gneisses have been prepared from several localities. The pattern of β-diagrams prepared from gneisses of the zone of transitional rocks strongly resembles that from schistose hornfelses: the β-maximum coincides completely with the *B*-maximum (statistical maximum of the lineation). While, on the β-diagrams prepared from gneisses of the zone of migmatites, there occur commonly two or more submaxima, which are usually tautozonal. The reason will be described and discussed later.

Macroscopic Structure

The writer has so far described features of various mesoscopic structure. In this chapter, the subjects what spatial relations these structures have and what structural-petrological meanings these spatial relations suggest, will be discussed.

The equalarea projection is used in preparing all diagrams. Symbols and modes of expression used in this paper are as follows:—

1) The direction of planar and linear structures is shown after the 360°-system: North is shown by zero, East by 90°, South by 180°, and so on.

2) The strike and dip of planar structures are shown as strike/dip: 116°/34°S.

3) *B*, β, and fabric axes: *a*, *b* and *c* are used after SANDER's definition.

Geometry of S_1

S_1, the foliation surface of schistose hornfelses and gneisses, was measured in the field only at places where folds on mesoscopic scale were not found or only weakly developed. Accordingly, most of the orientation of S_1 measured are to be related to the folds on macroscopic scale, but not to those on minor scale. Over 400 S_1 were measured from the Iwakuni-Yanai area and have been plotted and contoured in equalarea nets (Figs. 7, 8, and 9).

Zone of schistose hornfelses: In Fig. 8a are projected 231 πS_1, the pole of S_1, measured in this zone. πS_1 lies on a great circle (π-circle), in which two prominent maxima are

* As will be shown later, the *F*-folds have been formed later than the *B*-folds above described. When the *F*-folds were formed, the mechanical property of material is believed to have allowed plastic flow under the condition of high temperature and circulation of fluid, the condition of metasomatism or granitization. According to the condition of material, the folds are named the "*F*-folds".

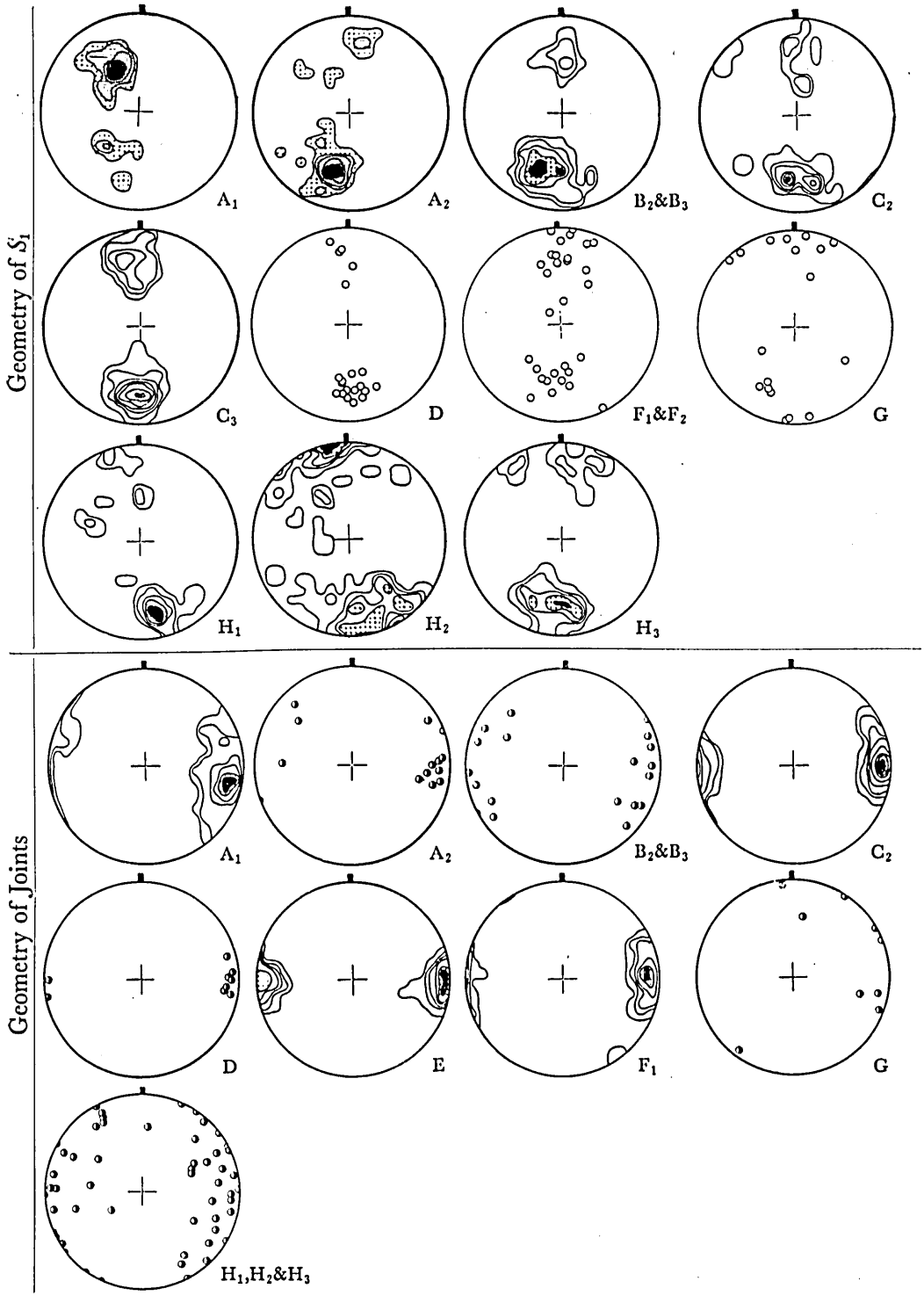
Geometry of S_1
A_1
A_2
B_2&B_3
C_2
C_3
D
F_1&F_2
G
H_1
H_2
H_3
Geometry of Joints
A_1
A_2
B_2&B_3
C_2
D
E
F_1
G
H_1,H_2&H_3

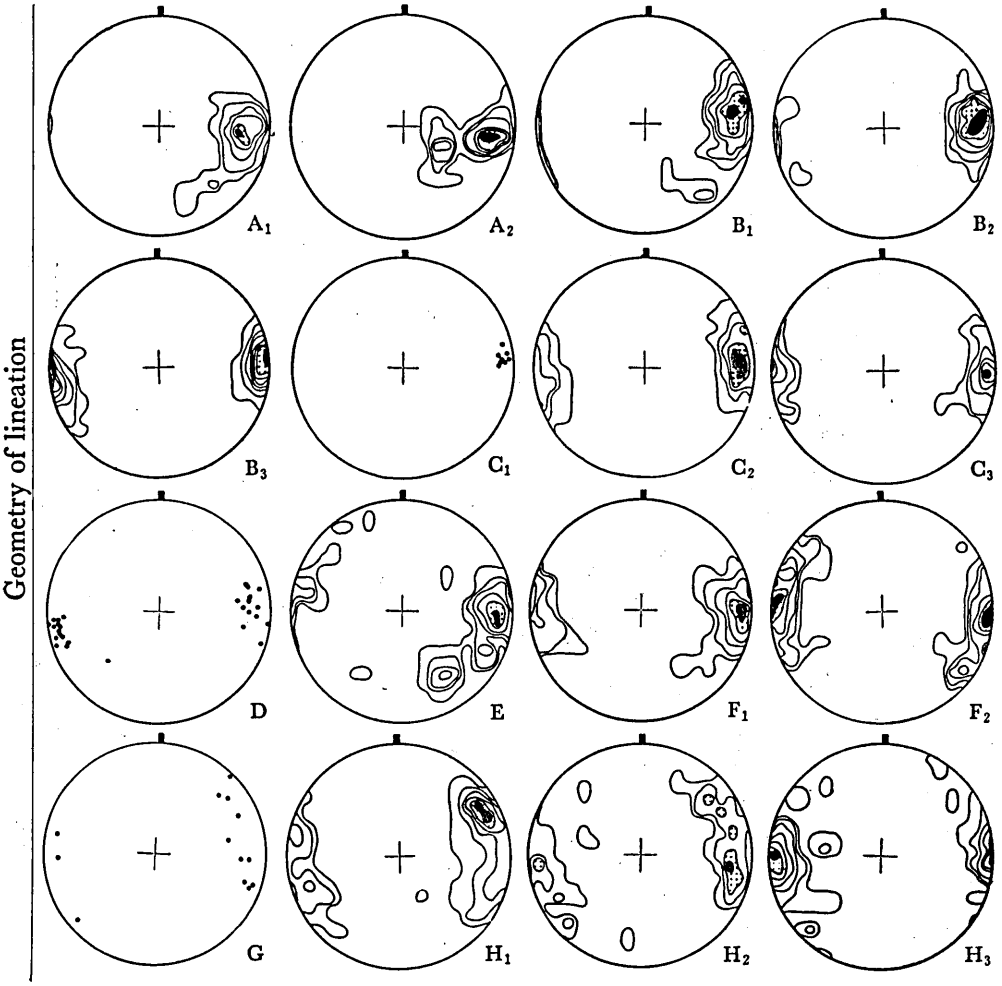

FIG. 7. Geometry of S_1, joints and lineation. The diagrams with marks A_1, A_2, B_1 and so on were prepared respectively from each subarea, A_1, A_2, B_1 and so on. The measurements and contours in each diagram are as follows:

Geometry of S_1 (S_1)···A_1, 34 πS_1; 25-13-7-4%. A_2, 31 πS_1; 32-25-16-10-6-3%. B_2 & B_3, 66πS_1; 15-12-8-4-1%. C_2, 34 πS_1; 26-22-16-10-6-3%. C_3, 33 πS_1; 18-15-12-9-6-3-1%. D, 20 πS_1; all measurements are marked. F_1 & F_2, 31 πS_1; all measurements are marked. G, 18 πS_1; all measurements are marked. H_1, 30πS_1; 25-18-12-7-3%. H_2, 73 πS_1; 10-7-4-3-1%. H_3, 51πS_1; 19-14-9-4-2%.

Geometry of joints (J)···A_1, 74 poles; 22-18-14-9-4-1%. A_2, 13 poles; all measurements are marked. B_2 & B_3, 18 poles; all measurements are marked. C_2, 74 poles; 30-25-20-15-11-7-3-1%. D, 9 poles; all measurements are marked. E, 41 poles; 25-18-13-8-5-2%. F_1, 38 poles; 29-21-15-9-5-3%. G, 9 poles; all measurements are marked. H_1, H_2 and H_3, 45 poles; all measurements are marked.

Geometry of lineation (L)···A_1, 70 axes; 24-20-16-12-7-3%. A_2, 39 axes; 26-19-14-9-5-3%. B_1, 65 axes; 20-17-12-8-4-1%. B_2, 72 axes; 23-18-13-8-5-2%. B_3, 83 axes; 25-23-19-16-12-8-5-2%. C_1, 8 axes; all measurements are marked. C_2, 102 axes; 16-12-8-5-2%. C_3, 75 axes; 20-15-11-8-5-2%. D, 27 axes; all measurements are marked. E, 54 axes; 17-14-10-7-4-2%. F_1, 80 axes; 19-15-11-8-4-1%. F_2, 68 axes; 14-11-8-5-3-1%. G, 13 axes; all measurements are marked. H_1, 52 axes; 18-14-11-7-4-2%. H_2, 40 axes; 10-8-5-2%. H_3, 63 axes; 20-17-14-10-6-4-2%.

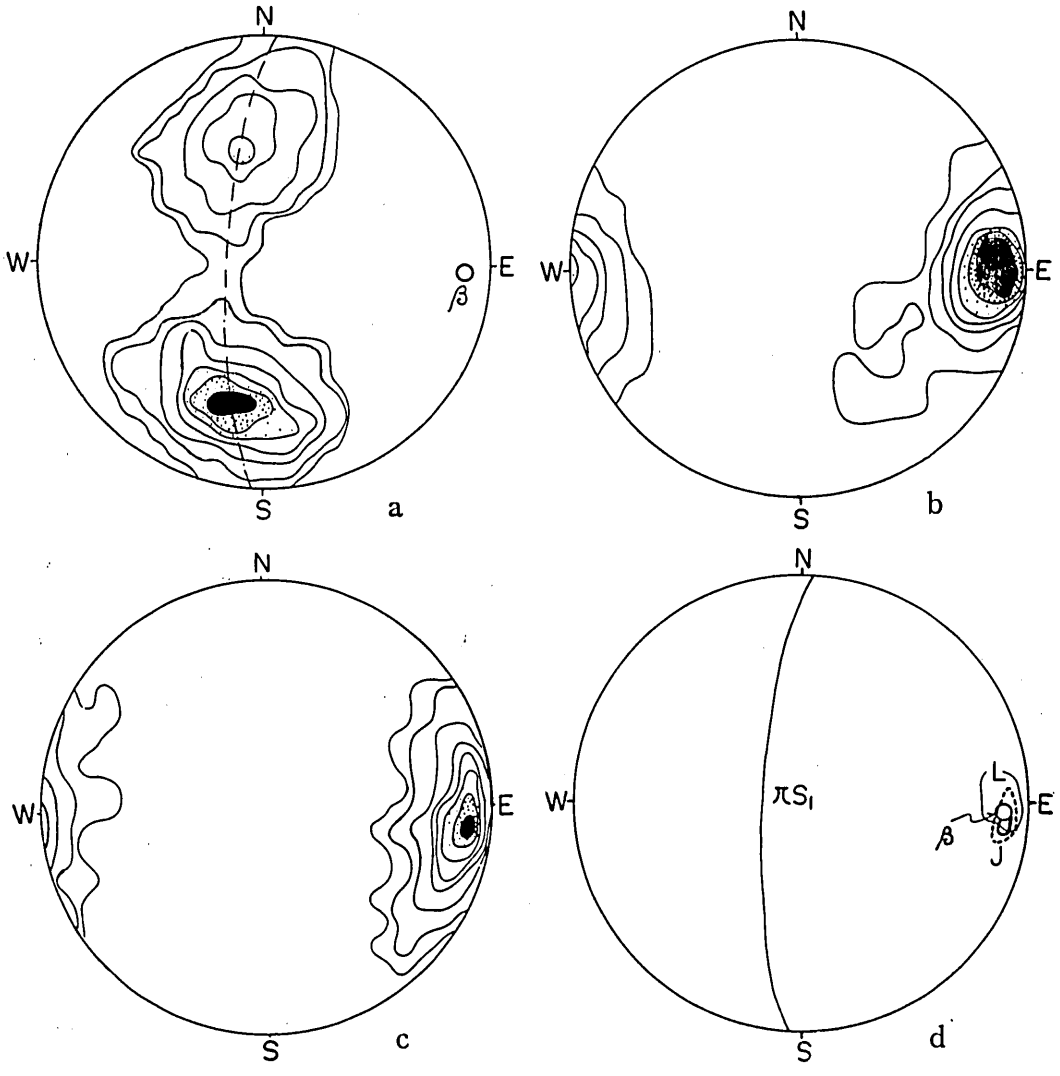

FIG. 8. Collective and synoptic diagrams for mesoscopic structures of schistose hornfelses. a, 231 πS_1 in schistose hornfelses; contours 11-9-7-5-3-2-1%. b, 531 axes of lineation in schistose hornfelses; contours 14-12-10-7-5-3-1%. c, 188 poles of joints in schistose hornfelses; contours 18-17-15-12-9-6-3-1%. d, Synoptic diagram for S_1, lineation and joints in schistose hornfelses.

found. The presence of the lowest concentration near the center of the diagram between the two prominent maxima suggests the relatively simple form of macroscopic folds, either anticlinal or synclinal, the limbs of which are nearly constant in orientation, making relatively angular hinges.

In order to examine in detail the pattern of orientation of S_1 expressed in Fig. 8-a, πS_1-diagrams were made for each subarea of this zone, the results being shown in Fig. 7. Each diagram in Fig. 7 generally shows two separate maxima, as found in Fig. 8-a. The

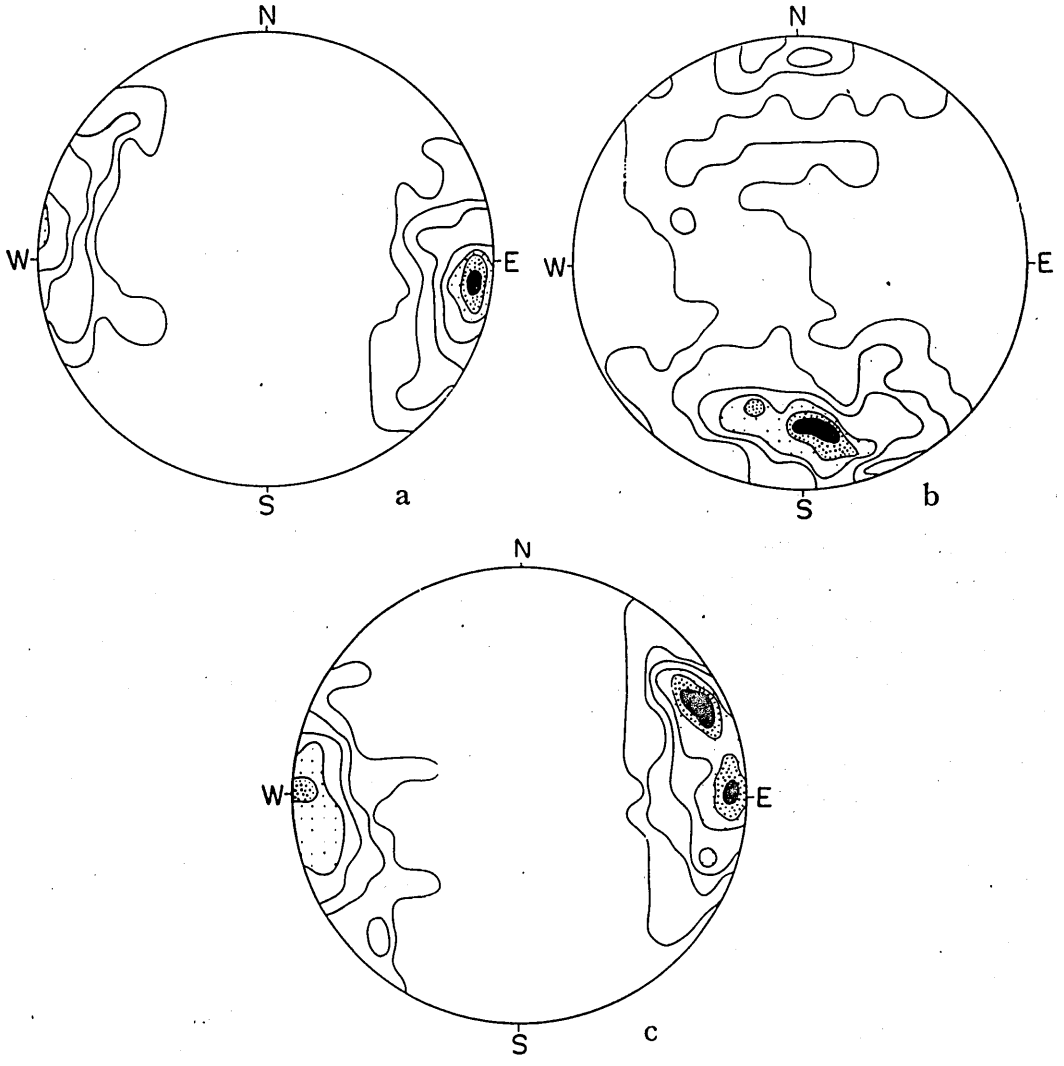

FIG. 9. Collective diagrams for mesoscopic structures in banded gneisses. a, 160 axes of lineation in banded gneisses of the zone of transitional rocks; contours 17-15-12-9-6-3-1%. b, 154 πS_1 in banded gneisses of the zone of migmatites; contours 9-8-6-4-2-1%. c, 155 axes of lineation in banded gneisses of the zone of migmatites; contours 10-8-6-4-2-1%.

presence of two separate maxima in each diagram suggests that one or more folds on macroscopic scale exist in each subarea. The resemblance in pattern of these diagrams indicates that the style of fold in each subarea has the similar characteristics as mentioned in the collective diagram, Fig. 8-a. Really in the field, the writer has been aware of the presence of folds on macroscopic scale with the wave-length of several hundred meters or less.

Zone of transitional rocks: The zone of transitional rocks was also divided into three subareas, E, F_1 and F_2 (Fig.3). Collective diagram for S_1 of this zone has not been completed, but πS_1-diagrams for subareas F_1 and F_2 are shown in Fig. 7. Data for S_1 collected from this zone are rather insufficietent, but the pattern of the diagrams fairly resembles that of the zone of schistose hornfelses.

Zone of migmatites: 154 S_1 in gneisses were measured from the zone and projected on an equalarea net, Fig. 9-b. The data measured from limbs of minor folds are excluded from the diagram; if any, they are very few.

Comparing the pattern of Fig. 9-b with Fig. 8-a, the former differs greatly from the latter in two points: (1) πS_1 does not lie on a great circle, but they are rather dispersed; (2) one prominent maximum occurs, and another maximum showing high concentration can not be found.

The zone in problem was also divided into three subareas, H_1, H_2 and H_3, in order to know in detail the macroscopic geometry of the structure. πS_1-diagrams for each subarea are shown in Fig. 7.

The principal maximum in the diagram for subarea H_1 is oriented in 75°/70°N., that for subarea H_2 is in 80°/90°, and that for subarea H_3 in 90°/55°N.. On the diagram for H_3, there is also another submaximum which is oriented in 110°/60°N.. It would seem,therefore, that there is continuous transition in strike of S_1 in gneisses from E.-W. in the western part (H_3) to ENE. in the north-eastern part (H_1) of the zone.* πS_1 is

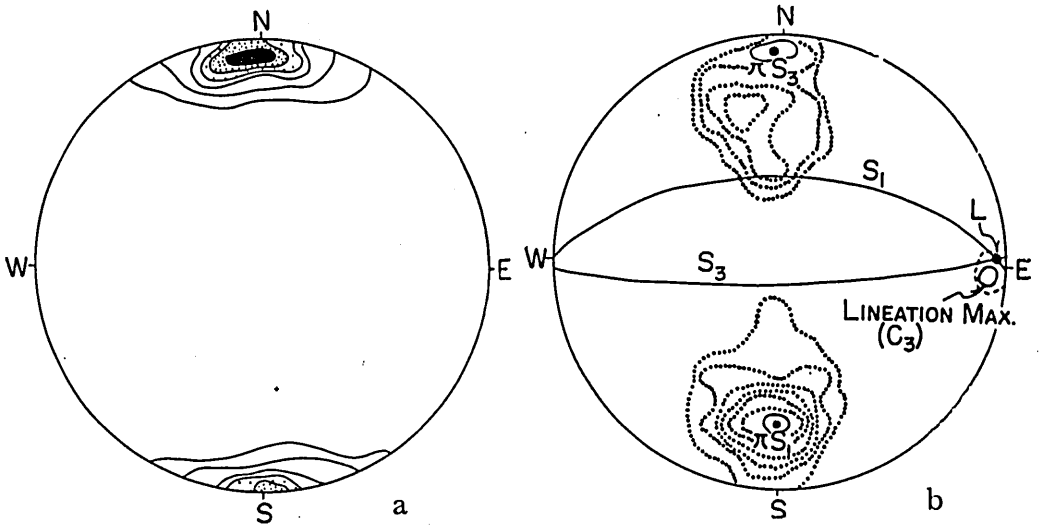

FIG. 10. Geometry of S_3. a, 103 πS_3 in the northern part of subarea C_3; contours 20-15-11-8-5-2%. b, Synoptic diagram for S_3, and S_1 and lineation in subarea C_3 (Figs. 10-a, and 7-C_3 (S_1 & L)). (see text).

* The general trend of the Ôbataké gneissose granodiorite draws a convex towards the south, and the eastern half of the mass runs actually in NE. (see, Plate XII). Thus, the general trend of the granodiorite is not strictly parallel to that of gneisses in subarea H_1 but sub-concordant or rather transverse to the latter.

highly dispersed in subarea H_2: the fact seems to be best explained by considering the remarkable development of the *F*-folds in subarea H_2.

The macroscopic geometry of subarea G (see, Fig. 3), data of which have been collected from islands of gneisses enclosed in the Gamano gneissose granodiorite, is remained unexplained, owing to the poorness of data.

Geometry of S_3

From the northern part of subarea C_3 were measured 103 surfaces of S_3, most of which were supplied from cuttings along the road running from Hashirano to Shimobata. The results of the measurements are shown in Fig. 10-a, in which only one principal maximum with concentric contours is found. The preferred orientation of S_3 is about E.-W. in trend and inclines steeply, nearly vertical, towards the south.

Fig. 10-b is a synoptic diagram for S_3, S_1 and the lineation.*

In Fig. 10-b, the maximum of S_3 lies on the great circle girdle of πS_1; that is, S_3 is tautozonal with S_1. This indicates that the formation of S_3 and the folding of S_1 may belong to one generation.

The general trend of S_1 and S_3 were drawn on the diagram, and the intersection of both was termed "L", which corresponds to the theoretical maximum point of the intersecting lineation $\widehat{S_1 S_3}$. In the foregoing section, the writer described that in schistose hornfelses lineations of various styles are mutually, strictly, parallel to each other; if it is so, the point L must fall within the maximum area of the lineation. In Fig. 10-b the point L is found within the submaximum area but not within the maximum area of the lineation. In actual cases, however, it is not unlike to regard that L coincides with the lineation maximum. The diagramatic result evidently elucidates that the intersecting lineation $\widehat{S_1 S_3}$ is also $B(=b)$-lineation.

Data for S_3 collected from the other localities in this zone have not been treated statistically, but, the similar macroscopic geometry of S_3 can be expected with high certainty.

Geometry of β

All β-diagrams for S_1 now concerned have been prepared from two or three adjoining exposures, and those based on the data over one subarea or of more larger scope have not been completed.

Zone of schistose hornfelses: As representative β-diagrams, the writer selected four diagrams which are shown in Figs. 11 and 12. Figs. 11-a, -b, -d, -e and Figs. 12-a, -b, are concerned with S_1 in banded chert, and Figs. 12-d and -e with S_1 in pelite.

Fig. 11-a shows the most common pattern of β-diagrams for S_1 in weakly folded banded chert. The 1 % great circle girdle is complete, but the pattern of the β-diagram

* The data for S_1 and the lineation in Fig. 10-b were prepared from diagrams for subarea C_3 in Fig. 7; accordingly, these data have not been necessarily collected from the same exposures where the data for S_3 were prepared. The writer believes, however, that there is no need to fear discrepancy in the source of these data, because, as will become evident in the later section, the structure in the zone of schistose hornfelses is geometrically very homogeneous over one or more subareas.

is rather concentric with one prominent maximum. Fig. 11-b is a lineation diagram prepared from the same exposure. In the synoptic diagram, Fig. 11-c, the β-maximum in Fig. 11-a coincides completely with the lineation maximum in Fig. 11-b.

In the adjacent of Sugaki (subarea C_3), the horizontal or westerly plunging lineation is most common, though the general plunge of the lineation in schistose hornfelses is in E.. In order to examine the geometrical relation between minor folds and the westerly plunging lineation, Figs. 11-d, -e and -f were prepared from folded banded chert near Sugaki. The pattern of the β-diagram is concentric (Fig. 11-d), and the maximum can be completely superposed on the lineation maximum (Fig. 11-f).

In and near the crest of the major anticline, the lineation and axes of minor folds

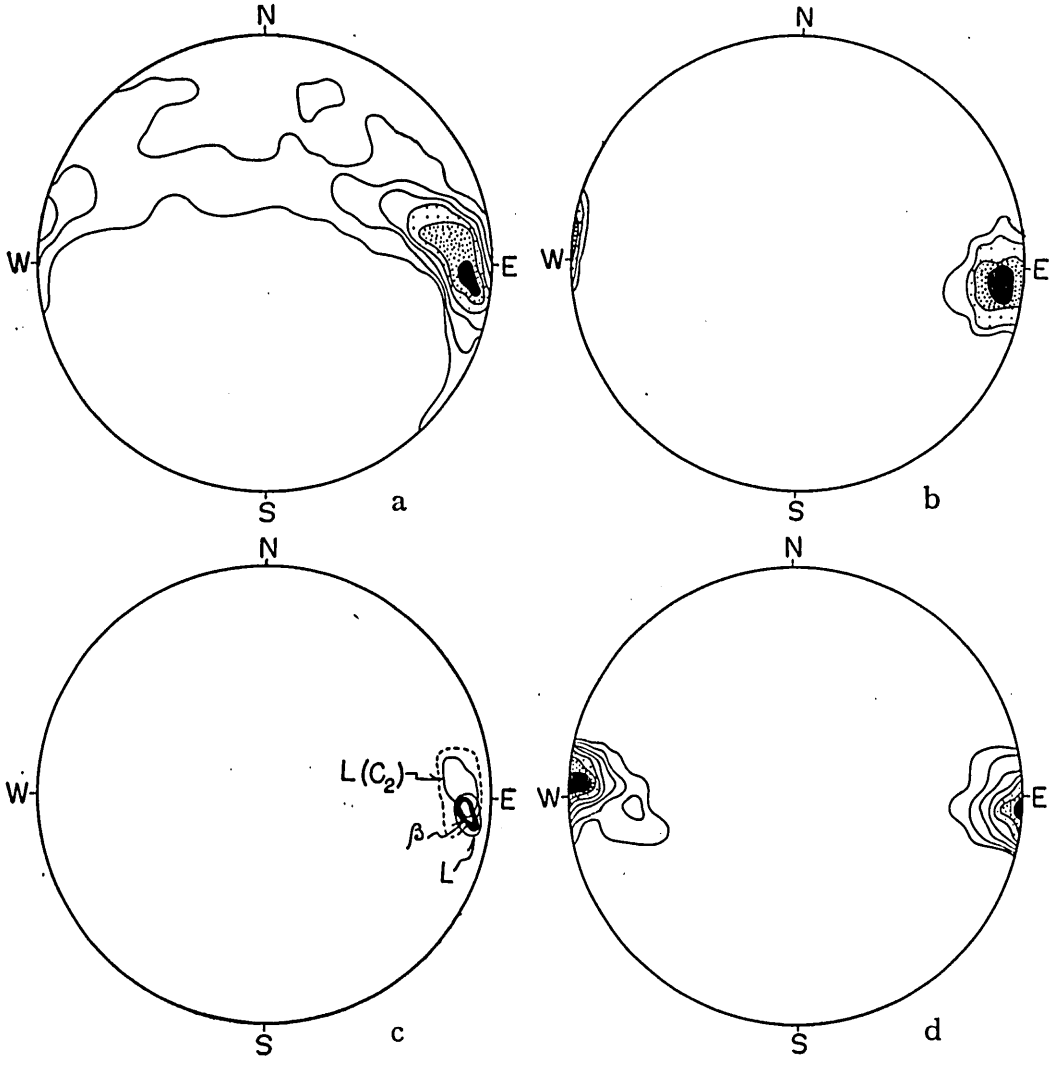

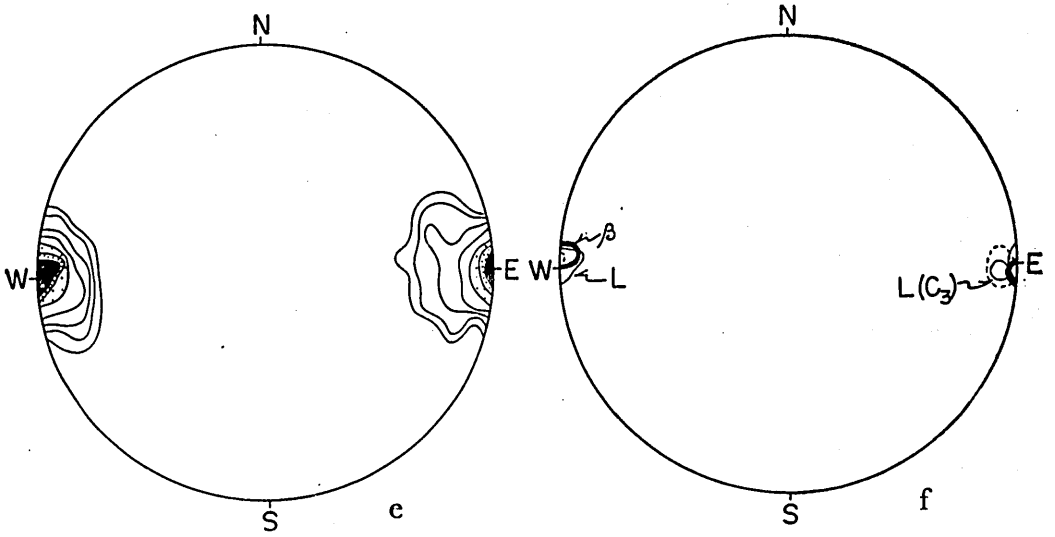

FIG. 11. Geometry of β: Schistose hornfelses (1). a, 564 β-axes for S_1 in banded chert, Tôgô (subarea C_2); contours 12-9-7-5-3-1%. b, 101 axes of lineation, in the neighbourhood of Tôgô; contours 40-30-15-5%. c, Synoptic diagram for lineation and β (Figs. 11-a, b and 7-C_2 (L)). d, 175 β-axes for S_1 in banded chert, Sugaki (subarea C_3); contours 50-40-30-15-8-4-1%. e, 98 axes of lineation, in the neighbourhood of Sugaki; contours 40-30-20-10-5-2-1%. f, Synoptic diagram for lineation and β (Figs. 11-d, e and 7-C_3 (L)). (see text).

plunge towards the east at relatively higher angles, 25°~40°. The results of measurements in two adjoining exposures are shown in Figs. 12-a, -b and -c. The pattern of β-diagram, Fig. 12-a, is concentric, and πS_1 is distributed on a great circle (Fig. 12-b). In the synoptic diagram, Fig. 12-c, the β-maximum is also superposed on the lineation maximum.

Figs. 12-d, -e and -f illustrate the type diagrams which are representative of those for pelite and semi-pelite. In Fig. 12-d, there are two prominent maxima within a complete great circle girdle. Reading Fig. 12-f, one can find that one of the β-maxima, trending in E. and plunging at lower angle, corresponds to the pole of πS_1 and coincides completely with the lineation maximum in Fig. 12-e. However, neither of two β-maxima in Fig. 12-d can be regarded as independent maximum, because the two maxima are completely included in the area of the second high concentration. The appearance of the two β-maxima seems to be only apparent in geometrical analysis.

Summarizing the results of the macroscopic geometry described above, it is probably concluded that folds on every scale in banded chert and pelite belong to a single style, "concentric", or one generation, and that in small field the β-maximum of S_1 coincides completely with the lineation maximum, regardless of the plunge angle of lineation and of the rock type, i.e., $\beta=B$.

Zone of transitional rocks: β-diagrams for S_1 (foliation surfaces in banded gneisses) prepared from this zone are very few, owing to poorness of good exposures.

An example from subarea F_1 is shown in Figs. 13-a, -b and -c. In Fig. 13-a, most of β-axes are concentrated in the principal maximum area, but gareat circle girdle is also traceable. Examining Fig. 13-c, synoptic diagrm for Figs. 13-a and -b, the β-maximum coincides almost completely with the lineation maximum; i.e., in subarea F_1, β corresponds also to $B(=b)$.

In each subarea of this zone, the similar geometrical relation of β to the lineation can be reasonably expected from the mesoscopic geometry of rocks. Folds on every scale found in this zone are most commonly the B-folds, axes of which are parallel to the lineation.

Zone of migmatites: Five β-diagrams for S_1 are illustrated as representatives, all of

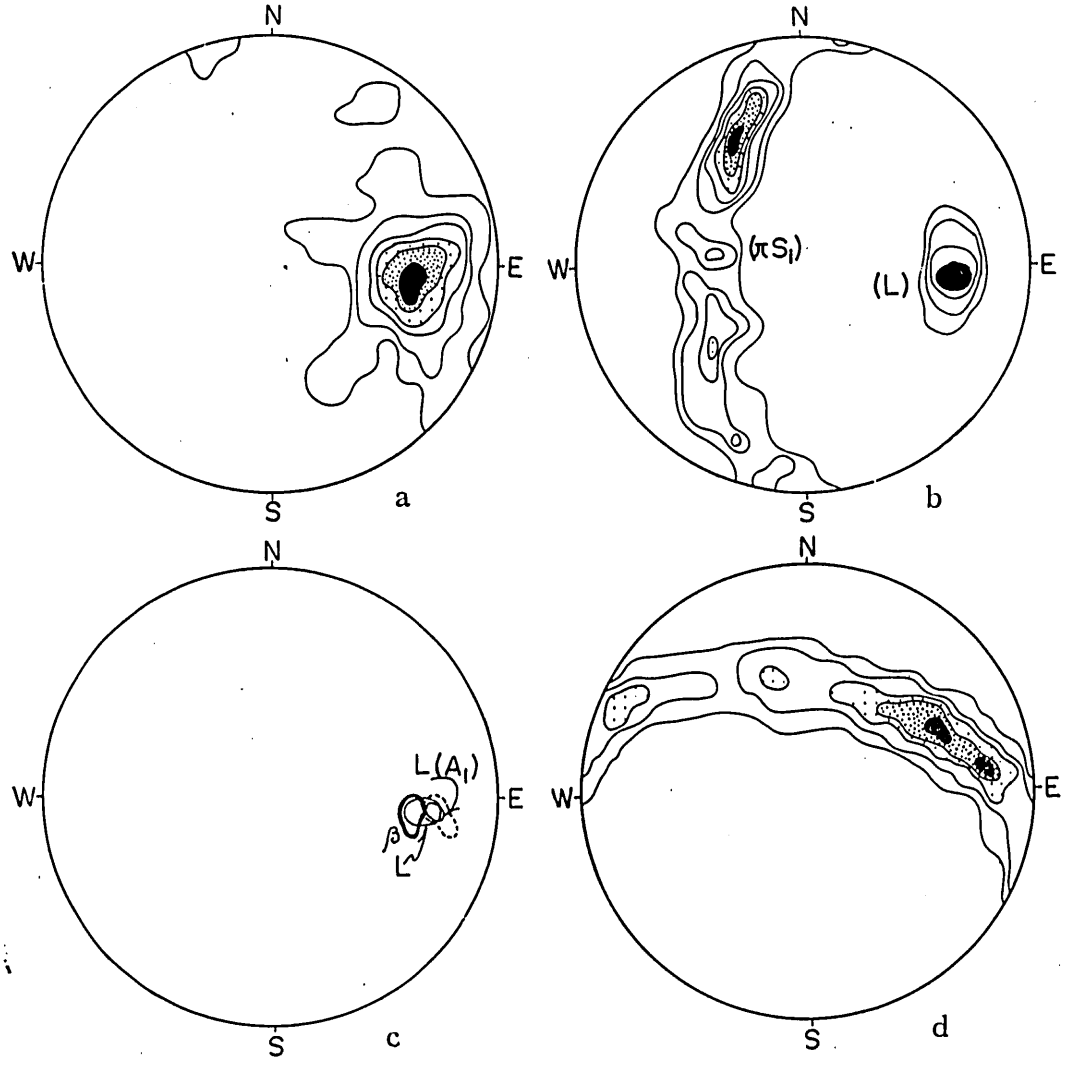

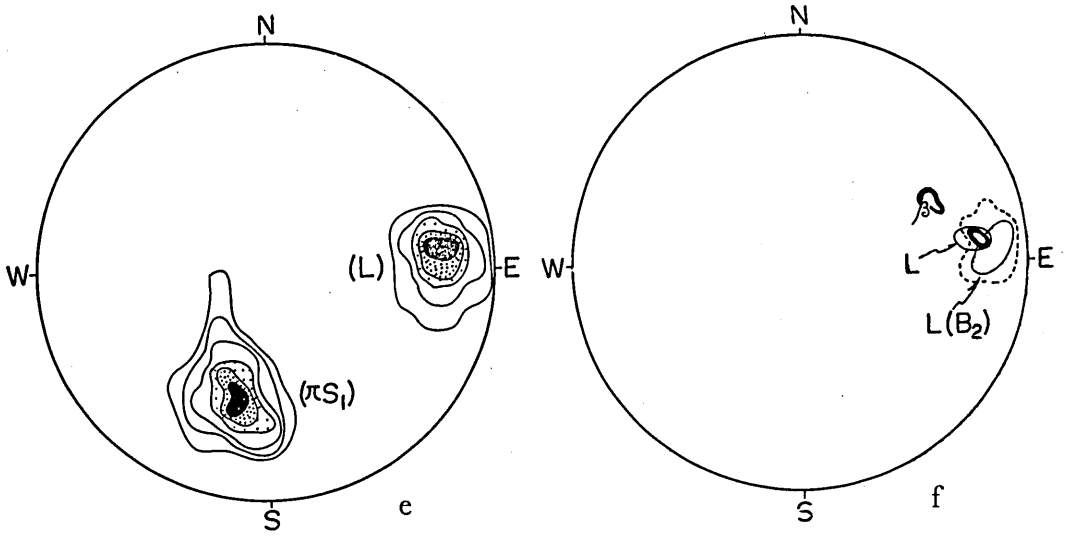

FIG. 12. Geometry of β: Schistose hornfelses (2). a, 561 β-axes for S_1 in banded chert, Kôbata (subarea A_1); contours 17-12-10-6-3-1%. b, 42 πS_1 and 30 axes of lineation in banded chert, Kôbata; contours 14-12-10-7-5-2% and 60-50-35-17%, respectively. c, Synoptic diagram for lineation and β (Figs. 12-a, b and 7-A_1 (L)). d, 219 β-axes for S_1 in pelite, just behind of the Shigino Primary School, Rokuroshi (subarea B_2); contours 8-6-4-2-1%. e, 34 πS_1 and 89 axes of lineation in pelite and semi-pelite, in the neighbourhood of Rokuroshi; contours 30-25-20-14-7-3% and 35-30-20-11-5%, respectively. f, Synoptic diagram for lineation and β (Figs. 12-d, e and 7-B_2 (L)). (see text).

which were prepared from siliceous banded gneiss. One β-diagram was prepared from subarea H_1, one from subarea H_3, and the remainders from subarea H_2.

In subarea H_1, B-folds are prominent, and the lineation is often observable. The results of measurements at three adjoining exposures are shown in Figs. 14-a and -b. A complete great circle girdle with one maximum characterizes the β-diagram, Fig. 14-a. In Fig. 14-b are plotted 16 lineations measured at the same exposures. Comparing Fig. 14-a with Fig. 14-b, the β-maximum falls within the distribution area of the lineation: the most common style of folds in subarea H_1 seems to be the B-folds; i.e., $\beta=B$, and the lineation is also the $B(=b)$-lineation.

Figs. 14-c and -d are concerned with subarea H_3. Siliceous banded gneiss at or near the exposure, from which the data were collected, is folded on moderate scale, but traces of the lineation are nearly completely obscured. The β-diagram, Fig. 14-c, is characterized by a great circle girdle with one maximum and another submaxima. 8-axes of folds were measured and plotted in Fig. 14-d. These axes of folds swarm about the β-maximum; however, it is difficult to examine the geometrical relation of β-axes to the lineation. Examining Fig. 14-e, the maximum in Fig. 14-a occurs closely near that in Fig. 14-c, but both β-maxima plunge at higher angles than the general plunge of the lineation in the zone of migmatites.

The F-folds are developed mainly in subarea H_2. The measurable lineation is mostly lacking in the subarea. Figs. 15-a and -b were based on measurements at separate

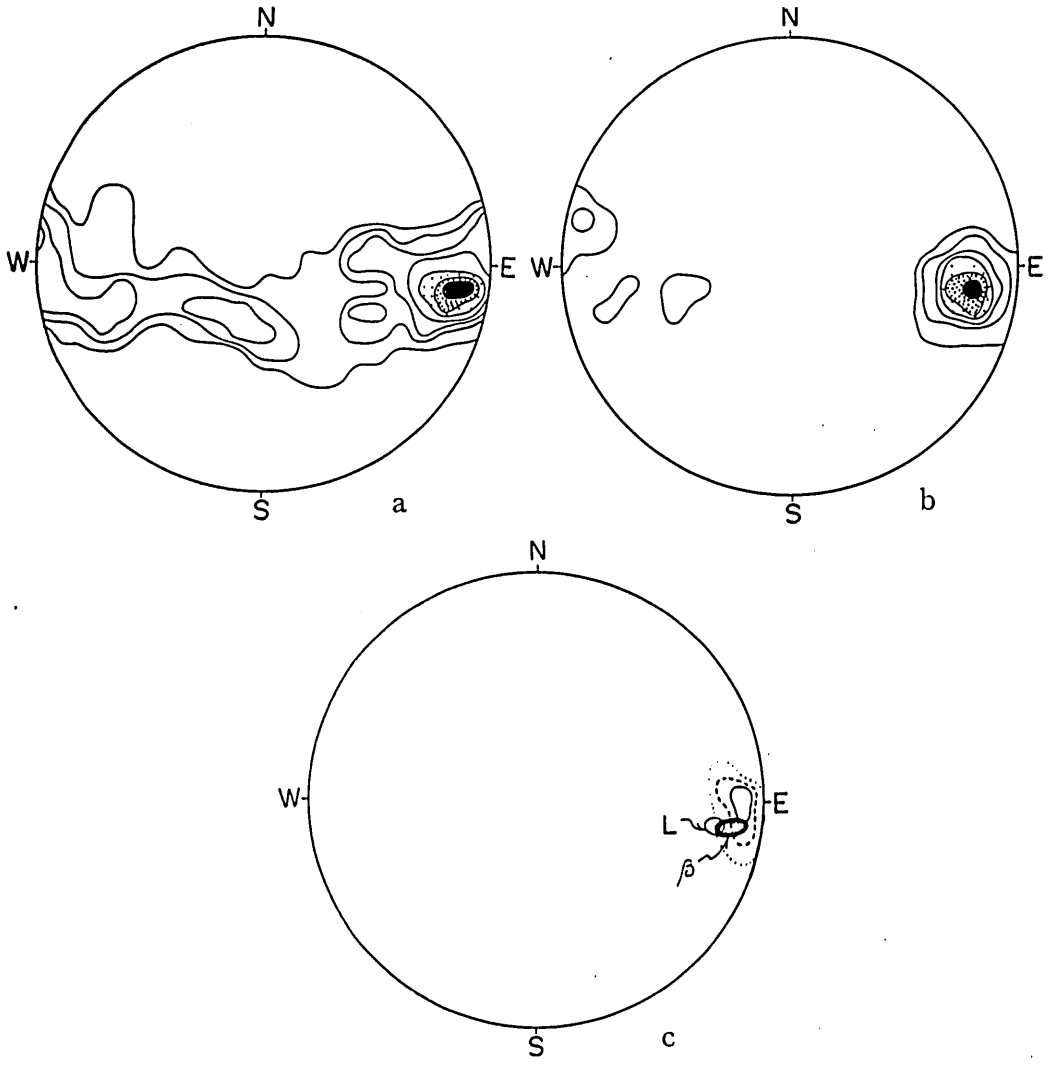

FIG. 13. Geometry of β: Banded gneisses of the zone of transitional rocks. a, 210 πS_1 in siliceous banded gneiss, Terasako (subarea F_1); contours 20-17-13-9-5-3-1%. b, 34 axes of lineation in siliceous banded gneiss, Terasako; contours 30-25-20-15-10-5%. c, Synoptic diagram for lineation and β (Figs. 13-a, b and 7-F_1 (L)). (see text).

exposures, where no folds with measurable axes were found. The β-diagrams are characterized by the presence of single great circle girdle, in which one prominent maximum is found; while, the orientation of each β-maximum differs remarkably in azimuth from each other (azimuth: 250°, plunge: 75° WSW. in Fig. 15-a; azimuth: 78°, plunge: 74° E. in Fig. 15-b).

The last β-diagram, Fig. 15-c, was prepared from a narrow exposure near Kanon-no-taki, where folds of two styles, B-folds and F-folds, are clearly observed, and the

lineation, along with axes of the *B*-folds, is gently folded about axes of the *F*-folds (Plate X-B). A complete great circle girdle with three or more submaxima characterizes Fig. 15-c. In Fig. 15-d, prepared from the same exposure at Fig. 15-c, the lineation and axes of the *B*-folds are plotted together with axes of the *F*-folds. Poles of the lineation are scattered but distributed near the periphery of the diagram. When Fig. 15-c is superposed on Fig. 15-d, the β-maximum and the peripheral submaxima in Fig. 15-c fall in the distribution area of the lineation, while, the central submaximum falls in that of the *F*-folds.

Judging from the synoptic diagram, Fig. 15-e, it becomes evident that in subarea H_2 the β-maxima do not always correspond to the lineation maximum but often to axes of the *F*-folds, and that the complex pattern of these β-diagrams seems to be due to superposition of folds of two generations, i.e., *B*-folds and *F*-folds.

Geometry of lineation

In the former sections, it has been proved geometrically that the lineation in the Iwakuni-Yanai area is without exception the $B(=b)$-lineation, to which axes of folds (*B*-folds) on every scale are strictly parallel. In this section, the degree of homogeneity of the lineation in each of the three zones will be treated statistically.

Zone of schistose hornfelses: Fig. 8-b is a collective diagram and Fig. 16-a is a synoptic diagram for the lineation in this zone as a whole. The maximum and submaximum areas in the collective diagram and 10 crosses which correspond to the lineation maximum in each diagram of Fig. 7 are traced in Fig. 16-a. 5 crosses completely fall into the maximum area, and 4 crosses near the maximum area. Thus, the orientation of the lineation is highly homogeneous through the zone of schistose hornfelses. 6-crosses (numbered) will, however, require some special explanations, that follows:—

1) Crosses 1 and 2 represent the maximum for subarea B_3 and C_3, respectively. The southern boundary of both subareas corresponds to axial zone of a subordinate anticline, which lies on the northern limb of the major anticline. The westerly plunging lineation is prominent in the southern half of subarea C_3, while easterly plunging lineation becomes conspicuous in the south-eastern part of subarea B_3.

Judging from the meso- and macroscopic geometry of folds, it appears reliable to assume that the lineation was initially nearly horizontal but subordinately, along with axis of the subordinate anticline, bent, suggesting axial flow normal to the tectonic transport. The axial flow was probably effective during the later phase of folding.

2) Crosses 3 and 4 represent the maximum for subarea A_1 and A_2, respectively. The boundary between these subareas corresponds also to the axial zone of the major anticline. In these subareas, the lineation generally plunges at relatively higher angles, 25°～40°, towards E. Such high angle lineation can probably be explained by the same assumption as explained in *1*).

3) Crosses 5 and 5' represent the maxima for subarea B_1. However, both the prominent (20%) maxima are completely enclosed in the 17% area. Accordingly, separa-

tion of the two maxima appears to be only a geometrical result.

Zone of transitional rocks: Fig. 16-b is a synoptic diagram for Figs. 7, 8-b and 9-a. Crosses designated as E, F_1 and F_2 show maximum points in each lineation diagram of Fig. 7, respectively.

Examining Fig. 16-b, all the maximum points thus plotted lie in or near the maximum area in the collective diagram, Fig. 9-a.* The preferred orientation of the linea-

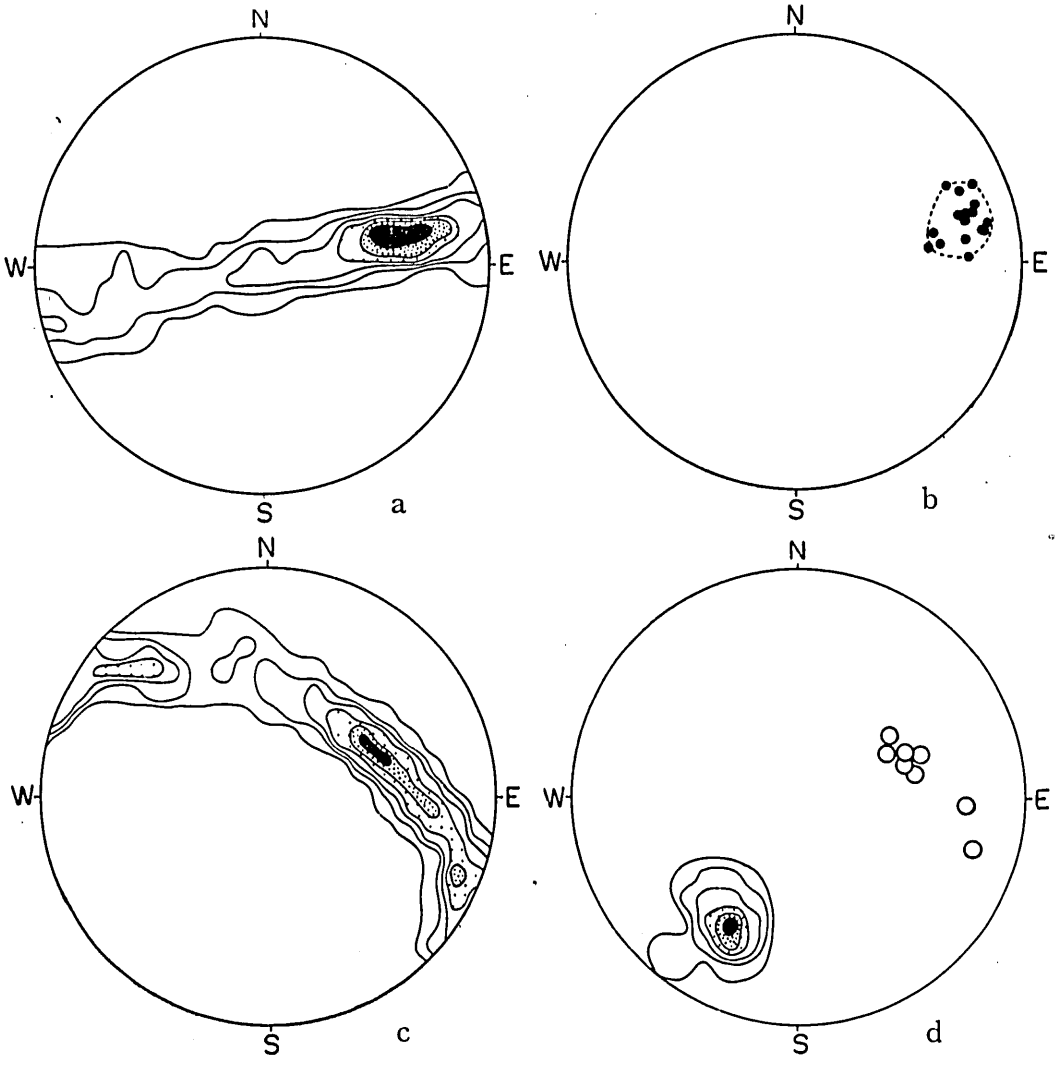

* On the lineation diagram for subarea E, Fig. 7, there are one maximum (17 %) and one submaximum (10%), both of which form separate concentration. The former trends 94° and plunges 15° in E., and the latter 146° and 30° SE., respectively. The abnormal position of the submaximum seems to be due to disordered lineation predominantly found near the thrust-fault (later described).

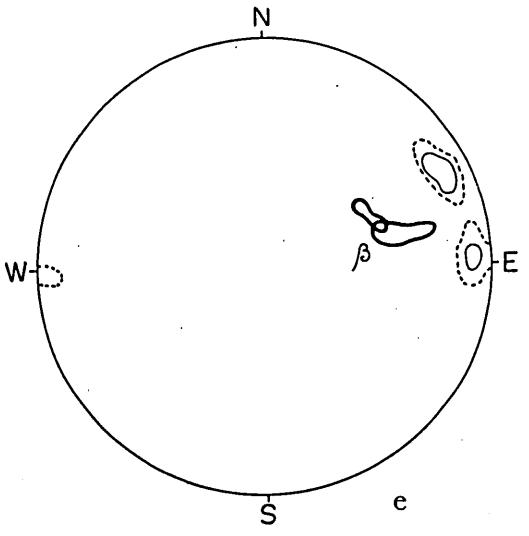

FIG. 14. Geometry of β: Banded gneisses of the zone of migmatites (1). a, 275 β-axes for S_1 in siliceous banded gneiss, Kirihata (subarea H_1); contours 17-14-10-6-3-1%. b, 16 axes of lineation in siliceous banded gneiss, Kirihata; all observations marked. c, 309 β-axes for S_1 of siliceous banded gneiss, Basara (subarea H_3); contours 11-10-7-5-3-2%. d, 30 πS_1 in siliceous banded gneiss (contoured) with 8-axes of folds on small scale (small circles), Basara; contours 53-43-33-22-10-3%. e, Synoptic diagram for lineation and β (Figs. 14-a, c and 9-c). (see text).

tion in this zone is likewise highly homogeneous, and is nearly parallel to that in the zone of schistose hornfelses.

Zone of migmatites: In this zone, in particular in subarea H_2, the lineation measurable is rather rare. The maximum areas in the collective diagram, Fig. 9-c, are traced in Fig. 16-c together with the maximum and submaximum points in each lineation diagram for separate subareas, Fig. 7. In the synoptic diagram, Fig. 16-c, the lineation maximum in H_1 trends 64° and plunges 17° towards NE., and that in H_3 270° and 6° towards W., respectively; however, in subarea H_2 there occur one maximum (98° in azimuth and 20° E. in plunge) and five submaxima whose trends are very variable.

Envisaging Fig. 16-c, the following facts can be pointed out:—

1) Poles of the lineation in subarea H_1, and those in subarea H_3, are relatively highly concentrated on one maximum, respectively; while, those in subarea H_2 are dispersed and seem to form an incomplete small circle girdle.

2) The general trend of the lineation draws a gentle convex towards the south, though orientations of the lineation in subarea H_2 are outstandingly disturbed.

3) In subarea H_1, the lineation most commonly plunges towards E.; while, in subarea H_3, it plunges towards W.: a gentle dome structure can be inferred. A kind of "swelling" might have occurred in regional scale.

Judging from the facts described above, it can safely be said that such characteristic

structures as found in the zone of migmatites, i.e., the convex trend of the lineation, a gentle dome structure, and the remarkable disturbance in orientation of the lineation in subarea H_2, partly in subareas H_1 and H_3, would be completed during the later deformation than the phase of folding of *B*-folds i.e., in the phase of *F*-folding.

Geometry of Joints

Data of joints collected from the zone of migmatites are too insufficient to examine statistically, but those collected from the zone of schistose hornfelses and the zone of transitional rocks may be appreciable.

68 poles of joints and 43 axes of the lineation, which were measured in folded

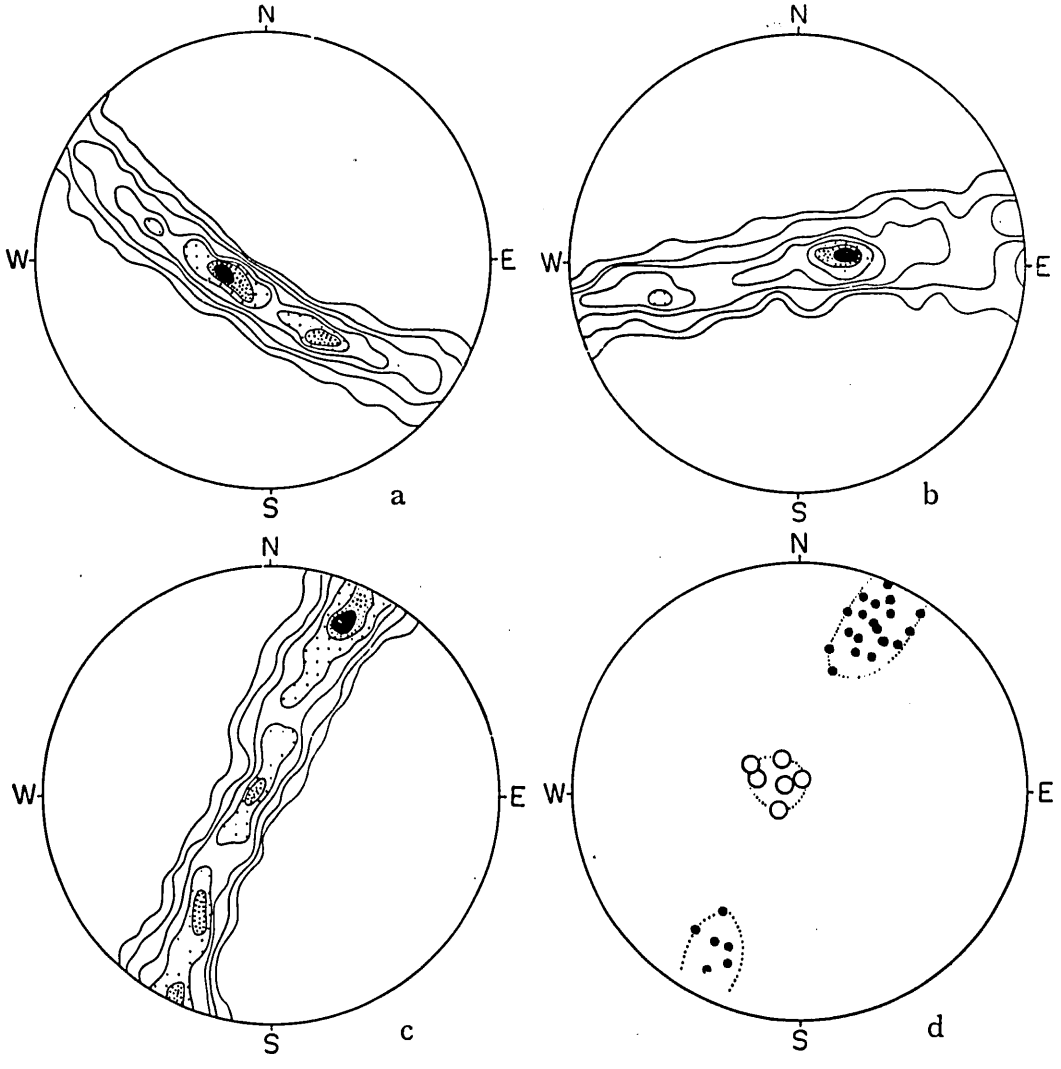

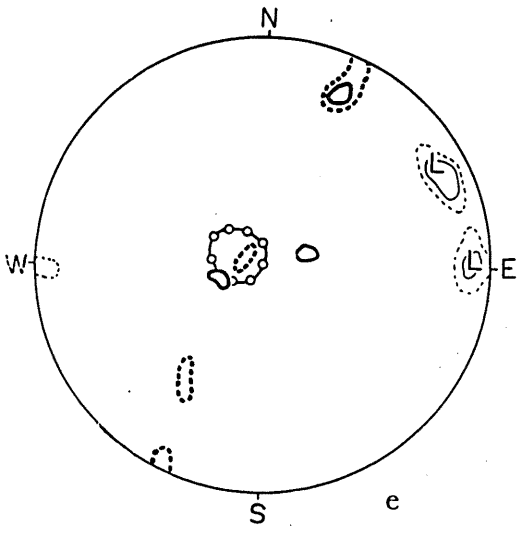

FIG. 15. Geometry of β: Banded gneisses of the zone of migmatites (2). a, 381 β-axes for S_1 in siliceous banded gneiss, Kotoishi-yama (subarea H_2); contours 12-11-9-7-5-3-1%. b, 370 β-axes for S_1 in siliceous banded gneiss, Ôkubo (subarea H_2); contours 12-11-9-7-5-3-1%. c, 480 β-axes for S_1 in siliceous banded gneiss, Kanon-no-taki (subarea H_2); contours 10-8-6-4-3-1%. d, Axes of lineation and *B*-folds (points), and axes of *F*-folds (small circle). e, Synoptic diagram for Figs. 15-a, b, c, d and 9-c. (see text).

banded chert at exposures near Kôbata (subarea A_2), are plotted in Figs. 18-a and 17-a, respectively. On the other hand, 57 poles of joints and 129 axes of the lineation, which were recorded from pelite within an small area in Rokuroshi (subarea B_2), are plotted in Figs. 17-b and -c, respectively. These examples illustrated above show that in banded chert as well as in pelite the joint maximum is nearly or completely superposed on the lineation maximum, and that the majority of joints is, at least within these small areas, probably referred to the "*ac*-joint" (E. CLOOS, 1937) which occurs almost strictly perpendicular to the lineation. In the synoptic diagram, Fig. 8-d, the three maxima are completely superposed on each other. This indicates that the majority of joints are normal to the lineation not only in small area but in the zone of schistose hornfelses as a whole.

Fig. 17-d is a synoptic diagram for joints, in which the concentration contours in Fig. 8-c (collective diagrm for joints found in schistose hornfelses) are drawn. Crosses designated as A_1, C_2, E and F_1 correspond to the maximum positions in each joint diagram for subarea A_1, C_2, E and F_1, respectively. All the maximum points fall in or near the maximum area in the collective diagram, though the maximum points E and F_1 are prepared from gneisses. The facts strongly suggest that the orientation of *ac*-joints is highly homogeneous through the two zones.

The regional trend of *ac*-joints would facilitate the development of consistent large N.-S. faults which are produced far later than the Ryôké phase but are hardly regarded to be younger than the intrusion phase of the Cretaceous intrusives. The Cretaceous acid dykes also have a consistent orientation that can be seen in Plate XII: the

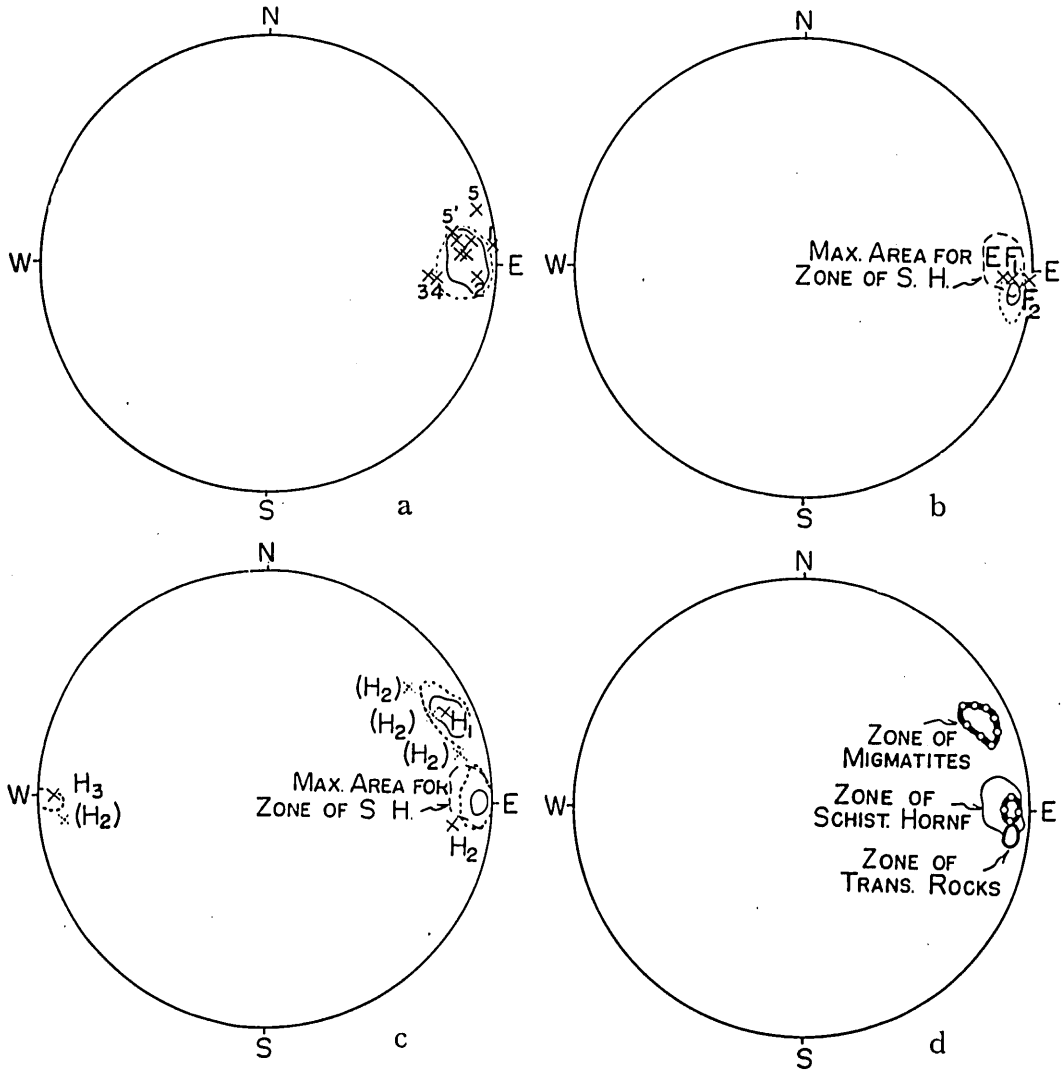

FIG. 16. a, Synoptic diagram for lineation in the zone of schistose hornfelses. b, Synoptic diagram for lineation in the zone of transitional rocks. c, Synoptic diagram for lineation in the zone of migmatites. d, Synoptic diagram for lineation over the three zones.

well-developed *ac*-joints would be a controlling factor for their intrusion.

In exposures near the crest of the major anticline, another system of joints is locally found. Fig. 18-a is, as already described, prepared from the northern limb, Fig. 18-b from the crest, and Fig. 18-c from the southern limb of the major anticline. A river-side from which data for Fig. 18-d were collected corresponds nearly to the axial zone of the major anticline but is lower about 100 m in altitude than the exposure from which Fig. 18-b was prepared.

Comparing these four joint-diagrams with each other, one may find that three are

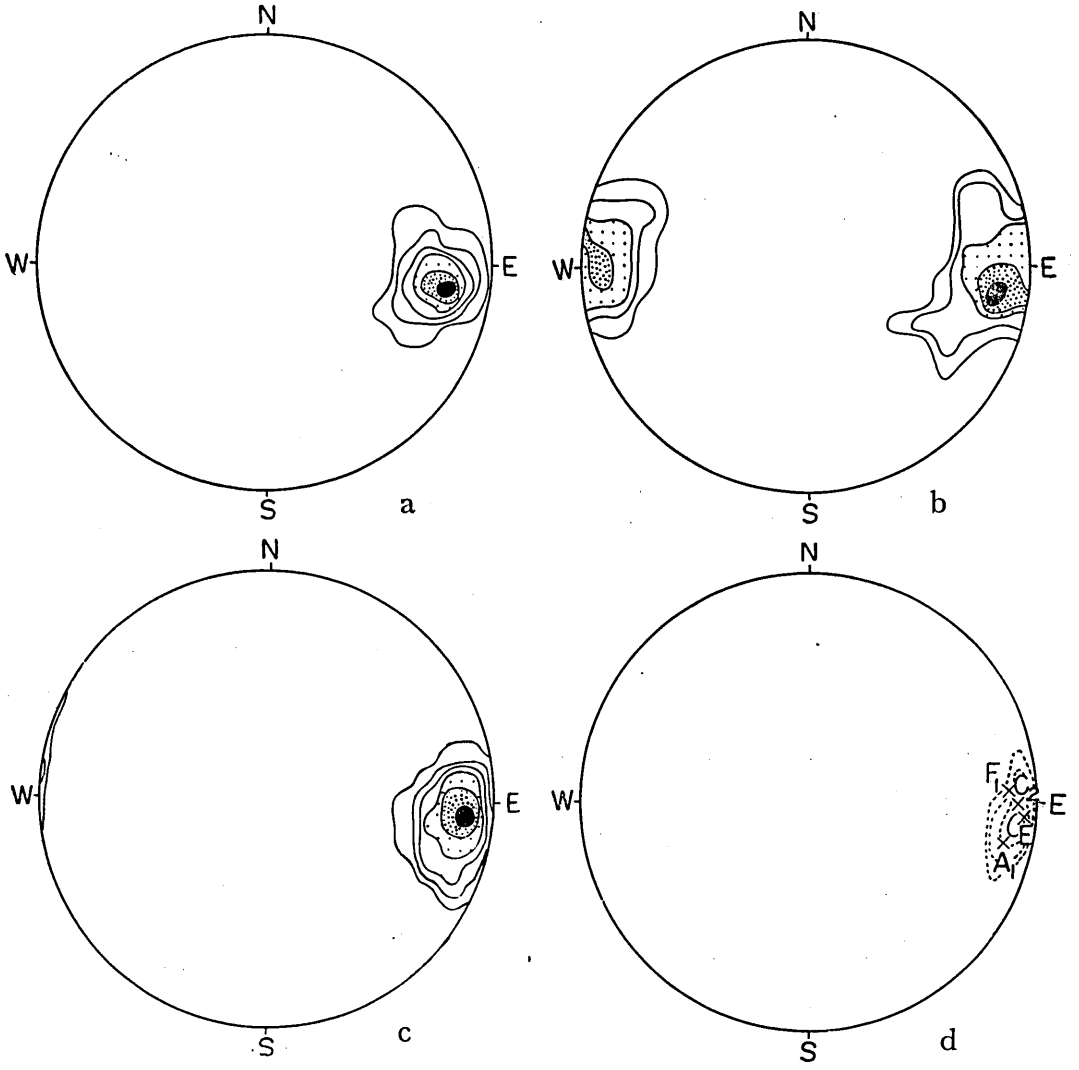

FIG. 17. Geometry of joints (1). a, 43 axes of lineation in banded chert on the northern limb of the major anticline (subarea A_2); contours 70-50-30-15-10-5%. b, 57 poles of joints in pelite in the neighbourhood of Rokuroshi (subarea B_2); contours 15-11-8-4-2%. c, 129 axes of lineation in schistose hornfelses in the neighbourhood of Rokuroshi; contours 22-19-16-11-6-3%. d, Synoptic diagram of Figs.7 and 8-c. (see text).

rather similar in pattern and in position of maximum and show various characteristics of *ac*-joints. While, Fig. 18-b shows a highly different pattern. In Fig. 18-b, there occur two separate maxima within nearly complete peripheral girdle (maximum, 144°/65° SW.; submaximum, 44°/85° NW.). The new joints in and near the crest of the major anticline can be referred to the oblique (*hk0*)-joints of E. CLOOS (1937) and others. These are not always found in pairs. Of most significant is that the occurrence of oblique joints is restricted only at the crest of the major anticline.

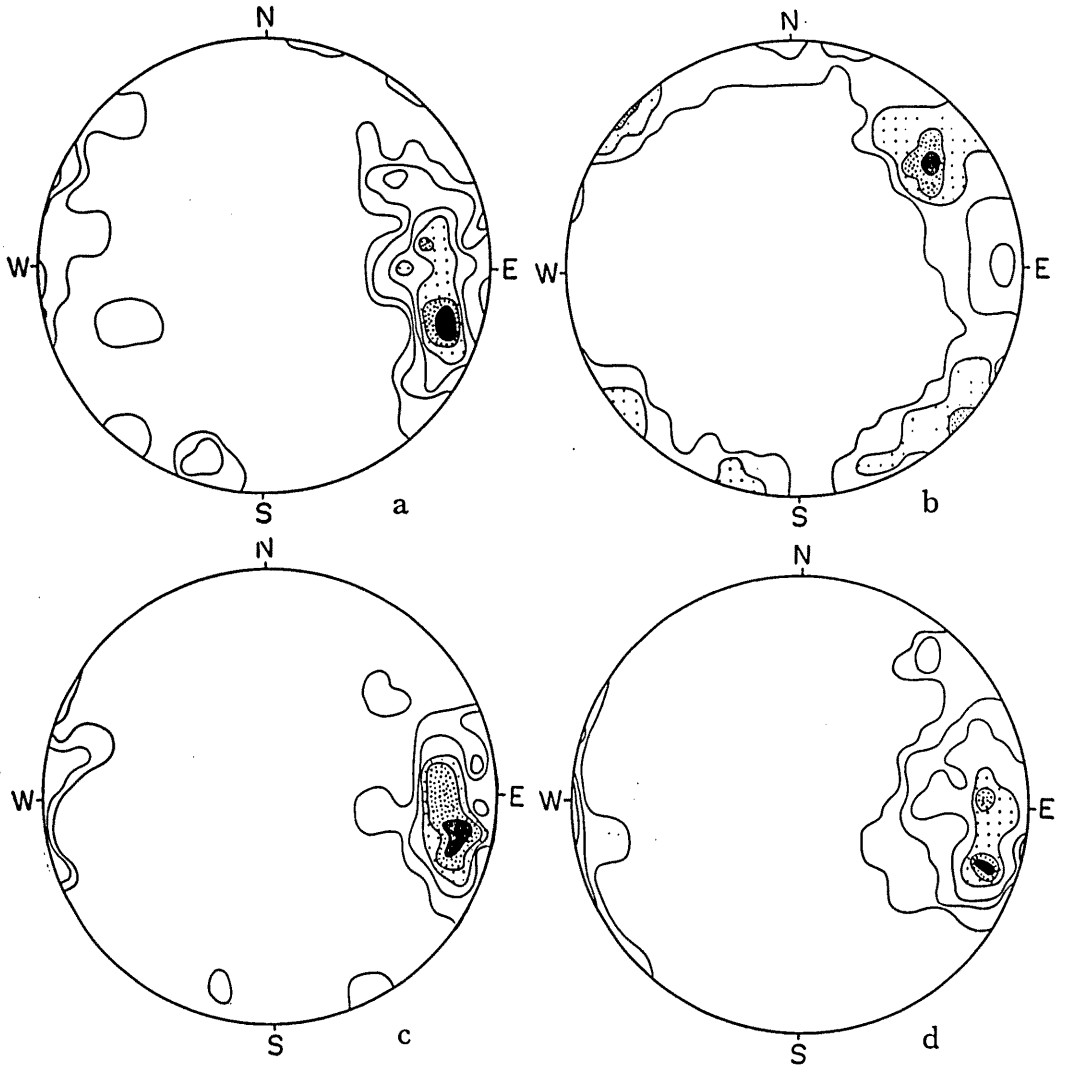

FIG. 18. Geometry of joints (2). a, 68 poles of joints in banded chert on the northern limb of the major anticline (A_2); contours 17–13–9–6–4–1%. b, 70 poles of joints in banded chert in the axial zone of the major anticline (higher horizon); contours 14–10–5–3%. c, 41 poles of joints in banded chert on the southern limb of the major anticline (A_1); contours 22–15–10–6–2%. d, 68 poles of joints in banded chert in the axial zone of the major anticline (lower horizon); contours 16–13–10–7–4–1%.

Geometry of thrust-fault

The thrust-fault is clearly observed at three exposures: (1) an exposure about 1500m east of Besshobata (near the entrance of the So-o Wireless Relay Station), (2) a riverbed about 300 m west of Hata and (3) a roadside about 300 m north of Honro-o. The sudden change in trend of S_1 within 5 m or less, and the abrupt appearance or disap-

pearance of different rock types near the strongly sheared zone, are expressions of the thrust-fault. Southerly plunging lineations, which are represented by crinkling axes and striae, are well developed in and near the thrust-fault. Slip surfaces, here termed S', are in most cases nearly or strictly parallel to S_1 in rocks. S' occurs every 2 cm or less in space, but the spacing becomes sometimes wider. No mineralization appears on S'.

Figs. 19-a, -b and -c are prepared from the exposure east of Besshobata, Figs. 19-d and -e are from that north of Honro-o, and Fig. 19-f is a synoptic diagram for Figs. 19-a ~-e.

In Fig. 9-a, all the linear elements are, together with 18 $\pi S'$, projected irrespective of their styles. The distinction of the lineation on the diagram can hardly be regarded as lying on single great circle but on two separate great circles, whose poles are shown as P_1 and P_2. The two great circles intersect at a low angle. P_1 is plotted near the distribution area of $\pi S'$, therefore it seems probable that southerly plunging lineations lie commonly on S' but that easterly plunging lineations do not lie on S'. While, the β-maximum in Fig. 19 -b the joint maximum in Fig. 19-c, and some of the lineation maxima in Fig. 19-a occur closely in the synoptic diagram. Such geometrical relation among these maxima is just similar to that explained in schistose hornfelses. However, the lineation maximum in Fig. 19-d and two β-maxima in Fig. 19-e do not coincide with each other.

In conclusion, some geometrical results of the thrust-fault, considered in conjunction with geological evidences, will be interpreted as follows:—

1) The NE.~ENE. trending lineation in Fig. 19-a may be the same style as that in schistose hornfelses: the $B(=b)$-lineation. The lineation in and near the thrust-fault seems to be dispersed from the regional trend during the late movement that completed the thrust-fault.

2) The lineation trending SW.~SES. with higher angles (Fig. 19-a, -d) has been found only in and near the thrust-fault, and may be referred to the so-called down-dip lineation.

3) The preferred orientation of *ac*-joints does not appear to have been dispersed in the thrust-fault: it seems probable to infer that the thrust-fault may have been displaced prior to or contemporaneously with the splitting of joints.

Synopsis of macroscopic geometry

In this section the results of the macroscopic geometry of the structure in the Iwakuni-Yanai area will be summarized, and, if possible, some kinematic and dynamic interpretation will be added.

Planar structures: The term "S_1" shows surfaces of original discontinuity in rocks regardless of schistose hornfelses and banded gneisses. The terms "S_2" and "S_3" have been used for secondary planar structures found only in schistose hornfelses: the former corresponds to "fracture-cleavage", and the latter to "slaty cleavage" in the sense

of DE. SITTER.

There are many positive evidences to suggest that S_1 has been in most cases surfaces of actual slip. πS_1 in schistose hornfelses forms a great circle girdle (π-circle) which defines β-axis for the zone of schistose hornfelses (Fig. 8-a). In banded gneisses of the zone of transitional rocks, the similar pattern of S_1 can be inferred. However, orientations of S_1 are more or less dispersed in the zone of migmatites; particularly, in subarea H_2 they are rather random. Great circle girdle can hardly be drawn on the collective diagram, Fig. 9-b. The general trend of S_1 in the zone of migmatites is gently curved with dips steeply inclined towards N.: E.-W.-trend in the western part (subarea H_3) turns gradually into NE.-trend in the eastern part (subarea H_1).

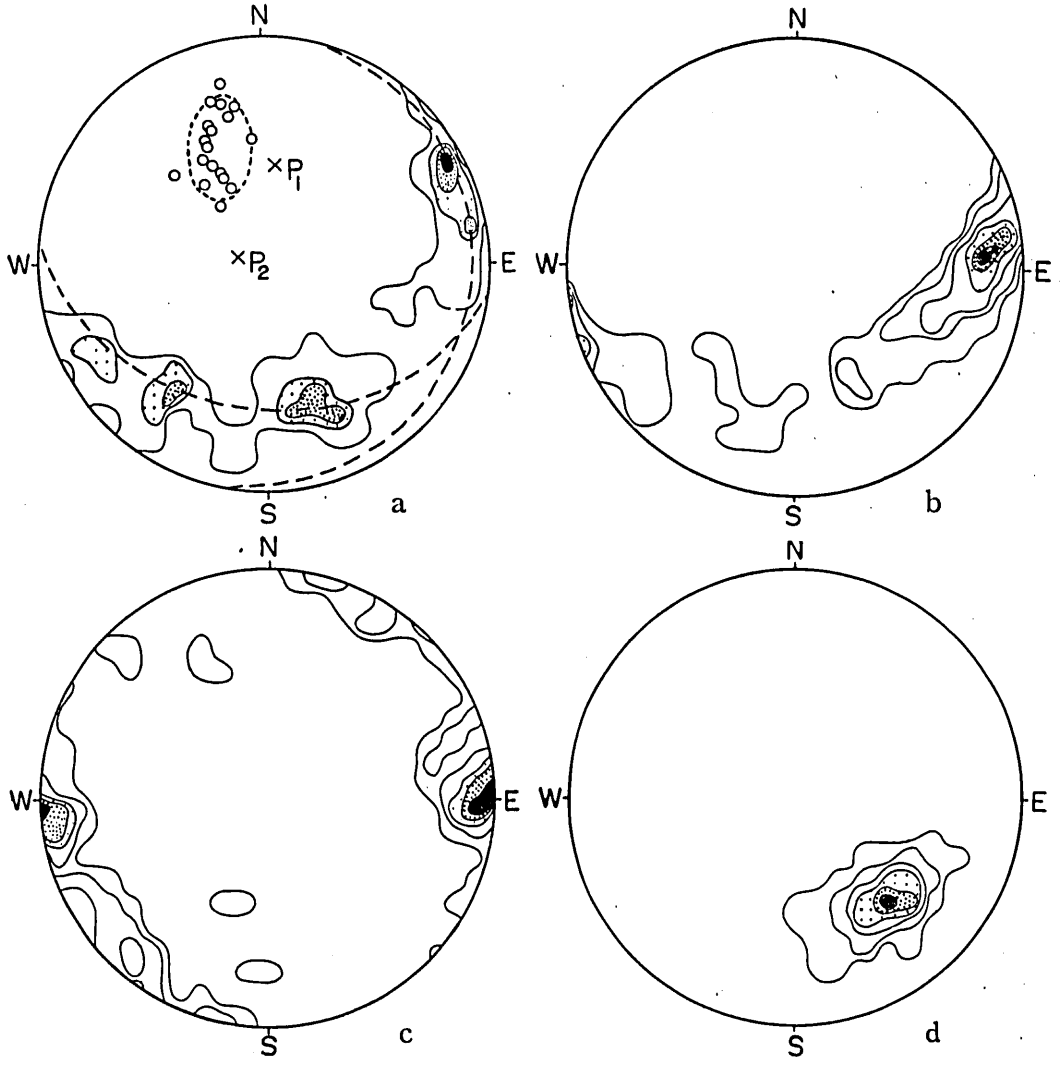

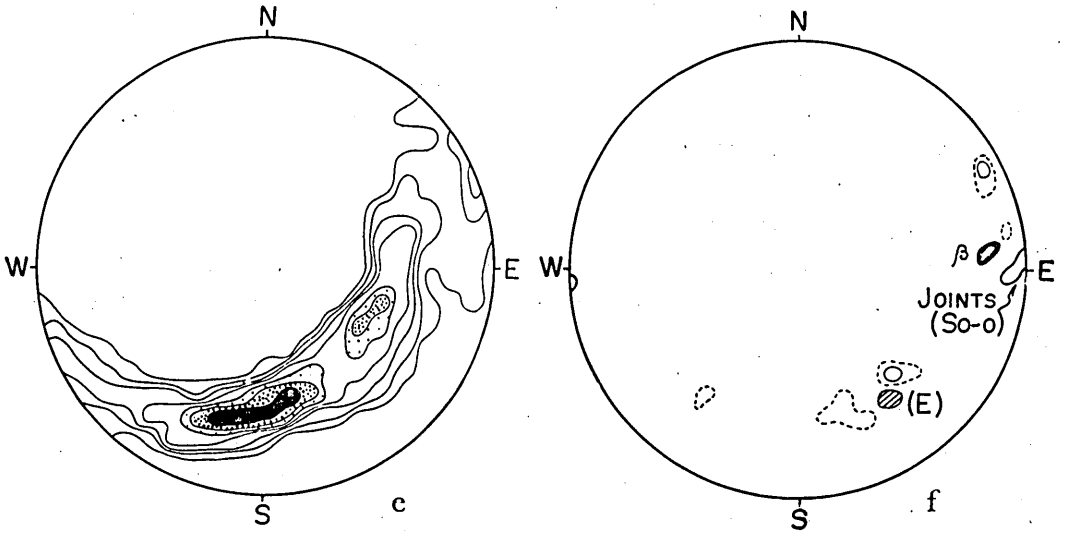

FIG. 19. Geometry of the thrust-fault. a, 56 axes of lineation and 18 $\pi S'$ in the sheared zone of the thrust-fault, near the entrance of the So-o Wireless Relay Station; contours 13-10-6-3%. b, 129 β-axes for S_1 in the same exposure as a; contours 23-19-15-10-6-2%. c, 43 poles of joints in the same exposure as a; contours 20-15-10-6-2%. d, 82 axes of lineation in banded chert at the northern part of Hon-ro-o; contours 50-40-30-20-10-3%. e, 531 β-axes for S_1 in an exposure north of Hon-ro-o; contours 9-8-7-5-3-2-1%. f, Synoptic diagram of Figs. 19-a, b, c, d and 7-E (*L*). (see text).

S_2 has been found locally in pelite and in semi-pelite. The macroscopic geometry of S_2 has not been carried out. It is accompanied by folds on small scale and most commonly nearly parallel to S_1 at limbs of folds, and converges towards crest of folds (Fig. 4).

S_3 has been found characteristically in the northern part and the southern part of the zone of schistose hornfelses, but hardly found in banded gneisses. These parts correspond to the extremes of both limbs of the major anticline. S_3 inclines in general steeply or nearly vertical. The statistic treatment has, however, been possible only at the northern part of the zone. Here, πS_3 shows high concentration (Fig. 10-a), and S_3 is tautozonal with S_1 (Fig. 10-b). Intersecting lineation $\widehat{S_1 S_3}$ is strictly parallel to axes of folds on every scale. These facts indicate that S_3 was formed under the same stress plan as flexural folding of S_1, possibly at the latest phase of folding.

The most consitently observable joints are "*ac*-joints", the regional trend of which is approximately N.-S.. The *ac*-joints must have facilitated the development of large faults trending N.-S.. Oblique (*hk0*)-joints occur characteristically at the crest of the major anticline. These oblique joints may be a kind of tension joints splitted probably at a later phase as a consequence of subsequent release of local confining pressure which had been especially high at the crest of the major anticline.

There is a thrust-fault, trending ENE. with southerly dips, between the zone of schistose hornfelses and the zone of transitional rocks. Down-dip lineation occurs in

and near the thrust-fault, but preferred orientation of *ac*-joints does not appear to have been dispersed in and near the thrust-fault. The thrust-fault would have been completed after the production of banded gneisses and migmatites but probably prior to the intrusion phase of the younger Ryôké granites (such as the Namera granite). The writer believes that the faulting might have occurred contemporaneously with or slightly prior to the splitting of *ac*-joints.

Linear structures: The lineation in schistose hornfelses is axes of microfolds and intersections of S_1 with S_2 or S_3, and of S_2 with S_3, but that observable in gneisses is restricted to axes of microfolds alone. The lineation is $B(=b)$-lineation throughout the whole area concerned.

The zone of schistose hornfelses and the zone of transitional rocks are highly homogeneous with respect to the lineation, the preferred orientation of which is about E.-W. in azimuth and 10°~20°E. in plunge. In the zone of migmatites, however, orientations of the lineation are fairly dispersed; especially, in subarea H_2 they become highly disturbed. The general trend of the lineation shows a gentle convex towards the south, though at the southern half of subarea H_2 it can not always be traceable. At the western part of the zone (subarea H_3) the lineation plunges most commonly towards W., while at the eastern part of the zone (subarea H_1) most of the lineation plunge towards ENE. or NE.. These facts indicate that a swelling movement occurred during the deformation, probably at the latest phase of production of gneisses and migmatite.

All β-diagrams for S_1 have been prepared essentially from restricted areas, but not prepared for regional scale. In schistose hornfelses as well as in gneisses of the zone of transitional rocks, the β-maximum coincides nearly or strictly with the lineation maximum, regardless of plunging angles of axes of folds and of rock types. Thus $\beta=B$, and the area as a whole had been folded about B. In gneisses of the zone of migmatites, the relation, $\beta=B$, can yet be traceable; but two or more β-maxima are generally found in each diagram. The prominent β-maxima often show high plunge angles, and may correspond to the axes of F-folds.*

Folds on every scale found in schistose hornfelses and the B-folds in gneisses are "concentric" in the sense of DE SITTER, and axes of these folds are strictly parallel to the lineation. Axes of these folds correspond, on the basis of symmetry, to the true fabric b-axis which can be equated with a kinematic B-axis (an axis of slip and external rotation normal to a deformation plane). In gneisses of the zone of migmatites, there is another style of folds, i.e., F-folds. The B-folds and the lineation aregently folded about axes of the F-folds which are generally steeply inclined but oriented in various directions. The F-folds are hardly related to the B-folds but are gentle wrinkles produced probably under fairly mobilized state.

* D. H. MACKENZIE (1957) reports the similar phenomena from Mid-Strathpay, Moine. In the interpretation of spread of β-axes in migmatites, MACKENZIE attached great importance to the opinion of C.E. WEGMANN (1929) that "the degree of mobility or competency of different rocks directly determines the degree of spread of their axial elements." The writer agrees also with the opinion of WEGMANN.

Summary: After these statistic treatment, it can be strongly asserted that structures in schistose hornfelses and in gneisses of the zone of transitional rocks are tectonically very homogeneous, while those in gneisses in the zone of migmatites become remarkably disturbed.

To conclude, there seems present at least two separate phases of deformation during the Ryôké metamorphism. The one, earlier, phase is characterized by penetrative movement which built up folds on every scale in schistose hornfelses and the *B*-folds in gneisses. The other, later, phase is characterized by a swelling movement in the zone of migmatites, during which the *F*-folds were probably produced.

The validity of this interpretation will be proved clearly by the results of the microscopic fabric analyses of the Ryôké metamorphic and granitic rocks.

IV. Microscopic Fabric

General Statement

Kinematic and dynamic interpretation of tectonic fabrics is conspicuous in the publications of the Innsbruck school. Interpretation of such fabrics by SANDER and SCHMIDT is based on an assumption that the symmetry of a tectonite fabric reflects the symmetry of movement responsible for the evolution of the fabric. The symmetry concept of SANDER and SCHMIDT has become strengthened by evidences derived from studies of experimentally deformed metallic aggregates, marble cylinders and so on; in particular, studies of deformed marble cylinders have been outstandingly developed by such investigators as GRIGGS and TURNER.

Interpreted according to the symmetry rule of SANDER and SCHMIDT, *a*-lineation represents a direction of differential movement or shear, whereas *b*-lineation is transverse to the direction of tectonic transport. While, opposition to the symmetry concept of SANDER and SCHMIDT has also been frequently reported by many investigators, such as STRAND (1944), KVALE (1948, 1953, 1954) and OFTEDAHL (1948) in Nowray; ANDERSON (1948) with reference to the Moine schists of Scotland; and BALK (1952, 1953a, 1953b) in North America.

Most of literatures dealing with lineation in deformed rocks abound in orientation diagrams for quartz, mica and others. So far many investigators have discussed and deduced the relation between the direction of movement and the fabrics of these minerals. However, as TURNER (1957) said, "since virtually nothing is known as to the mechanisms by which these minerals become oriented during metamorphism, the only property of the diagrams that could now be of value for kinematic interpretation is their symmetry."

Agreeing with the assertion of TURNER, the most significant object in this chapter has been lain on the symmetry of fabric pattern of essential constituent minerals. The following three points will be examined:—

1) To detect the characteristic fabrics of schistose hornfelses, gneisses and mig-

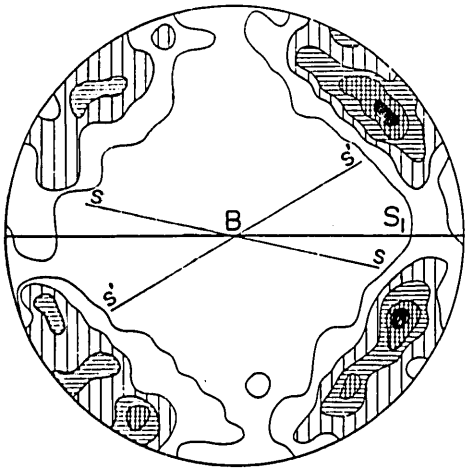

FIG. 20. 500 [0001] of quartz in Specimen TN56XI19-6; contours 5-4-3-2-1%.

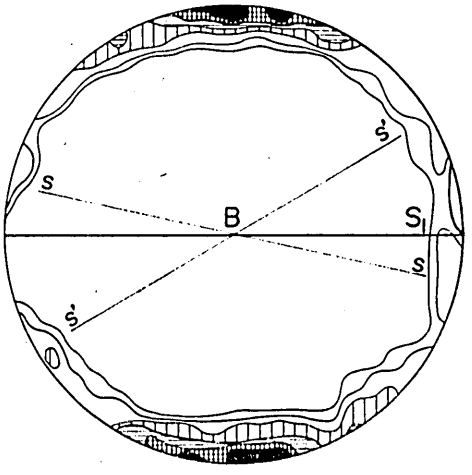

FIG. 21. 300 [001] of muscovitic mineral in Specimen TN56XI19-6; contours 14-12-10-8-5-2%.

matites, all of which have been produced presumably during the Ryôké metamorphism.*

2) If possible, to examine the time relation between two separate phases; i.e., the phase of production of schistose hornfelses and that of gneisses and migmatites.

3) To determine the microscopic fabrics of the Ryôké metamorphic rocks which were thermally metamorphosed by the younger intrusives, such as the younger Ryôké granites and the Cretaceous granite.

ORIENTATION DATA OF MINERALS FROM SELECTED SPECIMENS

Schistose hornfelses

Orientation data from unfolded banded chert: Four samples were selected.

Sample 1: TN56XI19-6; $\perp b$-section.

Locality: About 300 m to the northeast of Sugaki (subarea C_3).

Minerals measured: [0001] of quartz and [001] of muscovitic mineral from a chert band. Quartz shows no undulatory extinction and is equigranular. Quartz is 0.03 mm and muscovitic mineral 0.04 mm in average diameter.

Remarks: The lineation in the hand specimen plunges 5° towards ESE. The results are shown in Figs. 20 and 21.

Sample 2: TN57V3-3; $\perp b$-section.

Locality: About 200 m to the north of Shimobata (subarea C_3).

Mineral measured: [0001] of quartz from a chert band. Every petrographic feature of the sample is similar to those of *Sample 1*.

* Within macroscopic fields of observation, so far no appreciable fabrics imprinted by prior deformation has been observed. Provided that schistose hornfelses had suffered a certain deformation prior to the Ryôké metamorphism, some fabrics imprinted by earlier deformation are, as showed from other metamorphic terrains by many workers, can be expected to persist in rocks.

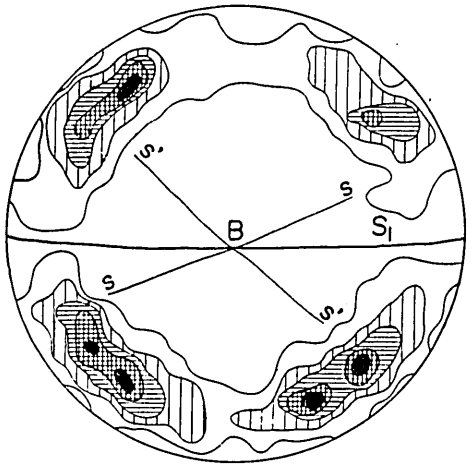

FIG. 22. 400 [0001] of quartz in Specimen TN57V3-3; contours 5-4-3-2-1 %.

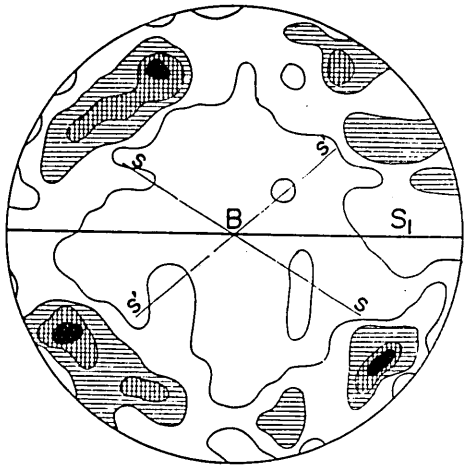

FIG. 23. 450 [0001] of quartz in Specimen TN56XI22-4; contours 4-3-2-1 %.

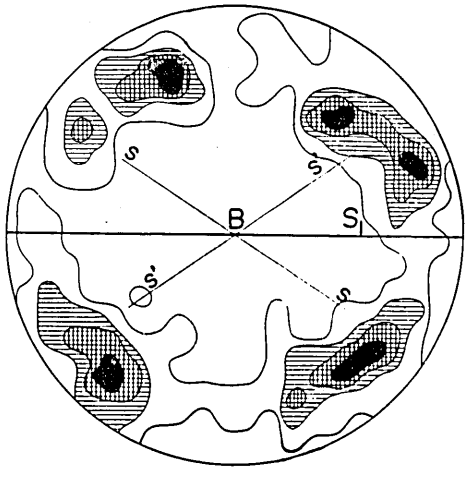

FIG. 24. 410 [0001] of quartz in Specimen TN56XI22-5; contours 4-3-2-1 %.

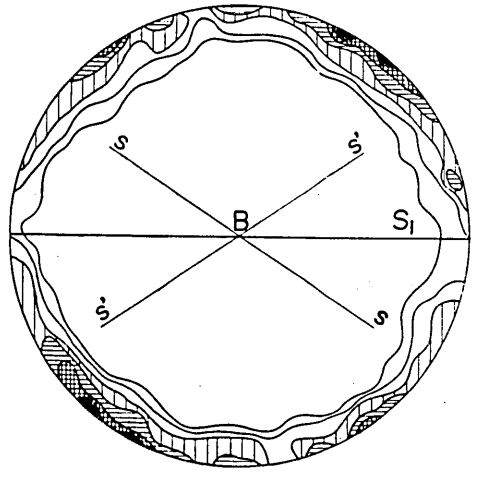

FIG. 25. 200 [001] of micas in Specimen TN56XI22-5; contours 9-8-6-4-2-1 %.

Remarks: The lineation in the hand specimen plunges 3° towards WNW. The result is shown in Fig. 22.

Sample 3: TN56XI22-4; $\perp b$-section.

Locality: About 500 m to the north of Hiuchi-iwa (subarea A_1).

Mineral measured: [0001] of quartz from a chert band. Quartz shows no undulatory extinction and is equigranular and 0.05 mm in average diameter, and micas (biotite predominant) are 0.05 mm.

Remarks: The average grain-size of quartz becomes larger than the former two samples, and biotite becomes predominant. The lineation in the hand specimen plunges 11° towards E. The result is shown in Fig. 23.

Sample 4: TN56XI22-5; $\perp b$-section.

Locality: Hiuchi-iwa (subarea A_1).

Minerals measured: [0001] of quartz and [001] of micas. The rock shows the same petrographic features as *Sample 3*.

Remarks: Many quartz veins have been observed in the section. The lineation in the hand specimen plunges 9° towards E.. The results are shown in Figs. 24 and 25.

Orientation diagrams for micas in unfolded banded chert are characterized by a sharply defined *ac*-girdle. The presence of three sets of surfaces are generally suggested: one corresponds to S_1, and the remainders are two intersecting sets of (*h0l*)-surfaces (here termed *ss* and *s's'*)* which can be found under the microscope only. *ss* and *s's'* intersect at variable angles, but they are commonly symmetrically paired about S_1. These surfaces do not seem to have acted as the actual slip surface.

Orientation diagrams for quartz have the following characteristics:—

1) Four or more prominent maxima are found in each diagram. There is, at least, one maximum in each quadrant, and these maxima generally form no *ac*-girdle but an incomplete small circle girdle which approximates to a great circle, *ac* of the fabric.

2) The symmetry approximates orthorhombic rather than triclinic. The positions of each maximum in separate quadrants correspond nearly to the position IV after SANDER with respect to S_1.

3) The surfaces of *ss* and *s's'* do not seem to be closely related to the preferred orientation of [0001] for quartz.

4) The patterns described from *1*) to *3*) are yet true in Figs. 23 and 24, in which [0001]-axes of quartz are slightly dispersed than those in Figs. 20 and 22.

Orientation data from pelite and semi-pelite: Three samples were selected.

Sample 5: TN56V2-4; $\perp b$-section.

Locality: Rokuroshi, just behind the Shigino Primary School (subarea B_2).

Minerals measured: [001] of muscovitic mineral and [0001] of quartz from a thin quartzose band in pelite. Quartz shows no undulatory extinction, and is equigranular and 0.03 mm in average diameter.

Remarks: The lineation in the hand specimen plunges 7° towards E.. The results are shown in Figs. 26 and 27.

In Fig. 26, *ss* and *s's'* are distinctive, but prominent maximum suggesting S_1 does not occur, though S_1 is the only megascopic surface in the sample. The two sets of surfaces, *ss* and *s's'*, are completely symmetrical with respect to S_1. It is not clear whether *ss* or *s's'* was ever a plane of actual slip.

The pattern of the quartz diagrams, Fig. 27, fairly resembles those of unfolded banded chert. The diagram is characterized by occurrence of two maxima in each quad-

* Each set of intersecting surfaces is spaced commonly at 0.05 mm or more. Both sets are usually well developed in chert bands; the one is more sharply observable than another under the microscope or in mica diagrams. The former has been for convenience' sake termed *ss* and another *s's'*. The intersection of *ss* with *s's'* coincides, in general, completely with the lineation.

Surfaces of *ss*, *s's'*, S_1, S_2 and so on were determined by preferred orientations of micas and traced on each fabric diagrams for quartz. However, the position of these surfaces were often approximately measured by reading the graduated stage of the microscope.

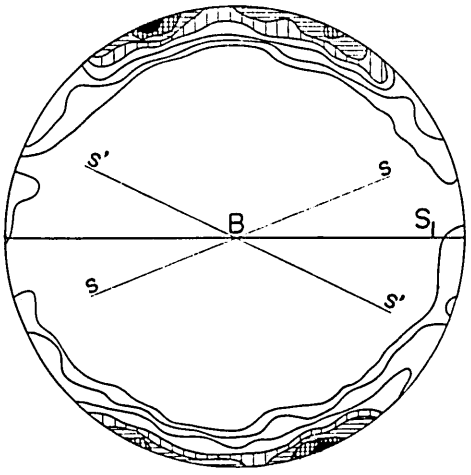

Fig. 26. 250 [001] of muscovitic mineral in Specimen TN56V2-4; contours 12-10-8-6-4-2-1%.

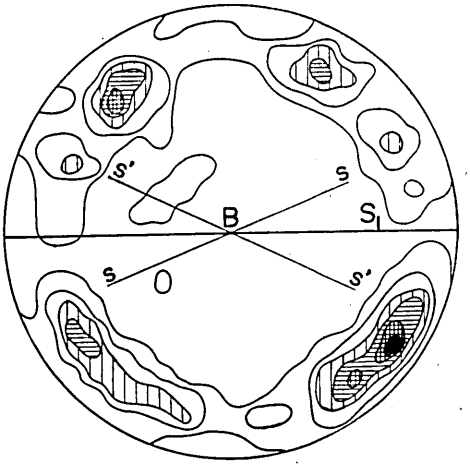

Fig. 27. 400 [0001] of quartz in Specimen TN56V2-4; contours 6-5-4-3-2-1%.

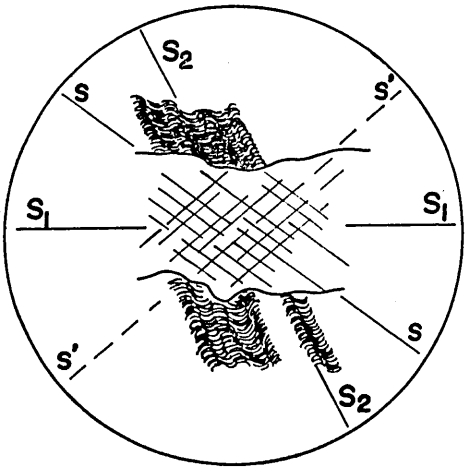

Fig. 28. Microscopic sketch of semi-pelite, Specimen TN56V6-5.

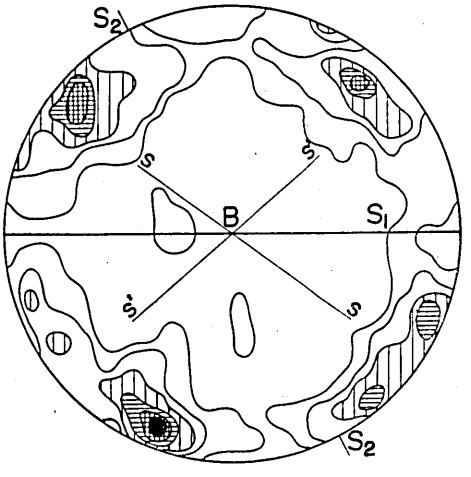

Fig. 29. 400 [0001] of quartz in Specimen TN56V6-5; contours 6-5-4-3-2-1%.

rant, except the third quadrant. Each maximum in the third and the fourth quadrant approximates the position IV with respect to S_1, while the maximum in the first quadrant and the submaximum in the second quadrant approximate the position IV with respect to one set of (*h0l*)-surfaces, *ss*: *ss* seems a plane closely related to the symmetry of quartz fabric.

Sample 6: TN56V6-5; $\perp b$-section.

Locality: Tôgô (subarea C_2).

Mineral measured: [0001] of quartz from a quartzose band in semi-pelite. Quartz is equigranular and 0.03 mm in average diameter.

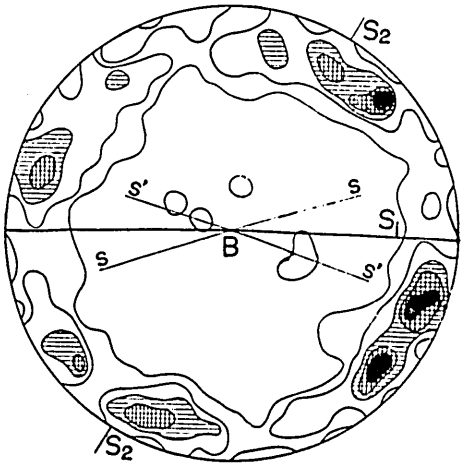

FIG. 30. 400 [0001] of quartz in a quartzose band, Specimen TN56IV30-4; contours 5-4-3-2-1%.

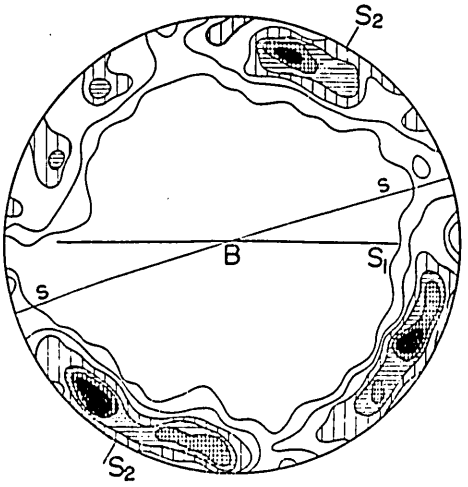

FIG. 31. 400 [0001] of quartz in a micaceous band, Specimen TN56IV30-4; contours 6-5-4-3-2-1%.

Remarks: S_2 is conspicuous within pelitic bands, but it is obscured in quartzose bands. The results are shown in Figs. 28 and 29.

Sample 7: TN56IV30-4; $\perp b$-section.

Locality: Rokuroshi (subarea B_2).

Mineral measured: [0001] of quartz from a quartzose band and the adjoining micaceous (pelitic) band. Petrographic features of the rock are similar to those of *Sample 6*. In the quartzose band, small flakes of plagioclase are rarely found.

Remarks: The pelitic band from which measurement was made shows weak microfolding of S_1. Axial planes of such microfolds may correspond to S_2. The results are shown in Figs. 30 and 31.

Fig. 28 is a microscopic sketch of the thin section. Under the microscope, S_1 within the quartzose band is very faint, whereas two sets of intersecting (*h0l*)-surfaces, in particular *ss*, are sharply defined. *ss* and *s's'* are completely symmetrical with respect to S_1. S_2 is also sharply defined in micaceous bands, and is completely parallel on both sides of the quartzose band.

In Fig. 29, [0001]-axes of quartz appear to form a small circle girdle, which approximates *ac* of the fabric. The symmetry of quartz fabrics is orthorhombic, but it is unreasonable to regard any of *ss*, *s's'*, S_1 and S_2 as a plane of symmetry.

Figs. 30 and 31 are quartz diagrams from quartzose band and from the adjoining micaceous band respectively. Comparing Fig. 30 with Fig. 31, there seems present no fundamental differences in pattern and in preferred orientation of [0001]-axes of quartz. Each of Figs. 30, and 31 illustrates a complete small circle girdle, which approximates *ac* of the fabric. In each quadrant, there presents at least one lanky area of high concentration, which generally encloses one or two prominent maxima. Then *ss* corresponds to one of symmetry planes, but S_1 does not seem to be a symmetry plane.

ss and *s's'* occur nearly symmetrically with respect to S_1.

At all events, the quartz diagrams for semi-pelite are, irrespective of chert band and pelite band, characterized by the presence of partial or complete small circle girdle which approximates to *ac* of the fabric, and by nearly orthorhombic in symmetry, *ss* being now regarded as one of symmetry planes.

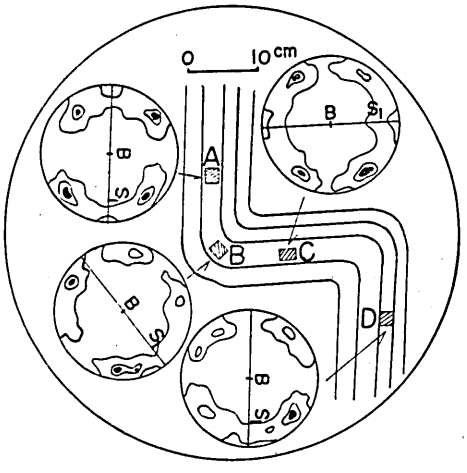

FIG. 32. Profile of a fold, the results of fabric analysis of which are shown in Figs.33–40.

Orientation data from folded banded chert: As examples two folds on small scale will be examined. The included angle of limbs of one fold is about 90°, and that of another about 60°. The petrographic features of these samples are just similar to those of *Sample 1*.

Example 1:— Sketch (on an *ac*-joint surface) of a fold near Sugaki and the parts from which four thin sections were prepared are shown in Fig. 32. S_1 on the limbs are strikingly even as shown in the figure. Simplified quartz diagrams of Figs. 35, 36, 37 and 38 are also illustrated in Fig. 32. Fabric diagrams for quartz and muscovitic mineral were prepared as follows:

Part (see, Fig. 32)	Sample no.	[001] of muscovitic mineral	[0001] of quartz from banded chert	[0001] of quartz from segregated quartz veins
A	Sample 8 N57X27-7-4	Fig. 33	Fig. 35	
B	Sample 9 TN57X27-7-3		Fig. 36	Fig. 39
C	Sample 10 TN57X27-7-5		Fig. 37	
D	Sample 11 TN57X27-7-1	Fig. 34	Fig. 38	Fig. 40

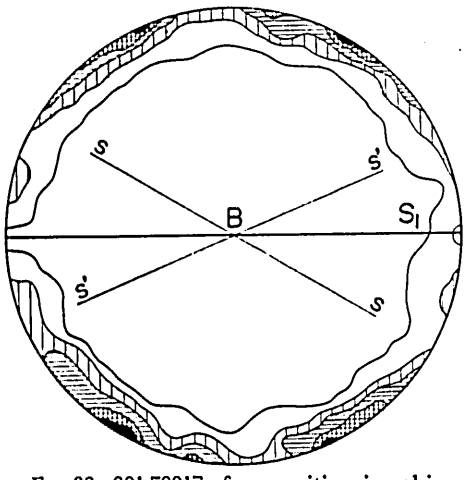

FIG. 33. 301 [001] of muscovitic mineral in Specimen TN57X27-7-4; contours 9-7-5-3-1%.

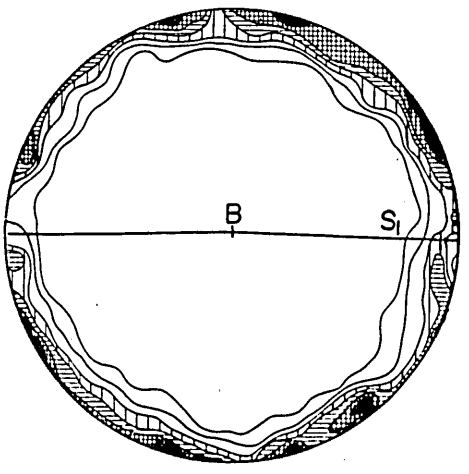

FIG. 34. 300 [001] of muscovitic mineral in Specimen TN57X27-7-1; contours 7-5-4-3-2-1%.

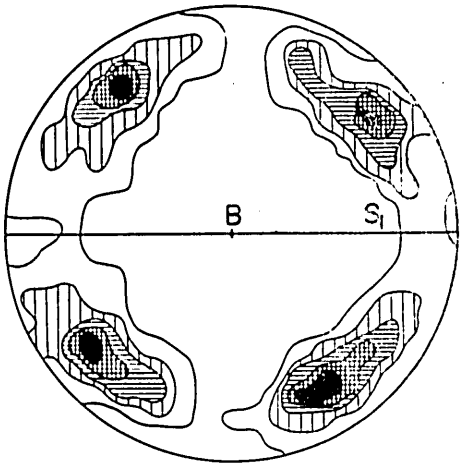

FIG. 35. 500 [0001] of quartz in Specimen TN57X27-7-4; contours 5-4-3-2-1%.

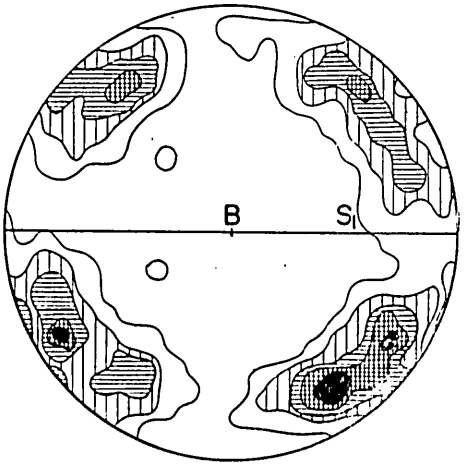

FIG. 36. 500 [0001] of quartz in Specimen TN57X27-7-3; contours 5-4-3-2-1%.

Figs. 33 and 34, which were prepared from two, strictly parallel limbs of the fold (see, Fig. 32), are characterized by complete *ac*-girdle, but the positions of the prominent maxima deviate from one diagram to another. S_1 is hardly traceable in these mica diagrams, while *ss* and *s's'* are sharply determined and found symmetrically with respect to S_1.

The pattern of Figs. 35, 37 and 38 is just similar to each other. The symmetry of these diagrams is orthorhombic, and the tendency to form a small circle girdle can be inferred. Positions of the prominent maxima in each diagram coincide nearly or completely with each other, namely at IV with respect to S_1. Thus, all characteristics of these quartz diagrams strongly resemble those of unfolded banded chert.

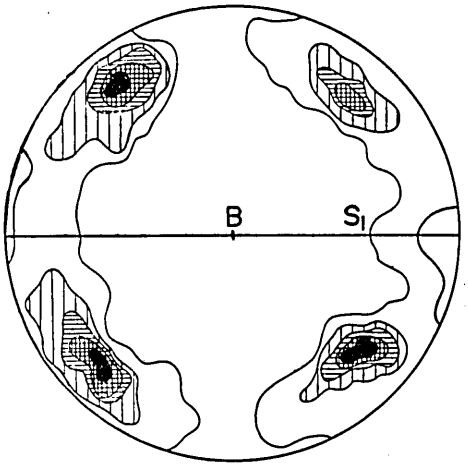

FIG. 37. 450 [0001] of quartz in Specimen TN57X27-7-5; contours 5-4-3-2-1%.

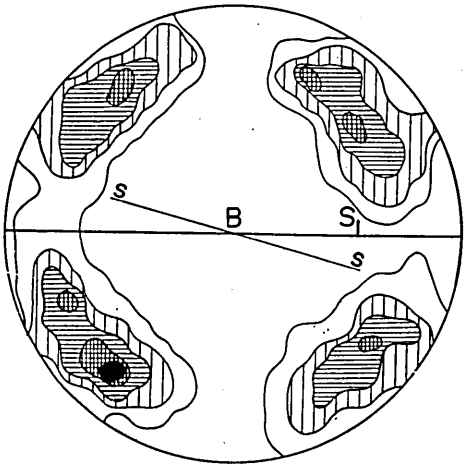

FIG. 38. 500 [0001] of quartz in Specimen TN57X27-7-1; contours 5-4-3-2-1%.

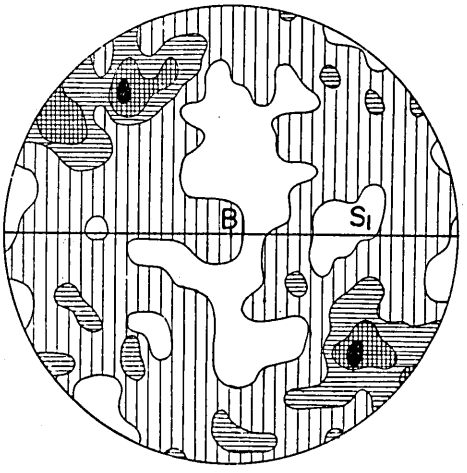

FIG. 39. 500 [0001] of quartz in Specimen TN57X27-7-3; contours 4-3-2-1%.

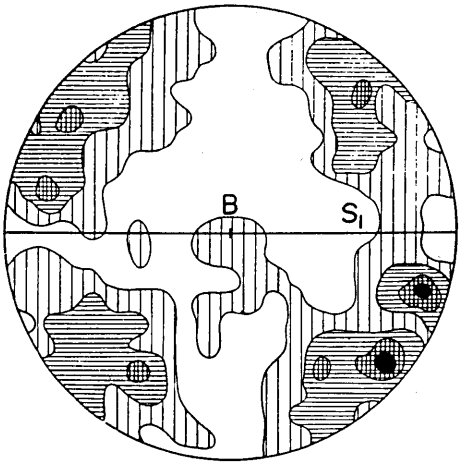

FIG. 40. 450 [0001] of quartz in Specimen TN57-7-1; contours 4-3-2-1%.

Fig. 36 was prepared from a crest of the fold (part B in Fig. 32), and is characterized by relatively lanky areas of high concentration in which one or two prominent maxima are enclosed. In this case, also, S_1 corresponds to a symmetry plane.

Conclusively, the pattern of quartz fabrics in folded banded chert is strictly similar to each other and, symmetrically, closely related to S_1 regardless of limbs or crest of the fold.

Before leaving the description of *Example 1*, fabric diagrams for quartz from segregated quartz veins will be examined. Under the microscope, they cut evidently the surfaces of S_1, ss and $s's'$.

In Fig. 39, [0001]-axes of quartz are strongly dispersed, but the diagram has yet two prominent maxima which are symmetrical with respect to *b* of the fabric; that is, it is slightly monoclinic in symmetry. The position of two prominent maxima in Fig. 39 almost coincides with those in Fig. 36. The same pattern of quartz fabrics can be observed in Fig. 40.

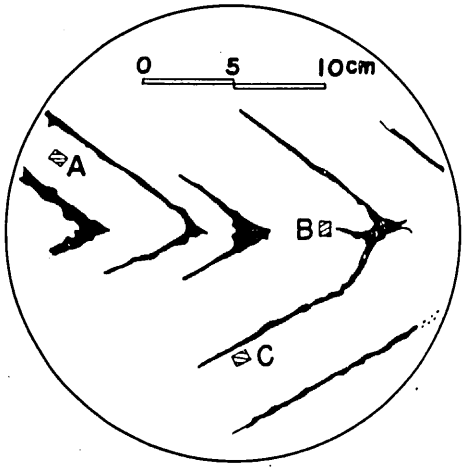

FIG. 41. Profile of a fold, the results of fabric analysis of which are shown in Figs. 42-47.

Example 2: Three samples were collected from a fold near Hashirano. Sketch of the fold (on an *ac*-joint surface) is shown in Fig. 41. Six fabric diagrams were prepared as shown in the following table.

Figs. 42, 43 and 44 are characterized by complete *ac*-girdle. *ss* and *s's'* are also indicative in Figs. 42 and 44, but S_1 which is a megascopically observable set of surfaces can not be decided in the diagrams. Fig. 43 is, however, characterized by one principal maximum indicating *ss*.

Patterns of three quartz fabric diagrams, Figs. 45, 46 and 47, strongly resemble each other. A complete small circle girdle occurs in Figs. 46 and 47, and a nearly complete

Part (see, Fig. 41)	Sample no.	[001] of muscovitic mineral	[0001] of quartz from banded chert
A	Sample 12 TN57X27-10-1	Fig. 42	Fig. 45
B	Sample 13 TN57X27-10-3	Fig. 43	Fig. 46
C	Sample 14 TN57X27-10-2	Fig. 44	Fig. 47

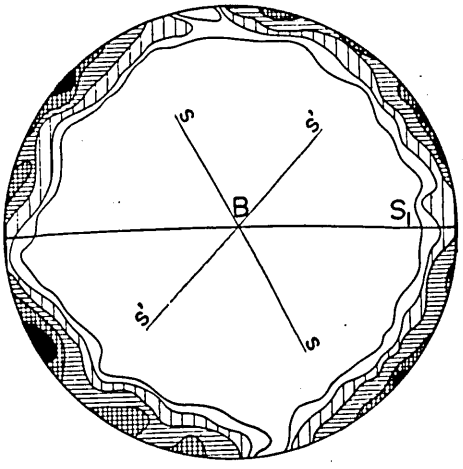

FIG. 42. 250 [001] of muscovitic mineral in Specimen TN57X27-10-1; contours 8-6-4-2 -1%.

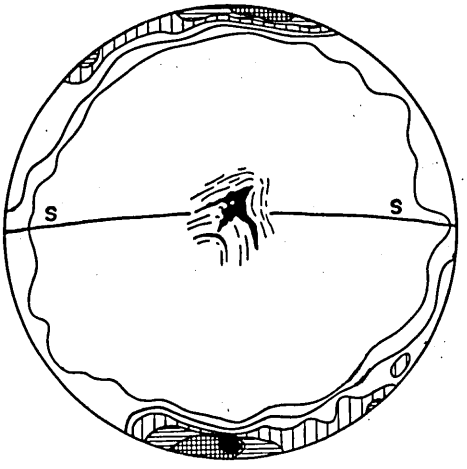

FIG. 43. 250 [001] of muscovitic mineral in Specimen TN57X27-10-3; contours 12-10-8-6 -4-2%.

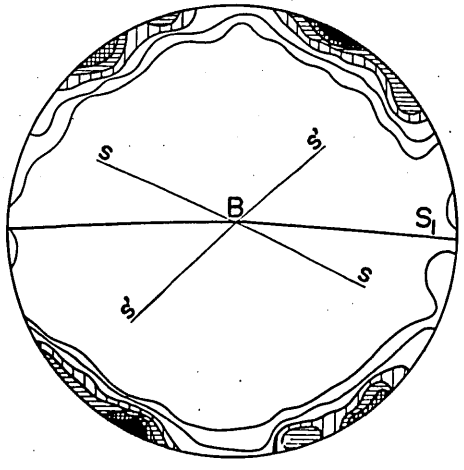

FIG. 44. 250 [001] of muscovitic mineral in Specimen TN57X27-10-2; contours 12-10-8-6 -4-2%.

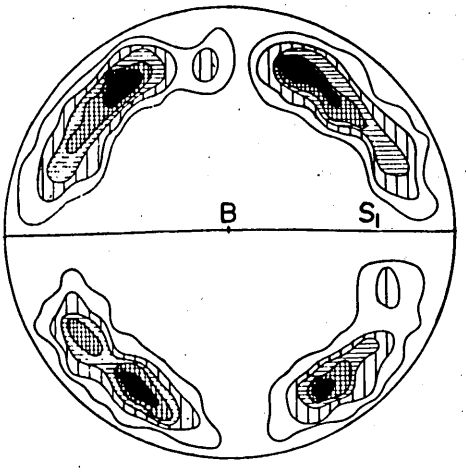

FIG. 45. 416 [0001] of quartz in Specimen TN57X27-10-1; contours 5-4-3-2-1%.

one in Fig. 45. Areas of high concentration are commonly lanky. Compared the first example with the second example, there is no fundamental difference in pattern of the quartz fabrics.

*Orientation data from "sheared flexure folds"**:

*"Sheared flexure folds" now concerned may not be referred strictly to "Totfalten" described by AMPFERER. FAIRBAIRN (1949, p. 178) has defined the folds as follows: "These are relict folds……Originally small scale, continuous flexures, they have been severed along micaceous zones by later shearing, and now lie suspended and inert insofar as further flexure is concerned. Their shape may be changed by shearing, but their deformation as a continuous unit ay flexure is bt an end."

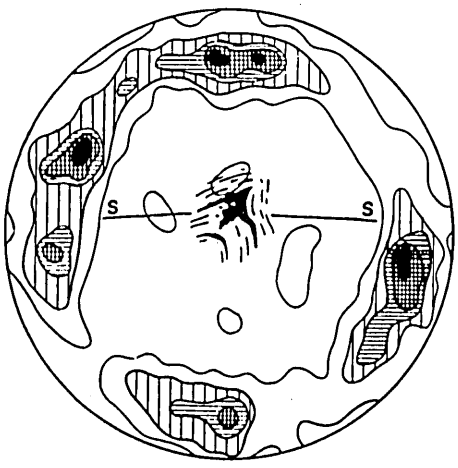

FIG. 46. 500 [0001] of quartz in Specimen TN57X27-10-3; contours 5-4-3-2-1%.

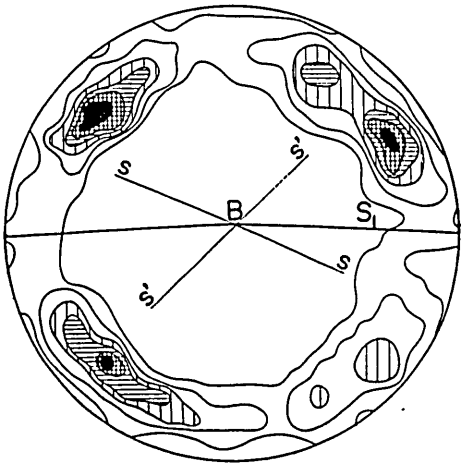

FIG. 47. 450 [0001] of quartz in Specimen TN57X27-10-2; contours 6-5-4-3-2-1%.

Sample15: TN57V22-2; $\perp b$-section.

Locality: About 400 m to the east of Datoko (subarea B_2).

Mineral measured: [0001] of quartz from quartzose bands in folded semi-pelite. Folded semi-pelite in problem shows no essential difference in petrography from ordinary semi-pelite. Well-developed micas, muscovite and biotite, are regularly oriented and parallel to the shear planes. The intersection of these shear planes with S_1 is parallel to the lineation. The shear planes are generally inclined at high angles, commonly 65°~75°. Quartz is equigranular and the average diameter measured is 0.03 mm.

Remarks: The results are shown in Figs. 48~51.

Fig. 48 is a microscopic sketch of sheared flexure folds in thin section normal to the lineation. The shear plane is strictly parallel to axial plane of folds, but it coincides with no set of (*hOl*)-surfaces such as *ss* and *s's'*. Three quartz diagrams, Figs. 49, 50 and 51, were prepared from parts A, B and C in Fig. 48, respectively.

The quartz diagrams, Figs. 49~51, for the sheared flexure folds are characterized by the presence of a nearly complete small circle girdle, within which prominent maxima are situated nearly at the position IV with respect to the shear plane. The symmetry of quartz fabric is orthorhombic; then, the shear plane becomes one of symmetry planes, but S_1, *ss* and *s's'* do not concern with the symmetry.

Orientation data from banded chert in which S_3 is well developed: Three samples will be described.

Sample 16: TN57XI29-2; $\perp b$-section.

Locality: The southern part of Hashirano (subarea C_3).

Minerals measured: [001] of muscovitic mineral and [0001] of quartz from banded chert. Quartz is equigranular and 0.03 mm in average diameter. The petrographic features of the rock are similar to the normal type of banded chert.

Remarks: The lineation in the hand specimen plunges at 5° towards E.. The results are

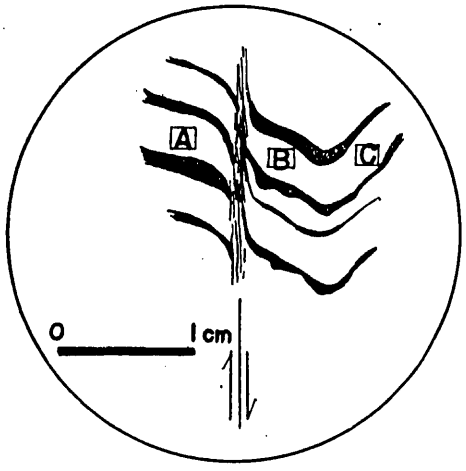

FIG. 48. Microscopic sketch of a "sheared flexure fold" in thin section (Specimen TN57 V22-2) normal to the lineation, the results of fabric analysis of which are shown in Figs. 49 -51.

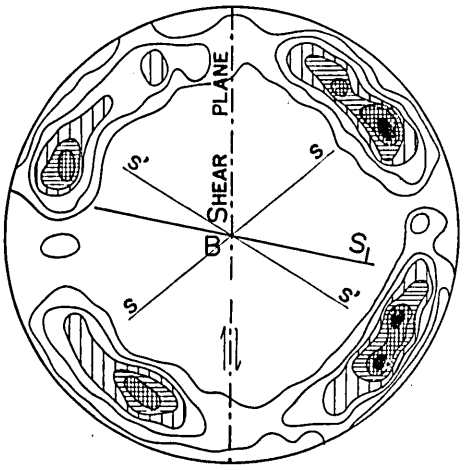

FIG. 49. 400 [0001] of quartz in Specimen TN57V22-2, A-part; contours 6-5-4-3-2-1%.

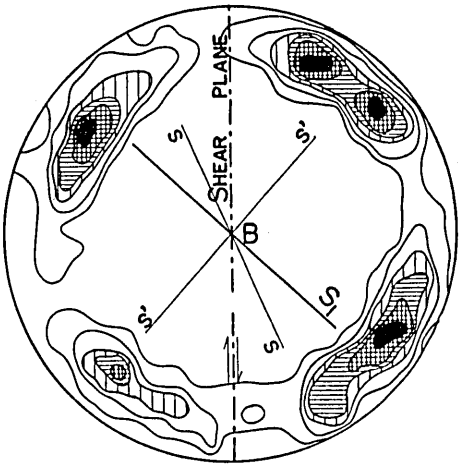

FIG. 50. 400 [0001] of quartz in Specimen TN57V22-2, B-part; contours 6-5-4-3-2-1%.

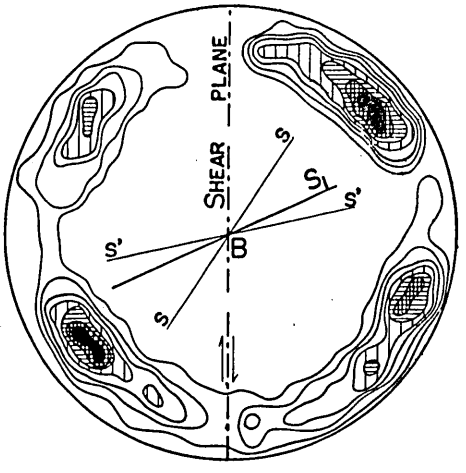

FIG. 51. 400 [0001] of quartz in Specimen TN57V22-2, C-part ; contours 7-6-5-4-3-2 -1%.

shown in Figs. 52 and 53.

Sample 17: GK57XI29-1B; $\perp b$-section.*

Locality: The southern part of Hashirano (subarea C_3).

Mineral measured: [0001] of quartz from a segregated quartz vein in banded chert. All petrographic features of the vein are just similar to those found in *Sample 9* and *11*. Quartz is equigranular and 0.05mm in average diameter.

* The *Sample 17* was tendered by G. KOJIMA, and its microscopic analysis was carried out in cooperation with him. The writer acknowledges his kindness.

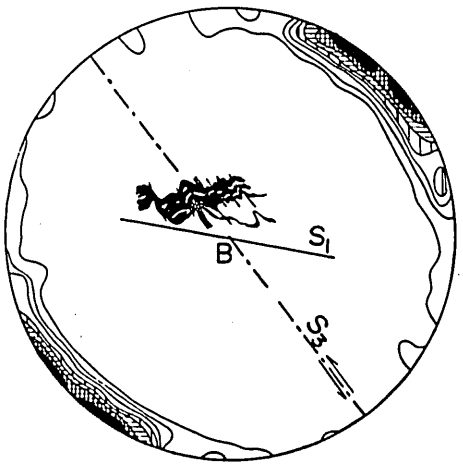

FIG. 52. 300 [001] of muscovitic mineral in Specimen TN57XI29-2; contours 14-12-10-8-6-4-2%.

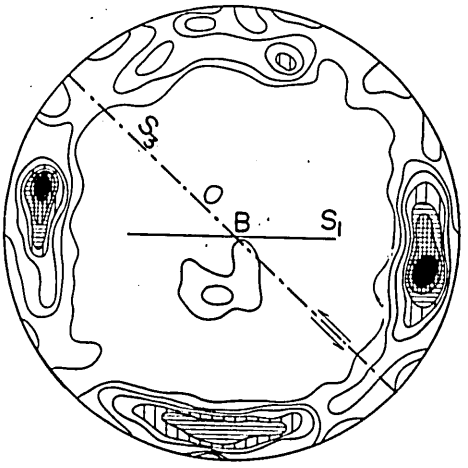

FIG. 53. 400 [0001] of quartz in Specimen TN57XI29-2; contours 7-6-5-4-3-2-1%.

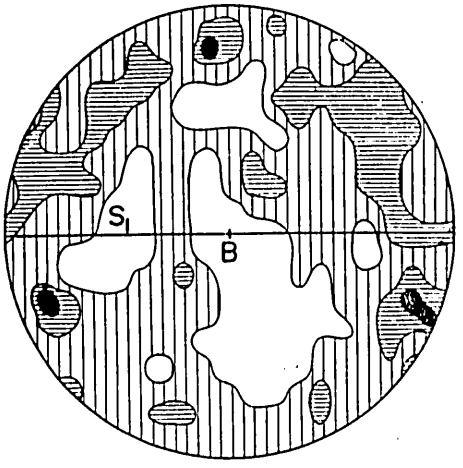

FIG. 54. 500 [0001] of quartz in Specimen GK57XI29-1B; contours 3-2-1%.

Remarks: When a $\perp b$-section and a $// b$-section from the same hand specimen are compared, it becomes evident that the veins are extended parallel to the lineation, and concordant or subconcordant often with S_3. The results are shown in Fig. 54.

Sample 18: TN57V9-2; $\perp b$-section.

Locality: 700 m to the north of Honro-o (subarea A_1).

Minerals measured: [001] of micas and [0001] of quartz from banded chert. But, the rock appears rather to be siliceous banded gneiss in petrographic character. Quartz is equigranular and 0.1 mm in average diameter, but sometimes attains 0.2 mm or more. Biotite is more predominant than muscovite.

Remarks: Segregated veins of quartz are observable in the hand specimen, but they can

not be distinguished from surroundings under the microscope. The results are shown in Figs. 55 and 56.

Fig. 52, fabric diagram for muscovitic mineral, shows an incomplete *ac*-girdle, in which two prominent maxima are found. One maximum corresponds to S_3, and another

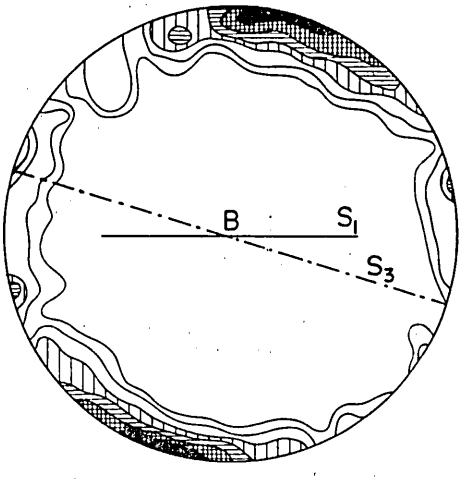

FIG. 55. 300 [001] of micas in Specimen 57V9-2; contours 10-8-6-4-2-1%.

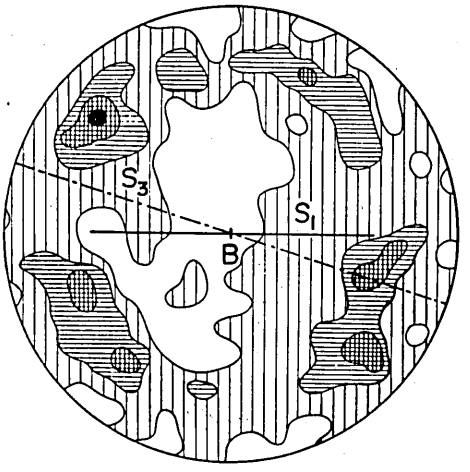

FIG. 56. 500 [0001] of quartz in Specimen TN57V9-2; contours 4-3-2-1%.

may correspond to *ss*. The quartz fabric diagram, Fig. 53, has a tendency to develop in an *ac*-girdle type. The diagram is characterized by the lanky areas of high concentration in each quadrant and by two prominent maxima which approximate to the position II after SANDER, with respect to S_3 but not to S_1. The symmetry of the diagram approximates monoclinic with an axis *b* of the fabric; however, the symmetry is yet orthorhombic and S_3 behaves just like as a plane of symmetry.

In Fig. 54, no preferred orientation of quartz axes can be found: it may be suggested that the quartz veins are probably segregated under a relatively static condition.

Fig. 55 is characterized by incomplete *ac*-girdle and one principal maximum which corresponds to S_3. S_1, *ss* and *s's'* can not be decided by preferred orientation of poles of (001) of micas. In Fig. 56, [0001]-axes of quartz are outstandingly dispersed, but a small circle girdle is yet traceable. Such pattern as shown in Fig. 56 is, however, the common type of quartz fabric diagrams for banded gneisses.

Gneisses

Orientation data from unfolded banded gneisses: Four samples were selected from unfolded banded gneisses, among which three were collected from the zone of transitional rocks, and one from the zone of migmatites.*

* Gneisses near the contact with the migmatite, Ôbataké gneissose granodiorite, are excluded in this section. Gneisses collected from the southern part of the zone of transitional rocks are also excluded in this section, because they have suffered regionally the thermal metamorphism by the younger Ryôké intrusives, such as the Kibé and Namera granites.

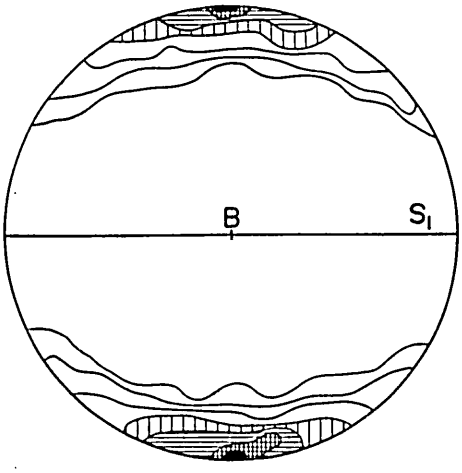

FIG. 57. 200 [001] of micas (mainly biotite) in Specimen TN56XI22-6; contours 11-9-7-5-3-2-1%.

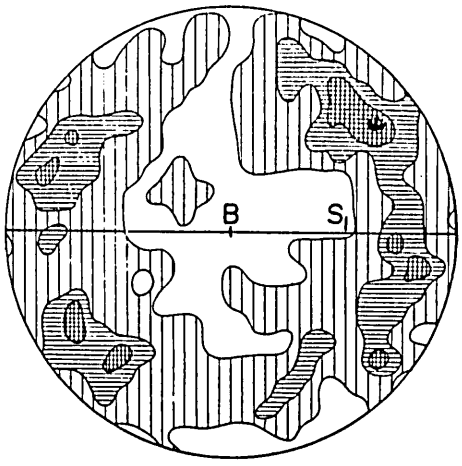

FIG. 58. 500 [0001] of quartz in Specimen TN56XI22-6; contours 4-3-2-1%.

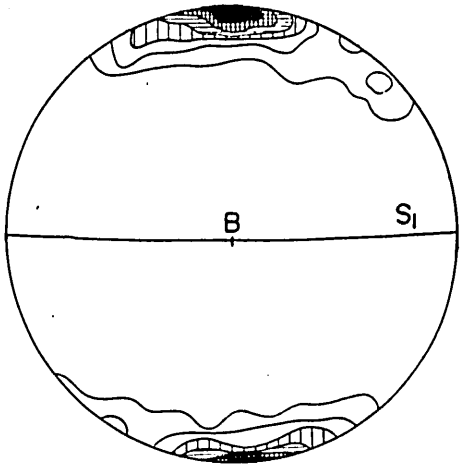

FIG. 59. 200 [001] of micas in Specimen TN56XI28-2; contours 17-14-11-8-5-2%.

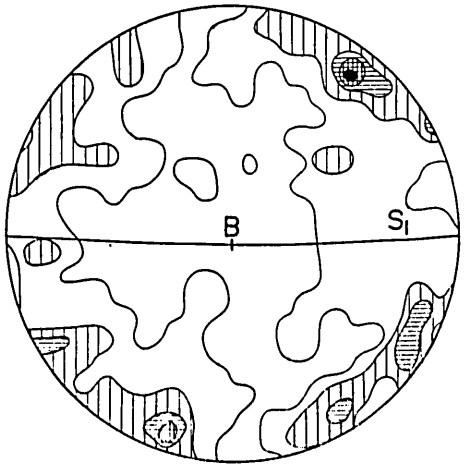

FIG. 60. 410 [0001] of quartz in Specimen TN56XI28-2; contours 5-4-3-2-1%.

Sample 19: TN56XI22-6; $\perp b$-section.

Locality: The western part of Honro-o (subarea E).

Minerals measured: [001] of biotite and [0001] of quartz from siliceous banded gneiss. The rock consists essentially of biotite and quartz, with cordierite and K-feldspar in small amount. Muscovite is lacking. Quartz is equigranular and 0.1 mm in average diameter. Undulatory extinction of quartz is rarely observed.

Remarks: The lineation in the hand specimen is relatively distinct and plunges 13° towards E.. The results are shown in Figs. 57 and 58.

Sample 20: TN56XI28-2; $\perp b$-section.

Locality: About 200 m to the west of Hata (subarea E).

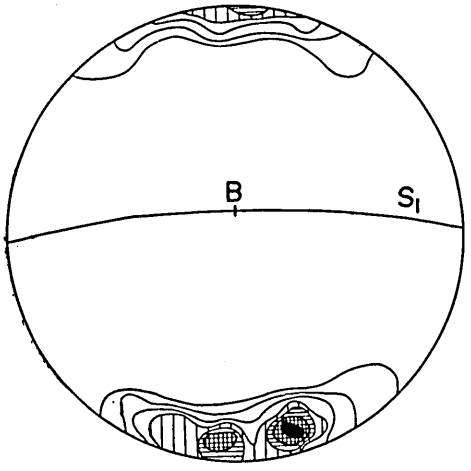

FIG. 61. 200 [001] of micas in Specimen TN56X22-5; contours 15-13-11-9-7-5-3%.

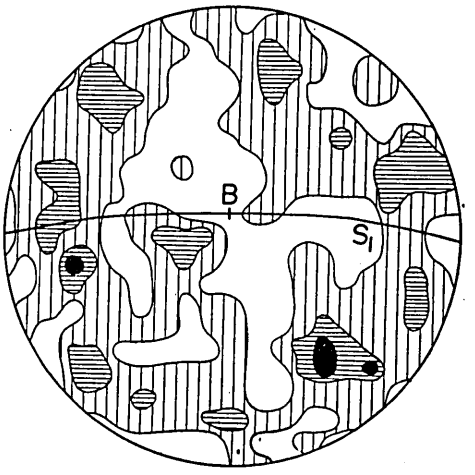

FIG. 62. 400 [0001] of quartz in Specimen TN56X22-5; contours 3-2-1%.

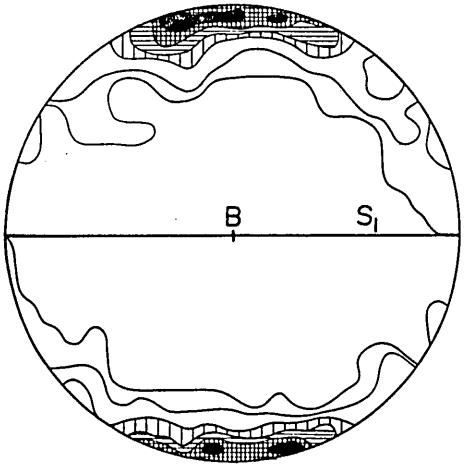

FIG. 63. 250 [001] of micas in Specimen TN56X7-6; coutours 10-8-6-4-2-1%.

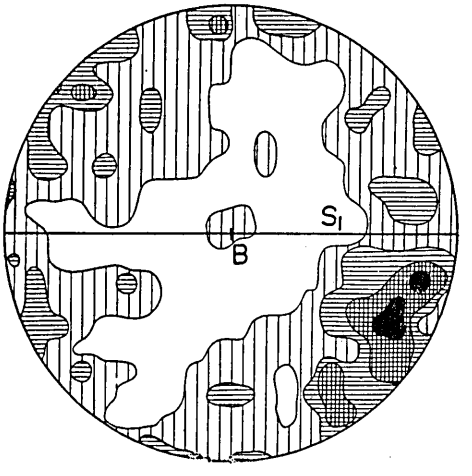

FIG. 64. 500 [0001] of quartz in Specimen TN56X7-6; contours 4-3-2-1%.

Minerals measured: [001] of biotite and [0001] of quartz from a quartzose band of micaceous banded gneiss. Cordierite, biotite, K-feldspar, plagioclase and quartz are the essential minerals of the rock. Larger grains of cordierite are found often in micaceous bands, and sporadically in quartzose bands. K-feldspar and plagioclase exist in small amount. Quartz is equigranular and commonly 0.1～0.2 mm in diameter. Undulatory extinction of quartz is very rare.

Remarks: The lineation of the hand specimen is distinct and plunges 2° towards E. The results are shown in Figs. 59 and 60.

Sample 21: TN56X22-5; $\perp b$-section.

Locality: Maimai (subarea F_1).

Minerals measured: [001] of biotite and [0001] of quartz from siliceous banded gneiss.

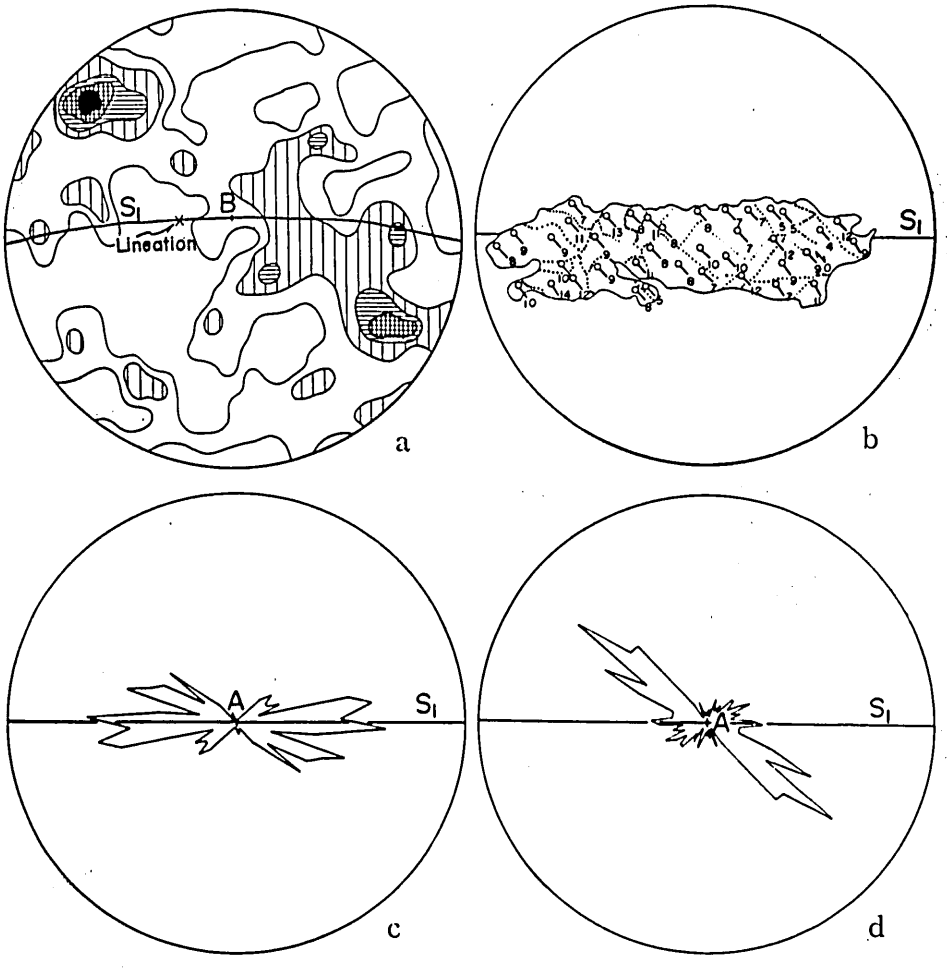

FIG. 65. a, 510 [0001] of quartz in Specimen TN56VIII19-2; contours 5-4-3-2-1%. b, Microscopic sketch of a porphyroblast of quartz and orientations of [0001] of each quartz grain, Specimen TN56VIII19-2; // *b*-section. c, Compass-rose diagram for elongation axes of quartz, Specimen TN56VIII19-2; //*b*-section; 100 points. d, Compass-rose diagram for undulatory zones in porphyroblasts of quartz, Specimen TN56VIII19-2; // *b*-section; 118 points.

The constituent minerals of the rock are similar to *Sample 19*. Quartz is equigranular and 0.2～0.3 mm in diameter. Undulatory extinction of quartz is not rare.

Remarks: The lineation is yet traceable. The results are shown in Figs. 61 and 62.

Sample 22: TN56X7-6; ⊥*b*-section.

Locality: About 500 m to the south of Mt. Mitsugadaké (subarea H_3).

Minerals measured: [001] of biotite and muscovite, and [0001] of quartz from siliceous banded gneiss. The petrographic features of the rock are rather similar to *Sample 21*, except the common appearance of quartz showing undulatory extinction.

Remarks: The lineation is traceable but not distinct. The rock seems to be free from

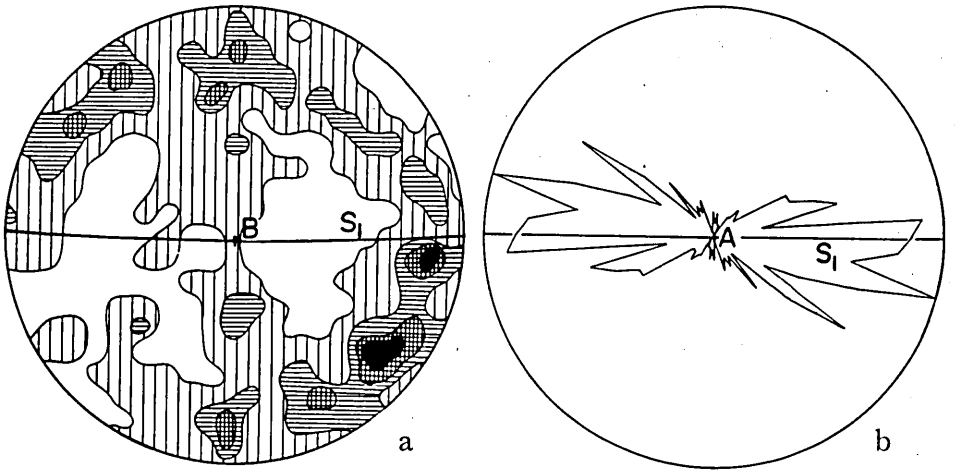

FIG. 66. a, 500[0001] of quartz in Specimen TN56X3-3; contours 4-3-2-1%. b, Compass-rose diagram for elongation axes of quartz, Specimen TN56X3-3; // *b*-section; 201 points.

"*F*-folding". The results are shown in Figs. 63 and 64.

Among four diagrams for biotite (and muscovite), two diagrams, Figs. 57 and 59, are characterized by one principal maximum in *c* of the fabric. While, in each of Figs. 61 and 63 occur two maxima which are completely enclosed by contours of slightly lesser concentration. It seems likely to infer that the two maxima in the latter two diagrams suggest no (*h0l*)-surface intersecting at *b* of the fabric but microfolds of S_1. All these diagrams indicate, therefore, that the cleavage plane of biotite is strictly parallel to the composition bands, S_1, in banded gneisses. Thus, the pattern of mica fabrics for banded gneisses are strongly contrasted to the general pattern of those for schistose hornfelses.

Four quartz fabric diagrams, Figs. 58, 60, 62 and 64, show various patterns of symmetry. The symmetry of these diagrams can not be distinctly decided, owing to strong spreading of quartz axes. It is to be remembered, however, that the pattern of Fig. 58 somewhat resembles that of quartz fabric diagrams for schistose hornfelses. Even in Fig. 58, the spreading of quartz axes is far stronger than quartz axes from schistose hornfelses. Nevertheless, it is considered likely that the quartz fabric pattern of banded gneisses is slightly symmetrical in the northern part of the zone of transitional rocks, but it becomes less symmetrical or lacking in symmetry in the southerrn part of this zone or in the zone of migmatites.

Orientation data from siliceous banded gneiss near the contact with the Obataké gneissose granodiorite:

Sample 23: TN56VIII19-2; approx. $\perp b$-section.

Locality: Ôkubo, 150 m to the north from the contact (subarea H_2).

Mineral measured: [0001] of quartz from siliceous banded gneiss. In the rock are intercalated thin calcareous bands, 3~2 mm in width, which consist of biotite, hornblende, diopsidic augite, plagioclase, and quartz. While, the quartzose bands consist of biotite, K-feldspar, plagioclase, and quartz, and less commonly hornblende. Porphyroblastic quartz is prevalent, which attains 2 mm or more in diameter. Undulatory extinction of quartz is common.
Remarks: The lineation is indistinct. The result is shown in Fig. 65-a.

Sample 24: TN56VIII19-2; approx. // *b*-section.
Measurements: Elongation axes and undulatory zones in grains of quartz.
Remarks: The results are shown in Figs. 65-c and -d.

Sample 25: TN56X3-3; $\perp b$-section.
Locality: Katano, 130 m to the north from the contact (subarea H_3).
Mineral measured: [0001] of quartz from siliceous banded gneiss. The petrographic features of the rock are just similar to *Sample 23*.
Remarks: The rock belongs to the same horizon as *Sample 23*. The lineation is traceable on the hand specimen. The result is shown in Fig. 66-a.

Sample 26: TN56X3-3; // *b*-section.
Measurement: Elongation axes of quartz grains.
Remarks: The result is shown in Fig. 66-b.

Each of the two quartz diagrams, Figs. 65-a and 66-a, includes two prominent maxima on both sides of S_1. Positions of these maxima close to the position IV with respect to S_1. The symmetry of these diagrams approximates monoclinic with axis *b* of the fabric, which does not necessarily coincide with axes of microfolds observable in the hand specimen.

Fig. 65-b shows a microscopic sketch of a porphyroblast of quartz and orientations of quartz axes of each grain. The variation of orientations of quartz axes within the porphyroblast is not beyond 9° in trend and 12° in plunge. Fig. 65-c and -d are the compass-rose diagrams after SCHMIDT.* The most common trend of the elongation axes for porphyroblasts is completely parallel to S_1, compositional banding, in siliceous banded gneiss (Figs. 65-c and 66-b). As can be easily inferred from Fig. 65-a, most of the undulatory zones** keep angles of about 40° with S_1 (Fig. 65-d).

The general pattern of quartz fabrics of banded gneisses was, as described above, characterized by lacking in symmetry. This was the most remarkable difference in fabric pattern between schistose hornfelses and banded gneisses. However, the pattern of quartz fabric becomes again a little symmetrical in banded gneiss near the contact with the Ôbataké gneissose granodiorite. The axes of crenulation, *B*-folds, coincide not always with axis *b* of the fabric. Of significance for the pattern of quartz fabrics of banded gneisses concerned are not axes of crenulation but surfaces of S_1.

---

*SCHMIDT, W. (1918), Statistische Methoden beim Gefügestudium kristalliner Schiefer, Sitz. Kaiser l. Akad. Wiss. Wien. FAIRBAIRN (1949) introduces the method of construction of the diagram (in page 305).
**Refer, H. W. FAIRBAIRN (1949, p. 14, Fig. 2-2).

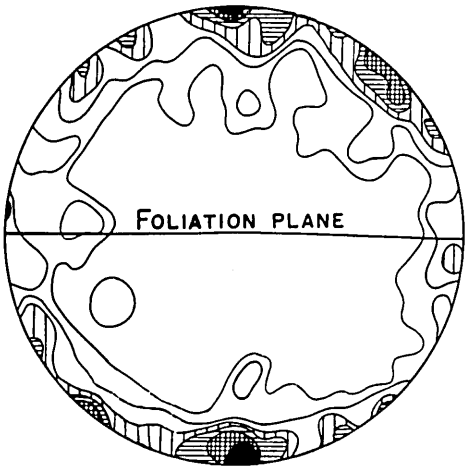

FIG. 67. 250 (010) poles of plagioclase in Specimen TN55XIII-5; contours 6-5-4-3-2-1%.

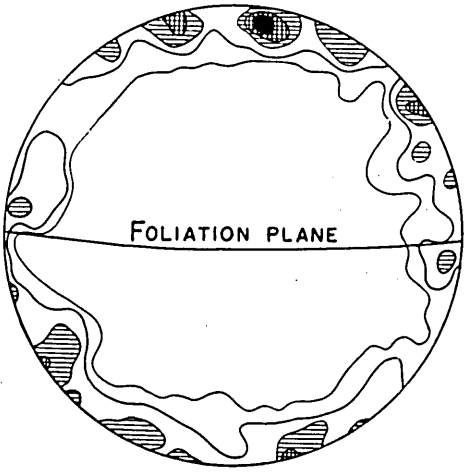

FIG. 68. 210 (010) poles of plagioclase in Specimen TN55XI22-5; contours 7-5.5-4-2.5-1%.

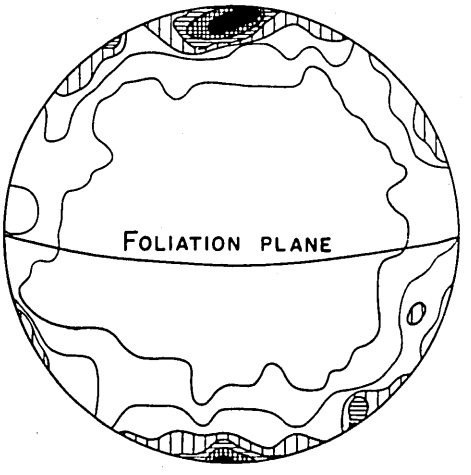

FIG. 69. 182 (010) poles of plagioclase in Specimen TN56VIII13-2; contours 6-5-4-3-2-1%.

Ôbataké gneissose granodiorite

Preferred orientation of quartz axes has not been examined, but poles of (010) of plagioclase were measured.

Sample 27: TN55XIII-5; $\perp S_1$-section.

Locality: Ôban (subarea H_1).

Mineral measured: [010] of plagioclase from the Ôbataké gneissose granodiorite. The rock consists essentially of augite, biotite, plagioclase, quartz; zircon, sphene occur as accessories. No zonal structure is found in plagioclase. 2V of plagioclase is $90° \sim +78°$ ($An_{38 \sim 49}$). Undulatory extinction of quartz is common.

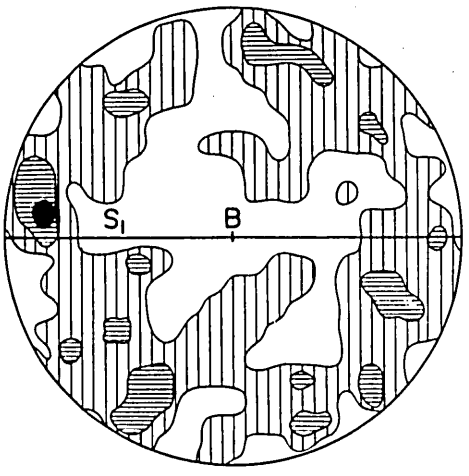

FIG. 70. 400 [0001] of quartz in Specimen TN55XI24-5; contours 3-2-1%.

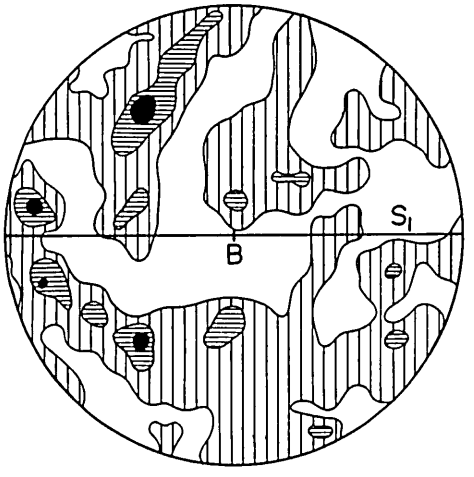

FIG. 71. 389 [0001] of quartz in Specimen TN56VIII10-4; contours 3-2-1%.

Remarks: S_1, compositional banding or foliation plane, is not so distinct. The result is shown in Fig. 67.

Sample 28: TN55XI22-5; approx. $\perp S_1$-section.

Locality: Tokimori (subarea H_1).

Mineral measured: [010] of plagioclase from the Ôbataké gneissose granodiorite. The rock is similar to *Sample 27* in every petrographic feature. 2V of plagioclase is 90°~ +80° ($An_{38\sim47}$).

Remarks: S_1 is relatively distinct. The result is shown in Fig. 68.

Sample 29: TN56VIII13-2; approx. $\perp S_1$-section.)

Locality: Ôkubo (subarea H_2).

Mineral measured: [010] of plagioclase from the Ôbataké gneissose granodiorite. The same essential minerals as in *Sample 27* are found. Porphyroblasts of plagioclase are common. 2V of plagioclase is 90°~+75° ($An_{38\sim52}$).

Remarks: S_1 is relatively distinct. The result is shown in Fig. 69.

Three diagrams, Figs. 67, 68 and 69, show the similar pattern to each other. S_1 in these diagrams has been decided directly by megascopic measurements of the hand specimens. Although many peripheral maxima occur in these diagrams, the prominent maxima show that most of (010)-planes of plagioclase are parallel or nearly parallel to S_1, foliation plane.

Banded gneiss and banded chert thermally metamorphosed by the younger intrusives

Orientation data from siliceous banded gneiss: Banded gneisses come into contact with the Kibé granite, the Namera granite and the Gamano gneissose granodiorite (see, Plate XII).

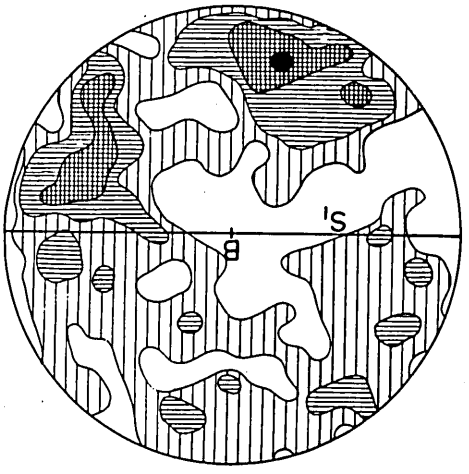

FIG. 72. 350 [0001] of quartz in Specimen TN56XI16-8; contours 4-3-2-1%.

Fig. 70 is a quartz diagram for siliceous banded gneiss coming into contact with the Gamano gneissose granodiorite, and Fig. 71 is that for siliceous banded gneiss to be exerted an intense thermal metamorphism by the Kibé granite.

These two diagrams show no definite pattern of symmetry. Such lacking in symmetry as illustrated by these diagrams, however, can not be safely regarded as the characteristic pattern of banded gneisses thermally metamorphosed, because banded gneisses proper show no definable symmetry with respect to the quartz fabric.

Orientation data from banded chert: A sample was selected from an exposure near Kôbata, apart about 200 m from the intrusion contact of the Cretaceous granite. The result of the fabric analysis of quartz axes is shown in Fig. 72. The diagram is characterized by lacking in symmetry. In the former examples so far described, schistose hornfelses have usually shown the distinct pattern of quartz fabrics. It seems likely to interprete, therefore, that the distinct pattern of quartz fabrics in schistose hornfelses was completely exhausted by the thermal metamorphism exerted by the Cretaceous granite.

SYNOPSIS OF THE ORIENTATION DATA:——WITH SOME KINEMATIC AND DYNAMIC INTERPRETATIONS

Fabrics of unfolded schistose hornfelses

In mica diagrams for schistose hornfelses occur generally two sets of (*h0l*)-surfaces, *ss* and *s's'*, which are completely or almost completely symmetrical with respect to S_1 and intersect at the fabric axis *b*. *b* coincides strictly with the lineation.

In banded chert, the symmetry of quartz fabric is orthorhombic, and S_1 is one of the symmetry planes. The prominent maxima are in common referable to the position IV after SANDER with respect to S_1. Such quartz pattern, considered in conjunction with mica fabrics, has been tentatively interpreted as that evolved during compression by a

force acting normal to the surface of S_1, as suggested by TURNER (1951). In banded chert, there seems to be no evidence rejecting the interpretation suggested by TURNER.

The symmetry of quartz fabric of semi-pelite is also orthorhombic with respect to one of (*h0l*)-surfaces, *ss*, but S_1 rarely represents one of symmetry planes. The area of higher concentration of [0001]-axis of quartz in each diagram is always lanky. Furthermore, the prominent maxima are situated between the position IV and II after SANDER. The quartz fabric characterizing semi-pelite may be best explained with such assumptions as follows:— (1) the quartz pattern of semi-pelite might have been similar to that of banded chert at the incipient phase of the deformation, but (2) later, with evolution of deforming movement, one set of subordinate (*h0l*)-surfaces becomes a plane of actual slip, and, consequently, (3) internal rotation of quartz grains was resulted. The pattern of quartz fabric in pelite can be explained by the similar way.

The difference between the quartz patterns of semi-pelite or pelite and that of banded chert may be attributable to difference in relative competency of rocks under the same deforming process. It is to be remembered, however, that the symmetry of quartz fabric in schistose hornfelses is always orthorhombic, irrespective of difference in competency of rocks.

Fabrics of folded banded chert

In quartz diagrams for folded banded chert, Figs. 35～38 (*Example 1*) and Figs. 45～47 (*Example 2*), it became evident that the pattern of quartz fabric is just similar to each other with respect to S_1, regardless of limb or crest of folds, and that it shows no essential difference from that of unfolded banded chert.

Thus, the symmetry is not changed, i.e., constantly orthorhombic, irrespective of limb or crest and of included angles of both limbs of folds. It is not unlikely to infer that the process through which folds in banded chert have been completed can be explained by an imaginary process of "unrolling".* In the explanation of unrolling mechanism, it is usual to use "*q*-Richtung"**; in other words, the studies of unrolling have been carried out only when one prominent maximum occurs in each of quartz fabric diagrams. In the present instance concerned, however, all quartz fabric diagrams show orthorhombic symmetry. Nevertheless, high concentration of quartz axes and four prominent maxima at the definite position with respect to S_1 indicate that no distinct internal rotation of quartz grains had occurred during folding of banded chert. During folding of abnded chert, shearing stress might have acted along the surface of S_1. The fact can be easily inferred and proved from the quartz pattern of the segregated veins of quartz (later described).

* A classic instance of the process of unrolling is provided by a folded quartzite near Brenner, Tyrol, investigated by SANDER (1930). Lately, ZOZMANN (1950) investigated in detail a folded quartzite from Bardufoss, Norway, which is interpreted by him as an example of fold of partial unrolling (teilweise abwickelbare Falte).

**"*q*-Richtung" means an orientation which is shown in the quartz fabric diagram by a line passing through one prominent maximum and the fabric axis *b* (I.S. ZOZMANN. 1950; J. LADURNER, 1954). In studying quartz folds, the angle which these *q*-Richtungen make with the tangent of folds has been used generally as a basis of interpretation of folding mechanism.

Fabrics of "sheared flexure folds" and rocks in which well-developed S_3 were found

Quartz fabric patterns in Figs. 49～51 and Fig. 53 resemble each other with respect to the shear plane in the sheared flexure folds and S_3. These are characterized by a complete or nearly complete small circle girdle which approximates *ac* of the fabric. The areas of higher concentration in these diagrams are generally lanky. The most significant feature of these diagrams is that planes along which actual slip occurred govern the orientation of quartz axes and that S_1 or other (*h0l*)-surfaces are no longer directly concerned with the orientation of quartz axes. In particular, the quartz pattern in Fig. 53 approximates a monoclinic symmetry and the position II after SANDER and fairly resembles the quartz pattern investigated by KOJIMA and SUZUKI (1958a).*

Judging from the complete girdle and the lanky areas of higher concentration in these quartz diagrams, it can be inferred that [0001]-axes of quartz, which might have been oriented initially in the position IV with respect to S_1, were rotated internally during the time of later shearing and reoriented in the position II with respect to surfaces along which actual slip occurred.

Fabrics of banded gneisses

In banded gneisses, (001)-planes of micas are strictly parallel to S_1, and no (*h0l*)-surface intersecting S_1 could have been found. Micas in banded gneisses would have been recrystallized under a condition of high temperature and high confining pressure, and, then, surfaces parallel to the compositional banding were probably those favourable to growth of micas.

On the other hand, quartz fabric diagrams for banded gneisses are most commonly characterized by poorness of symmetry.

In Chapter II the writer has described that the grain size of schistose hornfelses increases from the north to the south, and eventually schistose hornfeses gradually change their micro- and macroscopic features into banded gneisses. Examining all fabric diagrams for quartz axes from three zones, it seems to be probable that the quartz fabric pattern in schistose hornfelses changes its distinct, orthorhombic, symmetry into the less symmetrical in rocks of the zone of transitional rocks and, further, into complete lacking in symmetry in rocks of the zone of migmatites.

The quartz fabric of siliceous banded gneiss near the contact with the Ôbataké gneissose granodiorite, shows again monoclinic symmetry with axis *b* of the fabric which does not always coincide with the lineation (axes of microfolds or of *B*-folds). Quartz grains are elongated in the direction of *b*, parallel to S_1.

---

* They found a systematic relation between the quartz fabric pattern and the plane of actual slip, and established a working hypotheses concerning the preferred orientation of quartz sufficiently recrystallized during flow of a rock, that is:
1) *r* $(10\bar{1}1)$ and / or *z* (0111) of quartz lie on the shear plane, and 2) the sense of displacement of upper layers on these lattice planes is downward from the *c*-axis of quartz.

Such evidences may suggest, considered with the geological situation of the banded gneiss and with the fabrics of the Ôbataké gneissose granodiorite, that shearing would be active along S_1 at a later phase of the recrystallization of banded gnesses, and that the shearing movement seems to be closely related to the movement of the Ôbataké gneissose granodiorite. *F*-folds can not be characterized by any symmetrical quartz pattern. *F*-folds may be gentle waves produced during the swelling movement in regional scale, to which the movement of the Ôbataké gneissose granodiorite is probably attributable.

Fabrics of the Ôbataké gneissose granodiorite

The orientation diagrams for [010] of plagioclase, Figs. 67～69, illustrate that most of the (010)-planes of plagioclase are parallel or nearly parallel to the surface of compositional banding in the gneissose granodiorite.

Judging from evidences observed in the field, the plagioclase pattern in problem seems to be reasonably explained by assuming that the Ôbataké gneissose granodiorite should have been moved from the place where it had been produced, and that the movement of the gneissose granodiorite might have occurred preferably along the foliation, which is evidently a remnant of the original structure. The foliation in the gneissose granodiorite is generally inclined steeply or nearly vertical.

Fabrics of segregated quartz veins

Two alternative quartz patterns have been found: one is represented by Figs. 39 and 40, and another by Fig. 54. Figs. 39 and 40 show an incomplete monoclinic symmetry with axis *b* of the fabric and suggest that quartz was segregated during the phase of deformation of schistose hornfelses. While, Fig. 54 shows no distinct pattern of quartz fabric and suggests that the segregation of quartz veins was completed at the phase later than the cleaving of S_3, probably under a static condition.

It is evident, from the meso- and microscopic observations, that the cleaving of S_3 may set in at the later phase of folding of schistose hornfelses. The similar segregated quartz veins have been found everywhere in the zone of schistose hornfelses, but they have not been found in banded gneisses. It can safely be said, therefore, that the segregation of quartz would have been accomplished prior to or, probably, simultaneously with the recrystallization of banded gneisses. The segregation of quartz veins would have begun at the later phase of folding of schistose hornfelses, and had not been prolonged over the main phase of recrystallization of banded gneisses.

Summary

Summarizing the results of fabric analyses described above, the following points must be mentioned:—

1) Schistose hornfelses are products of regional thermal metamorphism, which is re-

ferable to the older Ryôké phase and have been accompanied by deformation by which folds on various scales have been completed. No pre-deformational fabric could be found from schistose hornfelses.

2) The quartz fabric pattern from rocks in which planes of actual slip are found, approximates a monoclinic symmetry with axis *b* of the fabric. Even in these cases orthorhombic symmetry is yet traceable, and, then shearing along the planes of actual slip appears to govern the pattern of quartz fabric.

3) The recrystallization of banded gneisses was probably completed under high temperature and high confining pressure, but may not be accompanied by such penetrative movement as that characteristic of production of schistose hornfelses.

4) The Ôbataké gneissose granodiorite can not be strictly referable to the autochthonous granite, but it seems to have been somewhat mobilized. The mobilization of the granodiorite would have occurred probably at the later, extended phase of production of banded gneisses and migmatites, and would have been caused by the swelling movement of a regional scale.

5) Judging from various evidences so far described, it must be strongly asserted that the "Ryôké metamorphism" can be divided into two phases of contrasted style: the earlier phase is characterized by the production of schistose hornfelses and the later phase by that of banded gneisses and migmatites. It may be inferred that the earlier phase and the later phase were not strictly continuous but probably interrupted.

V. Concluding Remarks

The greater part of this paper was expended in describing the geometrical relations of various structural elements and the petrofabrics of the Ryôké metamorphic and granitic rocks of the area between Iwakuni and Yanai. The respective topics of these investigations were summarized at the end of each chapter. Therefore, there seems to be no need to sum up again.

Considering the results described in the preceding chapters, the history of development of the Ryôké metamorphic and granitic rocks in the Iwakuni-Yanai area may be summarized as follows:—

The phase of Pre-Ryôké metamorphism: The phase is represented by the sedimentation of original Palaeozoic formations. The surface of bedding or lamination, here termed S_1, has been preserved as the most significant surface of mechanical inhomogeneity in the rocks throughout the whole history of metamorphism. At certain stage in the course of diagenesis of original sediments, basic (diabasic) rock was intruded as small dykes. Judging from the results of structural-petrological investigations in the area so far clarified, no evidences suggesting the Pre-Ryôké metamorphism have been found.

The Ryôké metamorphism: Palaeozoic sediments and diabasic dykes had suffered the thermal metamorphism of regional scale, accompanied by deformation, throughout the

whole area.*

The effect of the thermal metamorphism is outstandingly extended towards the north of the area concerned. During the deformation, folds on various scales, from minor to major folds, were formed. Axes of folds are strictly parallel to the lineation. The general trend of the lineation is E.-W.

Contemporaneously with the folding, a fracture-cleavage, here termed S_2, was developed locally in semi-pelite and pelite. At the later phase of folding a slaty cleavage, here termed S_3, was cleaved locally in the axial parts of the major anticline. The earlier phase of the Ryôké metamorphism had ceased with the formation of slaty cleavage S_3. Accordingly, the earlier phase is characterized by penetrative movement accompanied by thermal metamorphism of regional scale.

On the other hand, rocks in the southern half of the area concerned have suffered more intense metamorphism under high temperature. The metamorphism progressed gradually into metasomatism. Thus banded gneisses were produced. The surface of foliation in banded gneisses is relatively distinct and corresponds evidently to the original laminae of sediments.

The grade of metasomatism increases with distance towards the south, probably with depth.** In the southern extremes of the area, some banded gneisses have been altered to migmatites, "autochthonous granite" (the Ôbataké gneissose granite and granodiorite), by alkali-alumina-metasomatism accompanied by metamorphic differentiation. The original laminae of sediments remain yet in these migmatites. With progressive metasomatism, a greater part of the autochthonous granite might have become more and more mobile, and have given rise to "parautochthonous granite" (the Gamano gneissose granodiorite), and further, to "intrusive granite" (the Kibé and Namera granites).

The Ôbataké gneissose granodiorite also moved upwards at some distance, and banded gneisses had, subordinately, swelled up in regional scale prior to and/or during the intrusion of the Gamano gneissose granodiorite. "*F*-folds" and, probably, regional arcuation of banded gneisses were completed at this phase. As the result of the swelling movement, various structures, in particular linear structures, lost their tectonically homogeneous characters.

The progressive metasomatism characterizes the later phase of the Ryôké metamor-

* Some authors, e. g., G. KOJIMA, have formerly asserted that the Ryôké metamorphism began at a phase when the diagenesis of original sediments had not so far proceeded. The writer has, however, not observed any evidence suporting such opinion. Does the petrography of schistose hornfelses suggest the characteristics of "soft rocks" which were thermally metamorphosed? Every rock seems to have behaved as having respective characteristics in competency, when the deformation occurred. Furthermore, diabasic dykes have generally facies of "chilled margin", marked by the presence of relatively sharp intrusive boundaries, and they have suffered the thermal metamorphism and deformation together with the sedimentary rocks. The writer inclines to believe that the diagenesis of sediments had proceeded moderately, probably almost completely, when the Ryôké metamorphism had begun.

** It is uncertain, however, whether banded gneisses and migmatites in the zone of migmatites were actually produced at deeper levels than schistose hornfelses, because the stratigraphy of the original sediments has not been fully clarified. Now, the writer sets much value on the words of H.H. READ (1957, p. 359): "Of course, the grade of metamorphism often increases with depth, but it does not increase because of depth."

phism. And, the movement of the Gamano gneissose granodiorite seems to be an extended phase of the Ryôké metamorphism.

The original rock of the Ryôké metamorphic and granitic rocks had once experienced the penetrative movement of the first phase as a whole, but the metamorphism of the second phase was effective only in the southern half of the Iwakuni-Yanai area: rocks in the northern half of the area were free from the metamorphism of the second phase and have remained as schistose hornfelses. The intrusion of the younger Ryôké granites, such as the Kibé and Namera granites, belongs to a younger age than the Ryôké metamorphism.

A thrust-fault, which trends ENE. with moderate dips towards the south, occurs near the boundary between schistose hornfelses and banded gneisses. Judging from geological as well as structural evidences, the movement of the thrust-fault seems to have been completed after the production of gneisses and migmatites, but probably prior to the intrusion of the younger Ryôké granites.

The Post-Ryôké metamorphism: Thermal metamorphism by the Cretaceous granites and their derivatives. The Cretaceous granite exerted intense thermal effects upon schistose hornfelses. The effects can be verified under the microscope; in particular, the fabric pattern of quartz in schistose hornfelses thermally metamorphosed by the Cretaceous grainte is characterized by the lacking in symmetry.

LITERATURES

ANDERSON, E.M., (1948): On lineation and petrofabric structure and the shearing movement by which they have been produced. *Geol. Soc. London Quart. Jour.*, **104**, 99-132.

BALK, R., (1952): Fabric of quartzites near thrust fault. *Jour. Geology*, **60**, 415-435.

———, (1953a): Structure of graywacke areas and Taconic Range east of Troy, New York. *Geol. Soc. America Bull.*, **64**, 811-864.

———, (1953b): Faltenachsen in Überschiebungszonen. *Geol. Rdsch.*, **41**, 90-103.

CLOOS, E., (1937): Interpretation of the crystalline rocks of Maryland. *Geol. Surv. Maryland*, **13**.

———, (1946): Lineation, a critical review and annotated bibliography. *Geol. Soc. America Mem.*, **18**.

FAIRBAIRN, H.W., (1949): *Structural petrology of deformed rocks.* Cambridge Mass.

GINDY, A.R., (1952): The plutonic history of the district around Trawenagh Bay, Co. Donegal. *Geol. Soc. London Quart. Jour.*, **108**, 377-411.

GORAI, M., (1952): The formation of the Japanese Islands (in Japanese). *Shizen* (Nature), **7**.

ICHIKAWA, K., (1958): Bemerkungen zum tektonischen Werdegang Südwestjapans während des Paläozoikums. *Jour. Inst. Polytechnics, Osaka, Series G*, **3**, 1-13.

IWAO, S., (1936a): On some basic inclusions in granite of Kuga district, Nagato; a study on contamination. *Jap. Jour. Geol. Geogr.*, **13**, 155-162.

———, (1936b): On the metamorphic rock in the Yanai district (preliminary report, in Japanese). *Jour. Geol. Soc. Japan*, **43**, 386-388.

———, (1936c): Geological and petrological relations in the field between granitic rocks and the Ryôké metamorphics of the Yanai district, Yamaguchi Prefecture (in Japanese). *Jour. Geol. Soc. Japan*, **43**, 660-691.

———, (1938): Quartzose biotite schists from the Yanai district; a study in mineralization. *Jap. Jour. Geol. Geogr.*, **15**, 105-124.

———, (1940): The origin of the basic inclusions in the granitic rocks of the Yanai district, Japan, and their petrographic feature. *Jap. Jour. Geol. Geogr.*, **17**.

JOHNSON, M.R.W., (1956): Conjugate fold systems in the Moine thrust-zone in the Lochcarron and Coulin Forest areas of Wester Ross. *Geol. Mag.* **93**, 345-350.

KARI, F., (1952): Analytisch-tektonische Studien an Gesteinen des Gerlostales. *Neues Jahrb. Geol. Paläontol. Mh.*, 1, 5-24.

KOBAYASHI, T., (1941): The Sakawa orogenic cycle and its bearing on the origin of the Japanese Islands. *Jour. Fac. Sci. Univ. Tokyo, Sect II*, 5.

KOIDE, H., (1949): Dando granodioritic intrusives and their associated metamorphic complex (abstract of the above paper, in Japanese), mimeographed. *Monograph Assoc. Geol. Collab.*, No. 1.

KOJIMA, G. and OKAMURA Y., (1952): *Yanai district* (in Japanese). Guide-book of the excursion at the 59 th Ann. Meet. of Geol. Soc. Japan.

_____, (1953): Contributions to the knowledge of mutual relations between three metamorphic zones of Chûgoku and Shikoku, S.W. Japan, with special reference to the metamorphic and structural features of each metamorphic zone: *Jour. Sci. Hiroshima Univ., Series C*, **1**, No. 3, 17-44.

_____ & SUZUKI, T., (1958): Rock structure and quartz fabric in a thrusting shear zone: the Kiyomizu tectonic zone in Sikoku, Japan. *Jour. Sci. Hiroshima Univ., Series C*, **2**, 173-193.

KVALE, A., (1945): Petrofabric analysis of a quartzite from the Bergsdalen Quadrangle, Western Norway. *Norsk Geol. Tidssk.*, **25**, 193-215.

_____, (1948): Petrologic and structural studies in the Bergsdalen Quadrangle, Western Norway, Part 2. *Bergen Museums Årbok, Naturvit. rekke., Nr. 1.*

_____, (1953): Linear structures and their relation to movement in the Caledonides of Scandinavia and Scotland. *Geol. Soc. London Quart. Jour.*, **109**, 51-74.

LADURNER, J., (1954): Beiträge zur Typisierung von Quarzfalten. *Tschermaks Miner. u. Petrog. Mitt. Bd. II*, 3, 47-66.

MACKENZIE, D.M., (1957): On the relationship between migmatitization and structure in Mid-Strathpey. *Geol. Mag.* **94**, No. 3.

OFTEDAHL, C., (1948): Deformation of quartz conglomerates in central Norway. *Jonr. Geol.*, **56**, 476-487.

OKAMURA, Y., (1957): Structure of the Ryôké metamorphic and granodioritic rocks of the Yanai district, Yamaguchi Prefecture (in Japanese). *Jour. Geol. Soc. Japan*, **63**, 684-697.

READ, H.H., (1931): The geology of central Sutherland. *Mem. Geol. Surv. Scotland.*

_____, (1943): Meditations on granite. *Proc. Geol. Association*, **54**, 64-85.

_____, (1948): A commentary on place in plutonism. *Geol. Soc. London Quart. Jour.*, **104**, 155-205.

_____, (1949): A contemplation of time in plutonism. *Geol. Soc. London Quart. Jour.*, **105**, 101-152.

Ryôké Research Group, (1955): Geological collaboration on the Ryôké metamorphic zone, Japan (in Japanese). *Earth Science*, No. 25.

SANDER, B., (1948): *Einführung in die Gefügekunde der geologischen Körper*, Ier Teil, Allgemeine Gefügekunde und Arbeiten im Bereich Handstück bis Profil. Wien und Innsbruck.

_____, (1950): *Einführung in die Gefügekunde der geologischen Körper*, IIer Teil, Die Korngefüge. Wien und Innsbruck.

SATO, H., (1933): *Yanaizu-sheet* (Sheet 241, Geological map on scale of 1:75, 000), with Explanatory text. Imperial Geol. Surv. Japan.

SITTER, L.U. DE, (1956): *Structural Geology*, New York.

STRAND, T., (1944): Structural petrology of the Bydgin conglomerate. *Norsk Geol. Tidssk.*, **24**, 14-31

TURNER, F. J. and VERHOOGEN, J., (1951): *Igneous and metamorphic petrology*. McGraw-Hill Book Co., Inc.

_____, (1957): Lineation, symmetry, and internal movement in monoclinic tectonite fabrics. *Geol. Soc. America, Bull.*, **68**, 1-17.

WEGMANN, C.E., (1929): Beispiele tektonischer Analysen des Grundgebirges in Finnland. *Bull. Comm. géol. Finlande*, **87**, 98-129.

_____, (1953): Über gleichzeitige Bewegungsbilder verschiedener Stockwerke. *Geol. Rdsch.*, **41**, 21-33.

WEISS, L.E., (1954): A study of tectonic style: Structural investigation of a marble-quartzite complex in Southern California. *Univ. California, Publication in Geological Sciences*, **30**, 1-102.

_____ & MCINTYRE, D.B., (1957): Structural geometry of Dalradian rocks at Loch Leven, Scottish

Highlands. *Jour. Geol.*, **65**, 575-602.
ZOZMANN, I. S., (1950): Gefügeanalysen an Quarzfalten. *Neues Jb. Mineral. Abh.*, **87**, 321-350.

Explanation of Plate VIII

A: Profile of small folds in banded chert, southwest of Hashirano.
B: Profile of small folds in banded chert, north of Kôbata. Pelite bands (black seams) become remarkably wider at the crest of folds.
C: Profile of small folds in banded chert, southeast of Kôbata.
D: Profile of small folds in banded chert, north of Hiuchi-iwa.

C

D

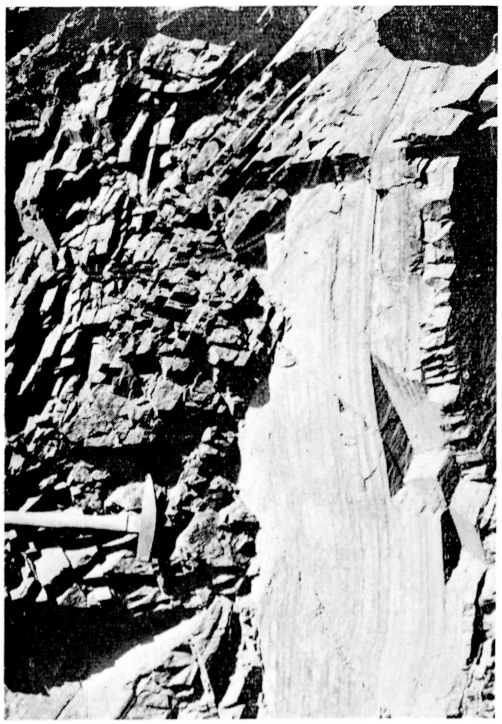

A

B

Explanation of Plate IX

A: *ac*-joints in pelite at Hiuchi-iwa.
B: *ac*-joints with oblique joints in banded chert, southeast of Kôbata.
C: Strongly lineated pelite at Hashirano. The hand of hammer is paralell to lineation.

A

B

C

Explanation of Plate X

A: Profile of small *B*-folds in siliceous banded gneiss, southwest of Kirihata.
B: Profile of *F*-folds in siliceous banded gneiss at Kanon-no-taki. Axes of *F*-folds are nearly vertical, and axes of *B*-folds and lineation are gently bent about axes of *F*-folds.
C: Strongly sheared siliceous banded gneiss within the thrust-fault near the entrance of the So-o Wireless Relay Station, east of Besshobata.
D: The thrust-fault running through banded chert, north of Honro-o.

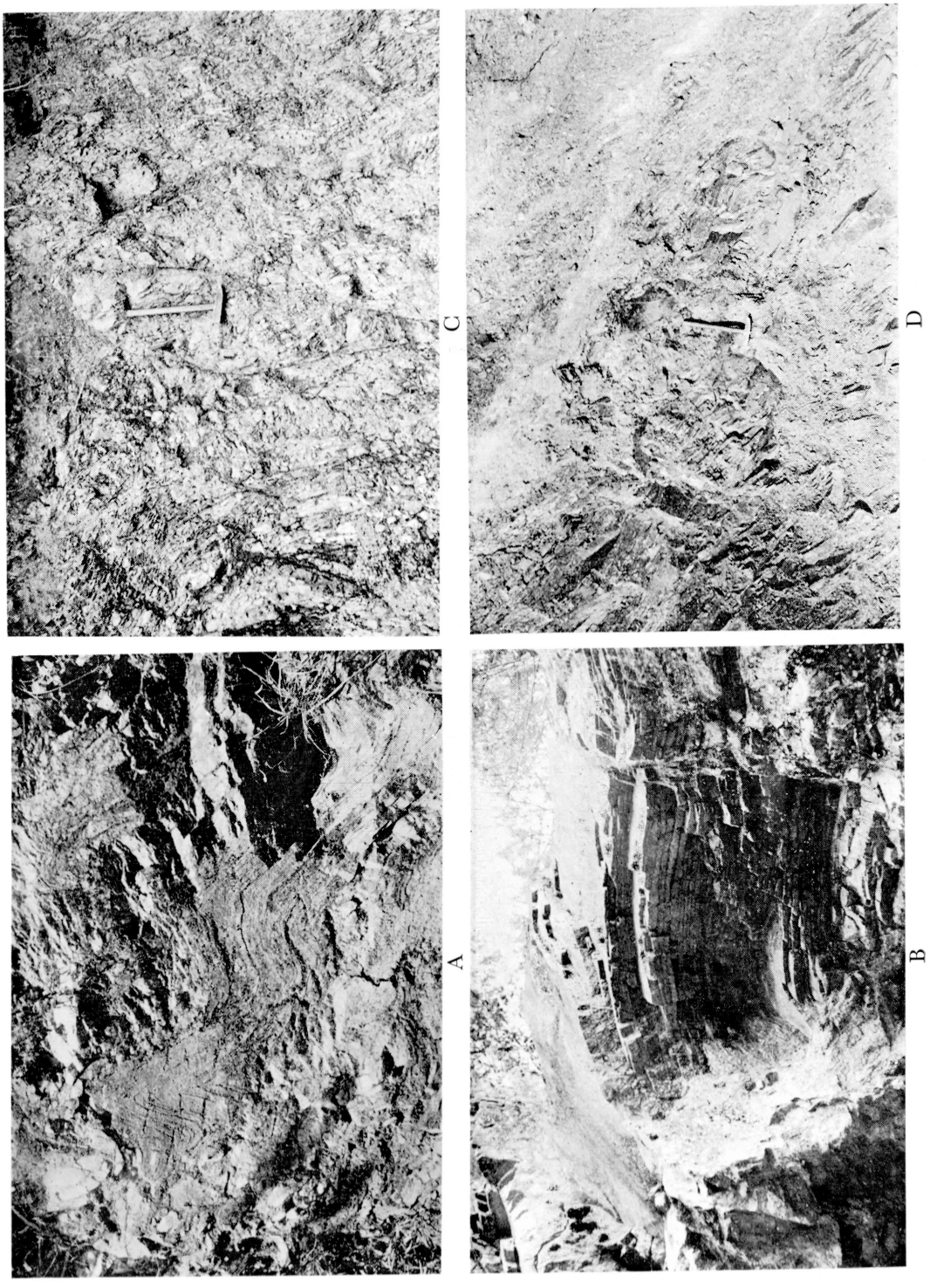
A
B
C
D

Explanation of Plate XI

A: Microphotograph of "sheared flexure folds" in Specimen TN57V22-2. Scale: 5 mm.
B: Microphotograph of banded chert, Specimen TN57XI29-2, in which S_3-surfaces are closely developed. Scale: 5 mm.

A

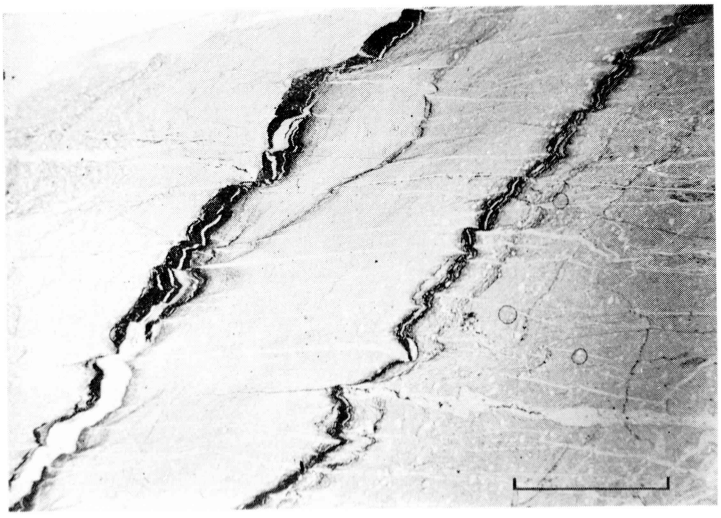

B

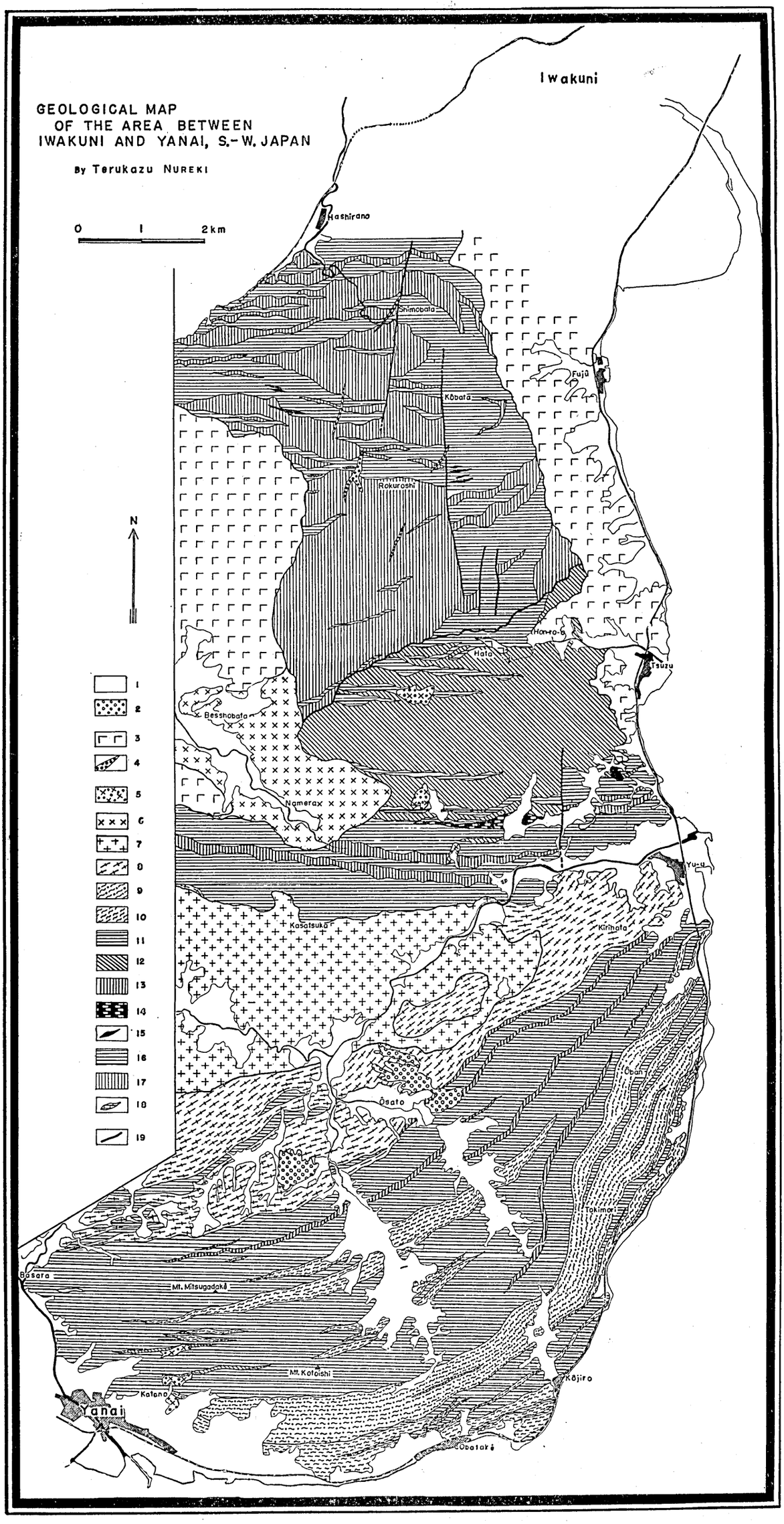

1 Alluvium; 2 Diluvium; 3 Cretaceous granite; 4 Dyke rocks (Cretaceous); 5 Fine-grained granite and aplite (Ryôké intrusive rocks); 6 Namera granite; 7 Kibé granite; 8 Gamano gneissose granodiorite; 9 Ôbataké gneissose granodiorite; 10 Ôbataké gneissose granite; 11 Siliceous banded gneiss; 12 Micaceous banded gneiss; 13 Micaceous gneiss; 14 Basic gneiss; 15 Basic (diabasic) rock; 16 Banded chert; 17 Pelite; 18 Limestone and calcareous-pelitic rocks; 19 Thrust-fault and fault.

STRUCTURAL MAP OF THE AREA BETWEEN IWAKUNI AND YANAI, S. W. JAPAN